5. RESEARCH ACTIVITIES

5.1 NUCLEAR PHYSICS

The main achievement in the last few months has been the setting up of the Indian National Gamma Array facility at IUAC. The mechanical structure for holding the Clover detectors has been installed in Beam hall II with motorised precision movement for the two halves of the array. The beam line along with a cylindrical scattering chamber has been set up with the beam dump inside the HYRA magnet for adequate radiation shielding. The detectors from the collaborating institutions TIFR, SINP and IUC-DAEF were received in Dec, 2007. During fabrication, the alignment of the mounting plates for individual Clover detectors was carried out with excellent precision (~±0.1°) to ensure that all the 24 detectors could be mounted without difficulty. Cabling work for the electronics has been completed and the testing of the data acquisition system has been going on.

A computer controlled LN2 filling system with a pressurised dewar of 1000 litre capacity has been set up. Off-line testing with radioactive sources has started and in-beam testing is expected to be carried during the end of Jan, 2008.

A workshop was carried out in August, 2007 asking for beam time proposals to be carried out with the first phase of INGA. Eleven experiments have been short listed for allocation of beam time during the first three months of operation.

The accelerated beam from the LINAC was delivered to the neutron array beam line in beam hall II. Fission dynamics for the reaction $^{16}O + ^{194}Pt$ at 120 MeV was studied with 16 neutron detectors in coincidence with complementary fission fragments.

The experiments carried out with Pelletron beams include (i) study of incomplete fusion reactions using ^{16}O beam (ii) Fusion-fission reactions near Coulomb barrier (iii) entrance channel effects in fusion dynamics and (iv) investigation of multi-neutron transfer reactions in ^{40}Ca on $^{68,70}Zn$.

5.1.1 Fission fragment angular and mass distribution measurements for the system $^{16}O + ^{194}Pt$ forming the compound nucleus $^{210}Rn^{*}$ at energies above and below the Coulomb barrier.

E. Prasad[1], K. M. Varier[1], B. R. S. Babu[1], N. Madhavan[2], K. S. Golda[2] , S. Nath[2], J. Gehlot[2], B. P. Ajith Kumar[2], J. J. Das[2], A. Jhingan[2], S. Muralithar[2], S. Kailas[3], A. K. Sinha[4], R. Singh[5], T. K. Ghosh[6], P. Bhattacharya[7], B. R. Behera[8], Hardev Singh[8], Rohit Sandal[8], Ranjeet[5]

[1] Department of Physics, Calicut University, Calicut

[2] Inter University Accelerator Centre, Aruna Asaf Ali Marg, New Delhi- 67

[3] Nuclear Physics Division, Bhabha Atomic Research Centre, Mumbai

[4] UGC-DAE Consortium for Scientific Research, Kolkata Centre, Kolkata

[5] Department of Physics and Astrophysics, Delhi University, Delhi

[6] Variable Energy Cyclotron Centre, Kolkata

[7] Saha Institute of Nuclear Physics, 1/AF Bidhan Nagar, Kolkata

[8] Department of Physics, Panjab University, Chandigarh-160014

In heavy ion induced fission reactions on heavy targets, anomalous enhancement of the angular anisotropy over the predictions of the Statistical Saddle Point Model (SSPM) has been observed near and below the Coulomb barrier [1]. This observation is a topic of extensive research for the last few years. Most of the existing models attribute this anomaly to the presence of non-compound nucleus mechanisms, such as pre-equilibrium fission, fast fission and quasi-fission. It is also known that the entrance channel mass asymmetry $\alpha = |A_T - A_P| / (A_T + A_P)$ with respect to the Businaro - Gallone critical value α_{BG} plays a decisive role in the dynamics of fusion process and hence in the angular distributions. At above barrier energies, for systems with $\alpha > \alpha_{BG}$, the anisotropies are consistent with SSPM predictions, while for systems with $\alpha < \alpha_{BG}$, the anisotropies are large due to non compound nucleus fission events. This anomalously large anisotropy can be explained by pre-equilibrium and pre-fission emission corrections. At below barrier energies also, anomalously large anisotropies are observed for systems involving deformed projectiles or targets irrespective of their α values. To explain this, Hinde et al., [2] proposed the nuclear orientation dependent quasi-fission reaction, where the di-nucleus before complete equilibration moves over the asymmetric conditional saddle point, leading to a narrow K distribution. Probable effects of this quasi-fission process, apart from the enhancement in anisotropy, could be an increase in the width of the mass distribution [3].

In order to further investigate the above mentioned effects, we have carried out measurements on the $^{16}O + ^{194}Pt$ system. The mass asymmetry value α for $^{16}O + ^{194}Pt$ system is 0.847 and α_{BG} is 0.856. The present experiment was performed at the Inter University Accelerator Centre, New Delhi, using pulsed ^{16}O beam with a pulse separation of 250 ns. The pulse width was about 0.9 ns – 1.1 ns and the target was 300 $\mu g/cm^2$ thick ^{194}Pt on 20 $\mu g/cm^2$ thick carbon backing [4]. The target was kept at an angle of 45° with respect to the beam and the fission fragments were detected in two multi-wire proportional counters with active area of 24 cm x 10 cm. The operating pressure was about 3.5 Torr of isobutane gas. These detectors were kept at 56 cm and 30 cm away from the target, subtending azimuthal angles of about 24° and 43°, respectively. The detectors were kept at folding angles for mass distribution measurements. Two ΔE-E telescopes (SSBD) were also used, one of which (ΔE ~8 μm and E~100 μm) was fixed near the MWPC on the moving arm (upper arm). The second telescope (ΔE ~ 14 μm and E~ 100 μm) was fixed at backward angle (174°) to collect the backward scattered particles. Two solid state detectors were kept at +10.5° and -9.5°, with respect to the beam direction to detect the elastically scattered ^{16}O beam. Signal from one of these detectors was used to get a TAC spectrum with RF as the stop signal to obtain the time structure of the beam and to rule out any time drift.

The angular distribution and mass distribution measurements were performed at energies ranging from 10% below the Coulomb barrier to 25% above the barrier. Data were collected at lab energies 102, 98, 94, 90, 86, 83, 81, 79, 77, 75 and 73 MeV.

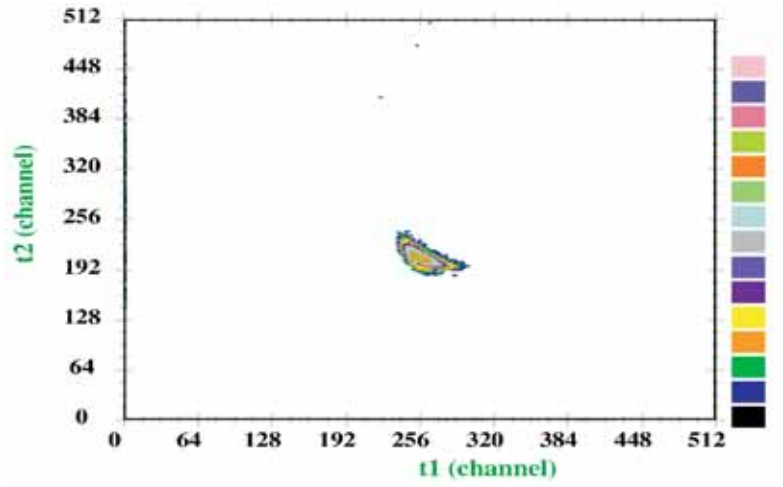

Fig. 1 The timing correlation between the detected fission fragments at 90 MeV (lab) beam energy. The fission fragments are well separated from elastic and quasi elastic channels

The MWPC provided very good position and time resolution. Fission fragments were well separated from the elastic and quasi elastic channels, both in time and energy loss spectra. The time correlation of the fission fragments detected is shown in fig. 1. The mass distributions of the fission fragments were obtained by knowing the time of flight and flight path very accurately. The mass resolution of the gas detectors was about 4 atomic mass units. The mass distributions of the fission fragments at different projectile energies are shown in fig. 2.

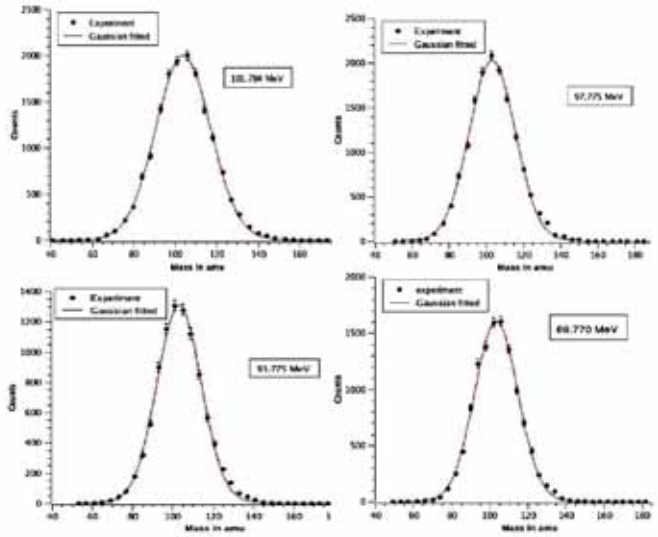

Fig. 2 Mass distributions of the fission fragments for the system ^{16}O + ^{194}Pt at different projectile energies (lab) (The solid lines are the Gaussian fits to the data)

REFERENCES

[1] S. Kailas, Phys. Rep. 284 (1997) 381

[2] D. J. Hinde et al., Phys. Rev. Lett. 77,(1996) 5027

[3] T. K. Ghosh et al., Phys. Rev. C 69(2004) 031603; Phys. Rev. C 70(2004) 011604

[4] E. Prasad, Proceedings of DAE-BRNS symposium on Nuclear Physics, Vol. 52(2007) 621

5.1.2 Effect of entrance channel mass asymmetry in fission of ^{216}Ra

Hardev Singh[1], Golda K. S.[2], Rohit Sandal[1], B. R. Behera[1], Ranjeet[3], A. Jhingan[2], R. P. Singh[2], P. Sugathan[2], S. K. Datta[2], Santanu Pal[4] and I. M. Govil[1]

[1] Department of Physics, Panjab University Chandigarh

[2] Inter University Accelerator Centre, Aruna Asaf Ali Marg, New Delhi - 67

[3] Department of Physics, Delhi University

[4] Variable Energy Cyclotron Centre, 1/AF Bidhan Nagar, Kolkata

The study of fusion-fission reaction dynamics has emerged as a topic of great interest in recent years. The light particle (neutron, proton, alpha) emission from the fissioning system has been used as a tool to understand these dynamical processes. Most of the experiments in this regard have been done using neutron as a probe. Experimentally measured pre-scission neutron yield is compared with the statistical model prediction and the excess yield, if any, is interpreted to be due to the damping of the fission process. In order to understand these dynamical effects and their dependence on the entrance channel, we have measured the pre-scission neutron yield from ^{12}C+^{204}Pb and ^{19}F+^{197}Au reactions at various lab energies. Since the above two systems populate the same compound nucleus ^{216}Ra, any difference in neutron yield measured from the two channels would reflect the entrance channel dependence of the fusion-fission dynamics as the two systems under consideration lie on two sides of Businaro-Gallone point.

The experiment was performed at the 15UD Pelletron of Inter University Accelerator Centre, New Delhi. Pulsed beams of ^{12}C and ^{19}F of various lab energies were used in the experiment. The targets were mounted at the centre of a 1.5 m diameter general purpose scattering chamber (GPSC). The fission fragments were detected using two large area (20 cm×10 cm) position sensitive multiwire proportional counters (MWPC). The neutrons were detected in coincidence with fission events by four neutron detectors which consisted of (12.7 cm dia×12.7 cm thick) organic liquid scintillator. Discrimination between neutrons and gammas was made by using pulse shape discrimination (PSD) based on zero cross technique and TOF. Time of flight (TOF) of neutrons and fission fragments were measured with respect to RF.

The observed TOF of neutrons was converted into neutron energy by considering the prompt ã peak in the TOF spectrum for time calibration and the energy spectrum was corrected for neutron detector efficiency using Monte Carlo computer code MODEFF. The components of pre- as well as post-scission neutron multiplicities were extracted by least square fitting of observed

neutron energy spectrum with Watt expression [4]. The calculations for the kinetic energies of the fission fragments and the folding angles were performed using the Viola [5] systematics for symmetric fission. The observed pre-scission neutron multiplicities for both the reactions are shown in fig 1.

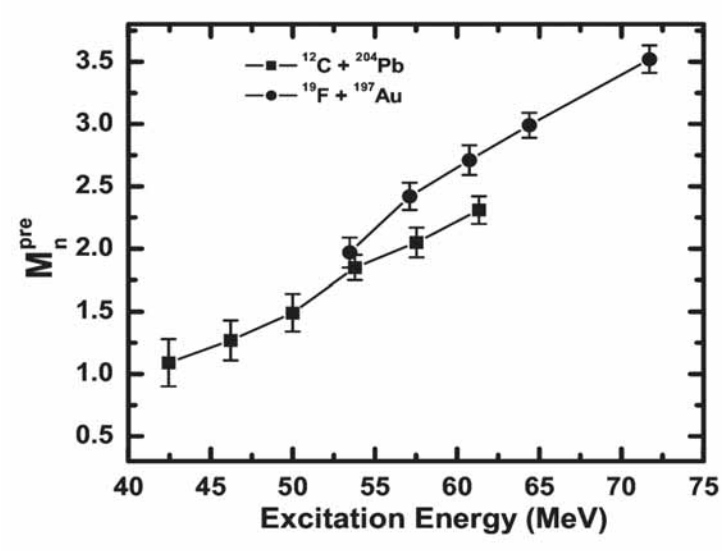

Fig. 1. Pre-scission neutron yield from both the reactions. Lines are drawn to guide the eye

The pre-scission neutron multiplicity is found to be higher for the system with entrance channel mass asymmetry á< $á_{BG}$ as compared to the system lying on the other side i.e. á> $á_{BG}$. This difference in multiplicities increases with the excitation energy of the CN. Thus the above observation indicates that the entrance channel mass asymmetry plays a crucial role in deciding the fusion-fission path of the composite system.

REFERENCES

[1] H. Rossner et al, Phys. Rev. C 40 (1989)2629

[2] A. Saxena et al, Phys. Rev. C 49(1994) 932

[3] Lestone et al, Phys. Rev. Lett. 70 (1993)2245

[4] D. Hilscher et al, Phys. Rev. C. 20 (1979)576

[5] V. E. Viola et al, Phys. Rev. C. 31 (1985)1550

5.1.3 Mass gated neutron multiplicity measurement to understand the fusion- fission dynamics for the system $^{16}O+^{194}Pt$

Rohit Sandal[1], B.R.Behera[1], R.K. Bhowmik[2], M.B. Chatterjee[2], R.K. Choudhury[3], Suneel Devi[4], S. Gautam[1], K.S. Golda[2], A. Jhingan[2], S. Kailas[3], A. Kumar[1], S.K. Mandal[4], M. Oswal[1], Prasad.E[5], Ranjeet[4], A. Roy[2], S. Ray[2], A. Saxena[3], H. Singh[1], R.P. Singh[2], K.P. Singh[1], Gulzar Singh[1], Varinderjit Singh[1], P.Shidling[6], P.Sugathan[2]

[1] Department of Physics, Panjab University, Chandigarh

[2] Inter University Accelerator Centre, Aruna Asaf Ali Marg, New Delhi- 67

[3] Nuclear Physics Division, Bhabha Atomic Research Centre, Mumbai

[4] Department of Physics and Astrophysics, Delhi University, Delhi

[5] Department of Physics, Calicut University, Calicut

[6] Department of Physics, Karnatak University, Dharwad

After the fusion of the two massive nuclei, the dominating channels in the decay of heavy and super-heavy nuclei are fusion-fission and quasi-fission processes [1]. In the last decade, there are several experiments for studies of the fusion of massive nuclei and their subsequent decay processes. The study of properties of fusion-fission and quasi-fission products helps us to understand the reaction dynamics and evolution of several degrees of freedom in the formation of the compound nucleus. This further helps in the selection of the proper target, projectile and bombarding energy combinations to maximize the formation probability of super-heavy nuclei. Measurement of fission fragment angular distribution, mass distribution and mass-energy correlation helps us to distinguish fusion-fission, quasi-fission and other non-compound nuclear components [2-3]. However, mass distribution, TKE distribution and mass-TKE correlation are not sufficient to distinguish above components in the fission path of the heavy elements [4-5]. In the past it was shown by dynamical calculations for the development of nuclear shape by Langevin equation that fusion-fission, quasi-fission and DIC have their own characteristic reaction times developing from the contact of the colliding partners to the scission point. The different reaction time means that each reaction process is associated with different pre-scission neutron multiplicity. The knowledge of the TKE of fission fragments and mean neutron allows us to calculate the energy balance of the reaction. This energy may depend on the shape of the evolving compound nucleus and might tell us whether this path can lead to compound nucleus component [3]. We can expect the total neutron multiplicity to be lower in the quasi-fission region and more neutron multiplicity in the fusion-fission region. Though all these effects have been studied in great details for entrance channel mass asymmetry, the effect of **'N/Z'** on the decay of the heavy nuclei has not been studied to a great extent. Keeping this in mind, we have started a programme to study the fission properties of the heavy nuclei by choosing different neutron-rich target and projectile combinations (i.g.^{16}O, ^{18}O+^{194}Pt, ^{198}Pt). As a first experiment of this series, we report here the summary of the mass gated neutron multiplicity measurement for the decay of the ^{16}O+^{194}Pt $\rightarrow$ ^{210}Rn reaction. Other experiments are planned in the next cycle.

120 MeV pulsed ^{16}O beam with an intensity of 7 to 30 nA, delivered by Pelletron plus First module of the super conducting linear accelerator facility (LINAC) of IUAC, was bombarded on a ^{194}Pt target having a thickness roughly 400 μg/cm^2. Time resolution of the beam out of the LINAC was continuously monitored by a BAF_2 detector positioned at the end of the Faraday cup. The pulse width was monitored to be roughly 600 ps throughout the experiment. The target was located at the centre of a thin walled spherical scattering chamber of 60cm diameter. The fission fragments were detected by a pair of Multi-wire proportional counter (5″ × 3″) kept at appropriate folding angle at a distance of 24 cm. from the target position.

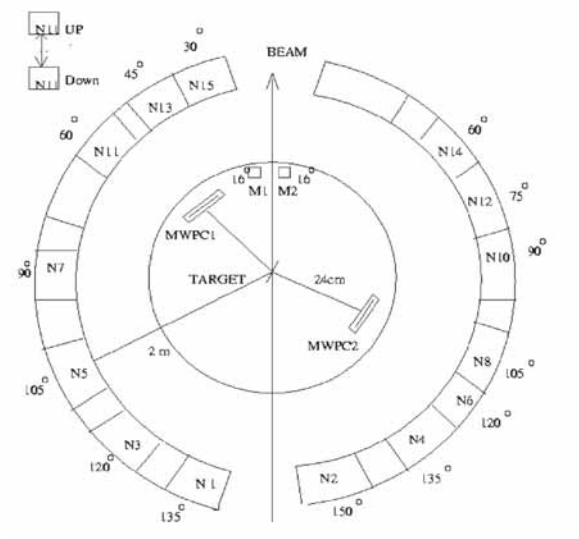

Fig. 1. Experimental set up at Beam Hall-II

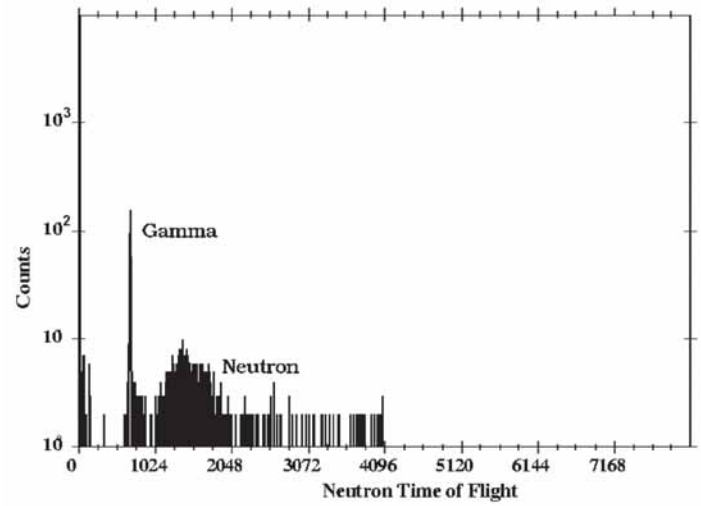

Fig. 2. Neutron Time of Flight Spectrum

14 neutron detectors (NE213 and BC501) of 5″ diameter and 5″ depth were kept at 2 meter distance from the target at angles ranging from 30°-150° (Fig.1 Two more neutron detectors were kept at 15° up and down out of the reaction plane. Because of the requirement of minimum gamma background in the neutron spectra, the beam dump was extended about 3m downstream from the target and the beam pipe was well shielded with lead and borated paraffin. The absolute neutron TOF was determined using the gamma peak in the TOF spectrum as a reference (Fig. 2). Two surface barrier detectors were placed 16° out of reaction plane for normalization purpose.

For n-γpulse shape discrimination, 12 IUAC home made [6] and 4 commercial (Canberra) PSD modules were used. The trigger of the data acquisition was generated by logic OR of the two

fission fragments (Cathode of the two MWPC) and ANDED with the RF of the beam pulse. The data analysis is in progress using the CANDLE offline data analysis package of the IUAC.

REFERENCES

[1] Yu. Oganessian et al., Nature (London) 400(1999) 242

[2] M. G. Itkis et al., Nucl. Phys. A 374 (2004) 136

[3] Y. Aritomo et al, Nucl. Phys. A759(2005) 342; Y. Aritomo et al, Nucl. Phys. A738(2004) 221.

[4] P.K. Sahu et al., Phys. Rev C 72 (2005) 034604

[5] R.G. Thomas et al., Phys.Rev. C 75 (2007) 024604

[6] S .Venkatramanan et al., Proc. DAE Symp. Nucl.Phys. Vol 51 (2006) 606

5.1.4 Evaporation residue cross section and γ-multiplicity distribution measurement for $^{19}F+^{184}W$ reaction

S. Nath[1], P.D. Shidling[2], J. Gehlot[1], E. Prasad[3], Ranjeet[4], K.S. Golda[1], A. Jhingan[1], J.J. Das[1], N. Madhavan[1], S. Muralithar[1], N.M. Badiger[2], A.K. Sinha[5], Santanu Pal[6] and R. Singh[4]

[1] Inter University Accelerator Centre, Aruna Asaf Ali Marg, New Delhi - 67

[2] Department of Physics, Karnatak University, Dharwad

[3] Department of Physics, Calicut University, Calicut

[4] Department of Physics and Astrophysics, Delhi University, Delhi

[5] UGC-DAE Centre for Scientific Research, Kolkata Centre, Kolkata

[6] Variable Energy Cyclotron Centre, 1/AF Bidhannagar, Kolkata

Fusion-fission dynamics of heavy systems is a topic of considerable current interest. Precise measurements of neutron, charged particle and GDR γ-ray multiplicities have revealed that these quantities are much larger than the values predicted by standard statistical model. This implies that collective mass flow from the equilibrium to the scission point is hindered by nuclear viscosity. However, neutrons, charged particles and γ-rays are emitted by the fused system while it moves from the equilibrium position to the saddle point and then from the saddle to the scission point. Therefore, these probes are not sensitive to whether the emissions occur before or after the traversal of the saddle point. Measurements of evaporation residues (ERs), on the contrary, can reveal information about pre-saddle dissipation. It has also been pointed out in our previous work [1-3] that the ER spin distribution is another sensitive tool to study dissipation in heavy systems.

To understand further the role of dissipation in fission of heavy nuclei, we carried out ER cross section and γ-multiplicity distribution measurements for the reaction $^{19}F+^{184}W$. The experiment was performed in HIRA [4] beam line. Pulsed ^{19}F beam, with 4 μs pulse separation, in the energy range of 90 – 110 MeV was bombarded on a 210 μg/cm^2 ^{184}W target on 110 μg/cm^2 carbon backing. Elastically scattered ^{19}F ions were detected in two silicon surface barrier detectors placed

at θ =±25° with respect to the beam direction. ERs were detected at the focal plane of HIRA using a 50×50 mm^2 two-dimensional position-sensitive silicon detector. A 14 element BGO multiplicity filter was placed in close geometry around the target to detect γ-rays from ERs. For clean and unambiguous identification of ERs, a TOF spectrum was recorded by setting up a TAC between the focal plane signal and the RF signal, used for beam pulsing. A two-dimensional plot between focal plane energy and the TOF is shown in Fig.1, which clearly identifies the ERs, free from any background contamination. For constructing γ-fold distribution, 14 TDC signals were recorded with ER as the common start and individual BGO signals as the stop.

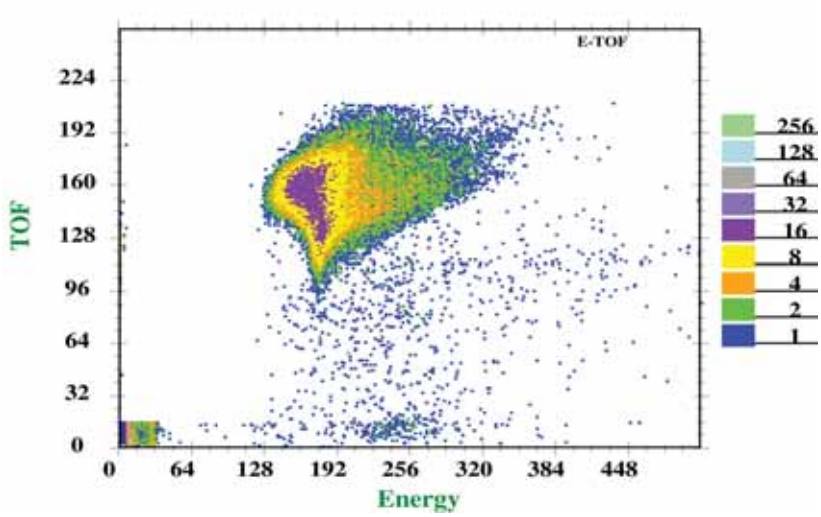

Fig. 1. Energy vs time of flight distribution for recoil products

REFERENCES

[1] S.K. Hui et. al., Phys. Rev. C 62, 054604 (2000)

[2] P. D. Shidling et. al., Phys. Rev. C 74, 064603 (2006)

[3] P.D. Shidling et. al., submitted to Phys. Rev. C

[4] A.K. Sinha et. al., Nucl. Instr. and Meth A 339, 543 (1994)

5.1.5 Study of complete and incomplete fusion dynamics in $^{16}O + ^{124}Sn$ system at 6.3 MeV/nucleon energy by measurement of spin distributions

D. Singh[1], R. Ali[1], M. Afzal Ansari[1], K. Surendra Babu[2], P. P. Singh[1], M. K. Sharma[1], Unnati[1], B. P. Singh[1], R. K. Sinha[3], Rakesh Kumar[4], S. Muralithar[4], R. P. Singh[4] and R. K. Bhowmik[4]

[1] Department of Physics, Aligarh Muslim University, Aligarh

[2] Department of Physics, G. B. Pant University, Pantnagar

[3] Department of Physics, Banaras Hindu University, Varanasi

[4] Inter-University Accelerator Centre, Aruna Asaf Ali Marg, New Delhi - 67

Study of incomplete fusion (ICF) reaction dynamics has been the subject of growing interest in the past few decades in the intermediate energy region. The first observation of PLFs by Britt and Quinton [1] in the bombardment of ^{197}Au and ^{209}Bi using ^{12}C, ^{14}N and ^{16}O projectiles at ≈10.5 MeV/nucleon led to the mechanism of 'massive transfer' of projectile to the target nucleus. Subsequently, Galin et al. [2] also observed 'fast' PLFs in forward cone and termed these reactions, leading to PLFs as 'incomplete fusion' (ICF). Inamura et al. [3] found more experimental evidence of ICF as a mechanism for ^{14}N + ^{159}Tb system at beam energy about ≈7 MeV/nucleons, wherein exclusive measurements of forward-peaked α–particles in coincidence with the prompt gamma rays of the different evaporation residues have been done. Furthermore they observed the lack of side feeding at low spins in the residual nuclei produced through ICF. Some earlier studies [4,5] on ICF by particle-gamma coincidence technique had mainly been focused on yield measurements in coincidence with emitted PLFs in forward cone. Observation of 'fast' alpha particles in forward cone in coincidence with prompt γ-rays of the populated evaporation residues provides an evidence of ICF.

In order to explain ICF reaction dynamics, several theoretical approaches have been proposed. The sum-rule model of Wilczynski et al. [6] has been quite successful in explaining the cross-section of all the PLFs at beam energies above 10 MeV/nucleon. According to the sum rule model, ICF reactions are localized in the angular-momentum space above the critical angular momentum for CF of the projectile and target. The Breakup fusion model [7] of Udgawa and Tamura is based on the distorted wave Born approximation (DWBA) formalism for elastic breakup of the projectile in the nuclear force field of the target nucleus, with the breakup amplitude multiplied by the factor representing the probability of fusion of one of the fragments with the target nucleus. This model qualitatively explained the kinetic energy spectra and angular distribution of ejectiles. On the other hand, Mermaz et al. [8] could explain the energy and angular distribution of the projectile-like fragments using a modified DWBA formalism for surface transfer reactions. However, no model so far proved successful at energy below 10 MeV/nucleon.

To study the CF and ICF reaction dynamics, we have performed an experiment at Inter-University Accelerator Centre (IUAC), New Delhi, using Gamma Detector Array (GDA) along with Charged Particle Detector Array (CPDA) set-up. The particle-gamma coincidence experiment has been performed with a view to study ICF reaction dynamics in the ^{16}O+^{124}Sn system at 100 MeV beam energy. Earlier most of the ICF reaction studies have been carried out by particle-gamma coincidence technique, with low-Z ($Z \leq 10$) projectile induced reactions with heavy targets ($A > 150$). However, there are few studies at lower beam energies and with medium mass spherical target nuclei. In order to investigate the role of target and residual nucleus deformation on the spin population in incomplete fusion reaction, the present experiment has been undertaken. These study show that the yields are almost constant up to a maximum angular momentum and then falls unlike in complete fusion where the yields falls exponentially with spin. However, no data on side-feeding population exist for the system ^{16}O+ ^{124}Sn. We have made an attempt to extract relative yields of the levels from the intensities of the gamma transition to decipher the side-feeding patterns. More experimental data are needed to have a better insight into the reaction mechanism that is involved at energies above Coulomb barrier and below 10 MeV/nucleon. With this view, we under took

studies on ICF reactions at beam energies 6.3 MeV/nucleon in the reaction of low-Z heavy ion ^{16}O with spherical target ^{124}Sn.

Self-supporting enriched target ^{124}Sn (enrichment ≈97.2%) of thickness 2.0 mg/cm^2 was mounted at 45^0 with respect to the beam direction inside the CPDA chamber. The target was bombarded with the 100 MeV ^{16}O with the beam current ≈20nA. Coincidences were demanded between particles (Z=1,2) and the prompt γ-rays emitted from the evaporation residues during the interaction of ^{16}O with ^{124}Sn. The CPDA is a group of 14 phoswich detectors. In the CPDA scattering chamber, seven CPD were placed on the top and seven in the bottom of the chamber. The 14 phoswich detectors of CPDA are divided in three angular zones: (i) 4 CPD in forward cone (10°-60°), (ii) 4 CPD in backward cone (120°-170°) and (iii) 6 CPD in sideways (60°-120°). In front of the each forward direction CPD an aluminium absorber of thickness 100 μm was used to stop the elastic scattered beam. This resulted in the removal of lower energy 'evaporation' alpha particles in the forward direction but allowed the fast α-particles produced in ICF to be detected.

Data analyses have been carried out off-line using software INGASORT. Identification of the CF and ICF channels in forward and backward cone were achieved by looking into various gated spectra. The main ICF reaction channels that were identified in the forward cone in coincidence with 'fast' α-particles are $^{124}Sn(O, \alpha 3n)^{133}Ba$, $^{124}Sn(O, \alpha 4n)^{132}Ba$, $^{124}Sn(O, \alpha 5n)^{131}Ba$, $^{124}Sn(O, \alpha p4n)^{131}Cs$, $^{124}Sn(O, \alpha 2pn)^{133}Xe$, $^{124}Sn(O, 2\alpha 2n)^{130}Xe$, $^{124}Sn(O, 2\alpha 4n)^{128}Xe$ and $^{124}Sn(O, 2\alpha p4n)^{127}I$. Three neutron channels produced in CF reactions $^{124}Sn(O, 5n)^{135}Ce$, $^{124}Sn(O, 6n)^{134}Ce$ and $^{124}Sn(O, 7n)^{133}Ce$ have also been identified from the singles spectra and are confirmed from gamma decay lines. In addition to these reaction channels identified in coincidence with particles in backward cone are: $^{124}Sn(O, p4n)^{135}La$ and $^{124}Sn(O, p6n)^{133}La$. Moreover, reactions channels identified in coincidence with 'compound' α-particles in backward direction are $^{124}Sn(O, \alpha 3n)^{133}Ba$, $^{124}Sn(O, \alpha 4n)^{132}Ba$, $^{124}Sn(O,\alpha 5n)^{131}Ba$, $^{124}Sn(O, 2\alpha 2n)^{130}Xe$, $^{124}Sn(O, \alpha p4n)^{131}Cs$ and $^{124}Sn(O, 2\alpha p4n)$ ^{127}I.

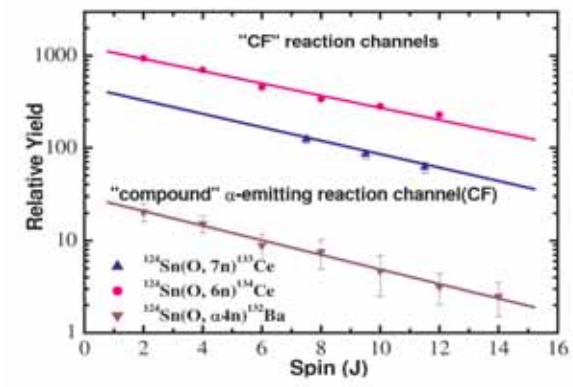

Fig. 1. Spin distribution for Complete Fusion channels

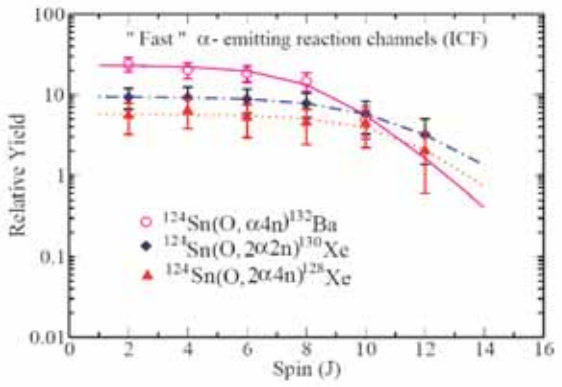

Fig. 2. Spin distribution for 'Incomplete Fusion Channels' in coincidence with fast α particles in forward direction

In the present work, to study the side feeding pattern intensities, the spin distribution of the energy levels of the evaporation residues populated by CF and ICF processes have been measured. As a representative case, the measured spin distributions for some the evaporation residues ^{134}Ce, ^{133}Ce, ^{132}Ba, ^{130}Xe and ^{128}Xe, produced in the ^{16}O+^{124}Sn systems are displayed in Figs. 1-2**.** In Fig. 1 the evaporation residue ^{134}Ce and ^{133}Ce produced in CF and ^{132}Ba, produced in coincidence with 'compound' α-particles emitted in backward cone, have been displayed. The yields of higher cascades show an exponential fall to high spin state, which indicates the presence of strong side feeding to the lowest member of yrast line transitions. Fig. 2 shows that the evaporation residues ^{132}Ba, ^{130}Xe and ^{128}Xe produced by ICF reaction, in coincidence with 'fast' α-particles emitted in forward cone. However, the intensities of the cascade transitions of evaporation residues ^{132}Ba, ^{130}Xe and ^{128}Xe have been found constant upto J=7$\hbar$, 9$\hbar$ and 9$\hbar$ respectively and then the yield successively decreases with high spin states, indicates the absence of side-feeding to the lowest members of yrast line transitions. It is interesting to find the spin at half yield in α and 2α-emitting channels associated with ICF. It comes out to be 9$\hbar$ and 11$\hbar$ respectively, while for CF it is 7$\hbar$, which clearly shows that the production of 'fast' forward PLFs associated with ICF are at higher input angular momentum and leads to peripheral interaction.

REFERENCES

[1] H. C. Britt and A. R. Quinton, Phys. Rev. 124 (1964) 877.

[2] J. Galin et al., Phys. Rev. C 9 (1974) 1126.

[3] T. Inamura et. al., Phys. Lett. B 68 (1977)51.

[4] R. I. Bardan et al., Euro. Phys. J. A 12 (2001) 317.

[5] K. Sudarshan et. al., Phys. Rev. C 69 (2004) 027603.

[6] J. Wilczynski et al., Nucl Phys. A 373 (1982)109.

[7] T. Udagawa and T. Tamura, Phys. Rev. Lett. 45(1980) 1311.

5.1.6 Disentangling of complete and incomplete fusion: Spin-distribution measurement at ≈ 4-7MeV/nucleon

Pushpendra P. Singh[1], B. P. Singh[1], Unnati[1], Manoj K. Sharma[1], D. P. Singh[1],R. Kumar[2], P. D. Shidling[3], D. Singh[1], Abhishek Yadav[1], R. Ali[1], R. P. Singh[2], S. Muralithar[2], M. A. Ansari[1], H. D. Bhardwaj[4], R. Prasad[1] and R. K. Bhowmik[2]

[1] Accelerator Laboratory, Department of Physics, A. M. University, Aligarh

[2] Inter University Accelerator Centre, Aruna Asaf Ali Marg, New Delhi - 67

[3] Department of Physics, Karnatak University, Dharwad

[4] Department of Physics, D. S. N. College, Unnao

The studies of incomplete fusion (ICF) dynamics at energies near and above the Coulomb barrier (CB) has been a topic of considerable interest in last decade or so, where complete fusion (CF) is expected to be dominant [1]. It is now an established fact that for incident energies a little

above the CB and for input angular momentum range $0 < l \leq l_{crit}$, heavy ion interaction is dominated by entire linear momentum transfer from projectile to target nucleus leading to CF process. As a consequence, a fully equilibrated excited compound nucleus of pre-determined charge, mass and angular momenta is formed, which decays by the light nuclear particle(s) and characteristic γ-radiations. However, at relatively high bombarding energies and for input angular momentum $l_{crit} \leq l \leq l_{max,}$ CF gradually gives way to ICF, where fractional mass and charge as well as the linear momentum of projectile are transferred to the target nucleus, due to the prompt-emission of α-clusters predominantly in the forward cone with almost projectile velocity. As a result of such process, projectile-like and target-like partners may appear in the exit channel. Such kind of reactions were first observed by Britt and Quinton [2], however, particle-γ-coincidence studies by Inamura *et al.*, [3] contributed a great deal to the understanding of underlying processes. Some of the important features of ICF dynamics are; (i) ICF contributes a significant fraction to the reaction cross-section in case of highly mass asymmetric systems [1]; (ii) the forward mean-ranges of recoils show relatively smaller depth in the stopping medium than that of CF residues [4], (iii) the outgoing projectile-like fragments are mainly concentrated in forward cone and their energy spectrum essentially peak at the projectile velocity; and (iv) the spin-distribution of evaporation residues populated via ICF are found to be distinctly different as observed for CF process [5].

In order to explain some of these features, several dynamical models have been proposed, but none of the existing models gave satisfactory fitting of the experimental data obtained at bombarding energies ≈4-7 MeV/nucleon. Moreover, the detailed conclusions regarding the multiplicity of linear momentum transfer, effect of mass asymmetry, role of different *l*-bins associated with ICF dynamics, could not be drawn from the available experimental data. As such, no theoretical model is available which can reproduce experimental data obtained at energies ≈ 4-7 MeV/nucleon. Further, ICF reactions are considered to be a promising route to produce high spin states in heavy residues at even low bombarding energies due to its peripheral nature. Therefore, in order to have better understanding of ICF dynamics in the framework of all these aspects, experiments have been carried at the Inter-University Accelerator Center (IUAC), New Delhi using Gamma Detector Array (GDA) alongwith Charged Particle Detector Array (CPDA), employing particle gamma-coincidence technique. The target projectile-combinations used in these experiments were; (i) $^{16}O+^{169}Tm$, and (ii) $^{12}C+^{169}Tm$. The beam energies were ≈90 MeV (^{16}O) and ≈55-90 MeV (^{12}C) with beam current ≈3-4pnA. The scattered beam was removed by an Aluminum absorber of appropriate thickness placed in front of each CPD. Fourteen detectors in the CPDA were divided into the three angular rings, *(i)* Forward angle (F) 10°-60°, *(ii)* Sideways (S) 60°-120° and *(iii)* Backward angle (B) 120°-170°. Depending on the fast component of the CPDA signal, proton and α-particles in each angular ring can be identified. Due to the extra absorber thickness required for stopping the scattered beam, only protons and α-particles could be detected in the forward ring. Coincidences were demanded between particles (Z=1,2) and prompt γ-rays. Data analysis has been carried out using INGASORT. Selection of αxn/2αxn-channels in forward, backward and 90° angles were achieved by looking into various gated spectra; however, xn-channels have been identified from the singles data. The main reaction channels that were identified in the forward ring in coincidence with fast α/2α-particles are $^{181-x}Re$ (αxn), $^{180-x}W$ (αpxn), $^{177-x}Ta$ (2αxn) and $^{176-x}Hf$ (2αpxn). The residues which have been identified in backward ring are $^{181-x}Re$ (xn) and $^{184-x}Os$ (pxn). Some xn-channels in $^{185-x}Ir$ (xn) reactions have also been identified from singles spectra.

The spin-distributions of various reaction products populated via CF and ICF dynamics identified from backward-α and forward-α gated spectra have been compared in Fig.1. For better comparison of spin-distributions of various channels in a window, yield of each residue has been normalized with the minimum observed spin at the maximum yield. As can be seen from this figure, the spin-distributions are distinctly different for direct-α/2α-emitting channels as that of fusion-evaporation xn/αxn-channels. It may, however, be pointed out that, the yield for the residues in coincidence with α/2α-particles emitted in forward-direction is almost constant up to J=10-12ħ and then falls with high spin states, indicating the absence of feeding to the lowest members of Yrast-line transitions or the population of lower spin states are strongly hindered in case of ICF. However, in case of residues populated via CF (xn/αxn-channels) reaction, yield is showing a sharp-exponential rise with low spin states, an indication of strong feeding towards the low spin states. It may however be pointed out that spin at half yield for direct-α/2α-channels associated with ICF are found to be ≈13ħ and ≈16ħ, while, spin at half yield for normal-α-channel is found to be ≈10ħ, same as in CF xn-channel. This striking feature of spin-distribution indicates the population of direct-α channels at relatively higher input angular momentum as compared to the fusion-evaporation channel. Several such channels have been compared. On the basis of above results, it can be inferred that, input angular momentum increases with fusion in-completeness [6].

With a view to have clear picture about the strong-feeding in CF and less feeding in ICF reactions, feeding-intensity for each reaction product has been estimated from experimentally measured spin-distributions. As a representative case, feeding intensity distribution for various channels is given in Fig.2. As can be seen from this figure, the feeding intensity shows an exponential rise toward low spin states, revealing strong-feeding towards band head. It may also be pointed out that, for 2α/α-channels (ICF), feeding intensity is shows an exponential rise up to ≈17ħ and ≈15ħ, respectively and then is found to decrease towards low spin states. This may be due to less feeding probability in ICF processes. Data analyses for both the systems have been completed. The results of above analysis have been submitted for publication [6]. It is also proposed to carry out theoretical calculations for explaining the experimental data, and more detailed experiments with other projectile-target combinations at different energies to develop some systematic for ICF reaction dynamics.

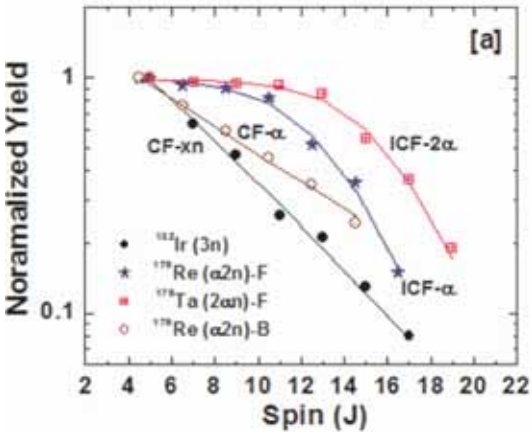

Fig. 1. Typical spin distribution for (i) ^{182}Ir (3n), populated via CF (3n-emission from CN), (ii) ^{179}Re (α2n), populated via direct-a and fusion evaporation a-emitting channels, and (iii) ^{174}Ta (2αn), populated via direct-2α-channel in forward cone

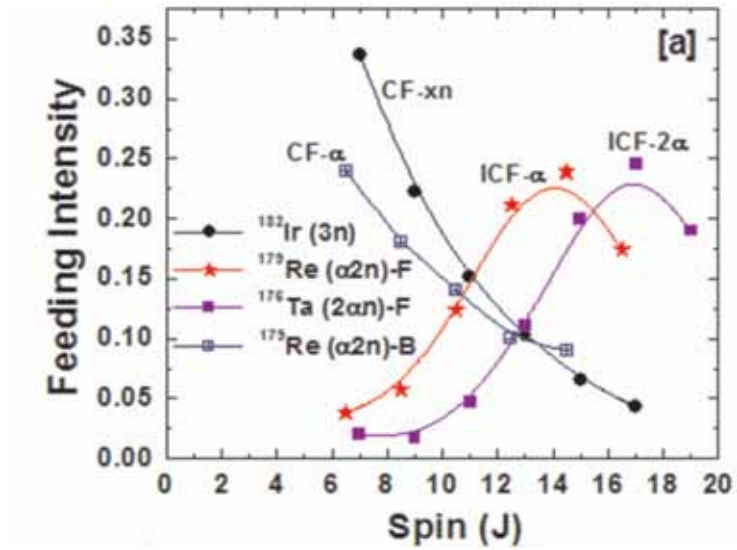

Fig. 2. Typical feeding intensity distribution for (i) ^{182}Ir (3n), populated via CF (3n-emission from CN), (ii) ^{179}Re (α2n), populated via direct-α and fusion evaporation α-emitting channels, and (iii) ^{174}Ta (2αn), populated via direct-2α-channel in forward cone.

(This work is partially supported by University Grant Commission (UGC), New Delhi as an Emeritus Fellowship to one of the authors)

REFERENCES

[1] Pushpendra P. Singh *et al.*, Phys. Rev. C77, 014607 (2008).

[2] H. C. Britt and A. R. Quinton, Phys. Rev. 124, 877 (1961).

[3] T. Inamura *et. al.*, Phys. Lett. B 68, 51 (1977).

[4] Pushpendra P. Singh *et al.*, Euro. Phys. J A34, 29-39 (2007).

[5] Pushpendra P. Singh *et al.*, Nucl. Phys. Symp. V52, 361 (2007).

[6] Pushpendra P. Singh *et al.*, Phys. Rev. C (RAPID) 2008 submitted

5.1.7 Spin Distribution studies of evaporation residues produced through complete and incomplete fusion in the collision of ^{16}O+ ^{160}Gd @ 90 MeV

[1]R. Ali, [1]D. Singh, [1]Dipti Pouchri, [1]M. Afzal Ansari, [1]M.K. Sharma, [1]Unnati,[1] P.P. Singh, [1]D.P.Singh, [3]P.D. Shidling [1]B. P.Singh, [2]Rakesh Kumar, [2]R. P. Singh, [2]S. Murlithar, [1]R. Prasad, [2]R. K. Bhowmik

[1] Department of Physics, Aligarh Muslim University, Aligarh

[2] Inter University Accelerator Centre, Aruna Asaf Ali Marg, New Delhi – 67

[3] Dept. of Physics, Karnatak University, Dharwad

It is now generally recognized that study of heavy ion induced reactions (like fusion, direct reaction, transfer reaction and deep inelastic collision) is of great interest at beam energies well above the Coulomb barrier. Predominant among them are complete and incomplete fusion reaction mechanism. For the mean input angular momentum lying in the range $0< l \leq l_{crit}$, complete fusion is considered to be the dominant mode the reaction. On the other hand, if the mean input angular momentum lies in the range $l_{crit} < l \leq l_{max}$, nuclear field is no longer hold to involve all the nucleonic degrees of freedom as a consequence projectile break-up takes place which leads to incomplete fusion reaction along with projectile like fragments (PLFs) in the forward direction. The PLFs were first observed by Britt and Quinton [1] in the bombardment of in the bombardment of ^{197}Au and ^{209}Bi by ^{12}C, ^{14}N and ^{16}O at energies > 10.5 MeV/nucleon. Advances in the study of CF and ICF reaction took place after the measurement of the spin distribution of evaporation residues produced by ^{14}N-beam on ^{159}Tb-target by Inamura et al. [2] at 6.7 MeV/nucleon energy.

Several models have been proposed to explain the characteristics of ICF viz; SUMRULE model [3], BREAK–UP Fusion (BUF) model [4], PROMPTLY EMITTED PARTICLES (PEP) model [5] etc. The SUMRULE model [3] of Wilczynski et al describes that the ICF reactions occur in the peripheral interactions and localized in the angular momentum space above the critical angular momentum of the complete fusion. The BUF-model of Udgawa and Tamura [4] is based on the distorted wave Born approximation (DWBA), where projectile is supposed to break-up in the field of the target nucleus. One of the fragments of the projectile is assumed to fuse with target nucleus and remaining fragments moves with unchanged velocity in the forward direction.

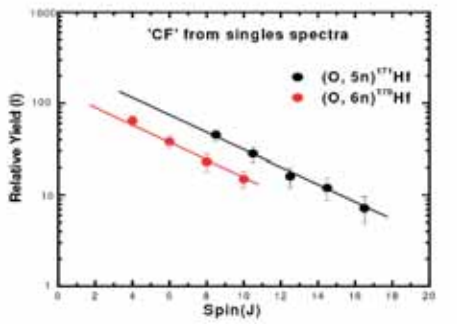

Fig. 1. Spin distribution for Complete Fusion channels

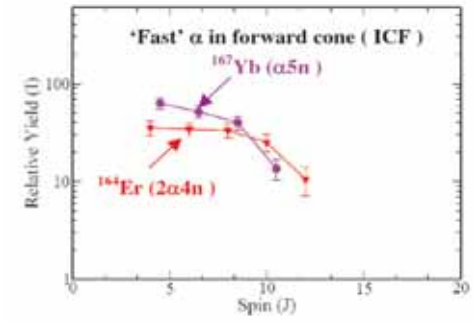

Fig 2. Spin distribution for 'Incomplete Fusion Channels' in coincidence with fast α particles in forward direction

In order to identify the CF and ICF reactions, particle-γ coincidence experiment has been carried out by using Gamma Detector Array (GDA) along with Charge Particle Detector (CPDA) facility at IUAC, New Delhi. The GDA consist of the twelve n-type Germanium detectors at 45°, 99° and 153° with respect to beam direction and fourteen Charged Particle Detector Array (CPDA) housed in small scattering chamber, which is surrounded by Ge-detectors. The CPDA were divided into three annular rings (i) Forward angle (10°-60°) (ii) Sideways angle (60°-120°) (iii) Backward angle (120°-170°), which covers nearly 90% of the total solid angle so that angular distribution of the charged particle in 4π-arrangement can be recorded. The self-supporting rare-earth target ^{160}Gd of thickness about 1.3 mg/cm^2 was mounted at 45° in the scattering chamber with special target holder. The target was bombarded by the ^{16}O-beam with energy 90 MeV. In order to distinguish the CF and ICF, Al-absorber of thickness 100 μm was used in the front of the CPDA-detectors to stop the evaporation α-particle and elastic scattered ^{16}O-beam. The coincidence has been demanded between prompt gamma rays and charger particle (p or α) in forward, 90^0 and backward direction.

Data analysis has been done by using INGASORT and CANDLE software. We have identified fourteen reaction products produced via CF and ICF by looking into various gated spectra. The incomplete fusion reaction products have been identified from 'fast' α particle gated spectra in the forward cone are ^{160}Gd(^{16}O, αxn) Yb, ^{160}Gd(^{16}O, αpxn) Tm, ^{160}Gd(^{16}O, 2α4n)^{164}Er and ^{160}Gd(^{16}O, 2αp4n) Ho. The CF reaction products ^{160}Gd(^{16}O, xn) Hf produced by neutron emission channel have also been identified from singles spectra. The reaction products identified by looking into 'compound' α particle gated spectra in backward cone are expected to follow the CF trend and this has been confirmed by spin distribution pattern for the reactions ^{160}Gd(^{16}O, αxn) Yb, ^{160}Gd(^{16}O, αpxn) Tm and ^{160}Gd(^{16}O, 2α3n)^{165} Er. The spin distribution of the residues produced through CF and ICF have been measured by studying the relative population of the levels in the deformed band to understand the side-feeding effect. Spin distributions i.e. relative yields of the levels of two residues produced as a function of level spins in the collision of ^{16}O + ^{160}Gd is shown in Figs.1and 2. As can be seen form the Fig.1 that relative yields of the neutron channel from singles spectra show exponentially fall with spin indicating hereby that strong side-feeding occurs in the lower members of the yrast line transition and the spin at half-yield for two neutron channels, produced in CF are found to be *7*ħ. On the other hand relative yield of the residue produced in coincidence with α-particles in forward direction shows constant yield at certain value of the spin and afterward exponentially fall with higher spin like complete fusion product is shown in Fig.2. It is observed that there is absence of side feeding to the lower member of the yrast line. Moreover, spin at half yield for ICF products are found to be 9 ħ and 11ħ in α and 2α-channel emission channels respectively. The angular momentum associated with α and 2α emissions in the projectile breakup increases with decreases in linear momentum transferred to the target nucleus, which leads to peripherals collision.

REFERENCES

[1] H.C. Britt and A.R. Quinton, Phys. Rev. 124 (1961) 877.

[2] T. Inamura et al; Phys. Lett. B68, 51(1977).

[3] J. Wilczynski et al Nucl. Phys. A 373, 109 (1982).

[4] T. Udagawa and T. Tamura, Phys. Rev. Lett. 45, 1311 (1980).
[5] J.P. Bondorf et al; Nucl. Phys. A 333, 285 (1980).

5.1.8 Fusion and incomplete fusion studies with heavy targets using ^{16}O beams

Devendra P. Singh[1], Manoj Kumar Sharma[1], Unnati[1], Pushpendra P. Singh[1], Abhishek Yadav[1], B. P. Singh[1], K. S. Golda[2], Rakesh Kumar[2], A. K. Sinha[3] and R. Prasad[1]

[1] Department of Physics, Aligarh Muslim University, Aligarh (UP)-202 002

[2] Inter University Accelerator Centre, Aruna Asaf Ali Marg, New Delhi - 67

[3] UGC-DAE, Consortium for Scientific Research, Kolkata

In recent years, dynamics of complete fusion (CF) and in-complete fusion (ICF) processes in heavy ion (HI) reactions has been a topic of considerable interest [1, 2]. The points of interest are; relative contribution of ICF and CF components at a given energy, their dependence on input energy and the target projectile pair etc. The measurement of excitation functions for the production of reaction residues via CF and ICF processes using off line γ- spectroscopy [2, 3, 4] has often been used. Angular distribution of the residues and their recoil range distributions have also [3, 4, 5] provided information of considerable value. In order to obtain the production cross-sections of the residues populated via CF and ICF processes an alternate method based on the delayed X-ray detection technique may also be used. This method is particularly suited for the residues which decay by electron capture (EC).

In the present work, delayed X-ray detection technique has been used to investigate HI reaction dynamics. A stack having target samples separated by catcher foils was irradiated by the incident ions of interest. After irradiation, target and catcher foils were counted by a HP(Ge) detector. The X-ray spectrum of interest was studied to investigate the evolution of reaction dynamics. By measuring the number of X-rays from various residues, one can follow the time evolution of the activities. From this, and by knowing the absolute intensities of the transitions it is possible to extract the cross-sections for different residues.

Experiment for the $^{16}O+^{181}Ta$ system has been carried out using 15 UD Pelletron accelerator facility of the Inter University Accelerator Centre (IUAC), New Delhi. Spectroscopically pure self-supporting foils of natural Ta were u sed. The thickness of sample foils were measured by α-transmission technique. The measured thicknesses of the ^{181}Ta foils were ≈1.25 mg/cm^2. In between two successive ^{181}Ta samples an Al-catcher of thickness ≈ 1.50 mg/cm^2 was kept which served both as energy degrader as well as catcher foil. Two stacks containing three and one stack containing four ^{181}Ta samples were irradiated with a $^{16}O^{7+}$ beam at H ≈ 88, 98 and 100 MeV, respectively. Keeping in mind the half-lives of interest, the irradiations were performed for ≈ 8h duration each, in the general purpose scattering chamber (GPSC) of 1.5 meter diameter, having in-vacuum transfer facility. For the detection of X-rays, a HP(Ge) detector with high gain option was used. The activities induced in various samples were recorded by counting the target and catcher foils together

using HPGe γ-ray spectrometer coupled to a CAMAC based FREEDOM software. The HPGe detector was pre-calibrated both for energy and efficiency employing various standard sources. The X-ray lines of interest were in the energy range of 55 to 73 keV. A typical X-ray spectra of ^{181}Ta bombarded by 100 MeV ^{16}O is shown in Figure 1.

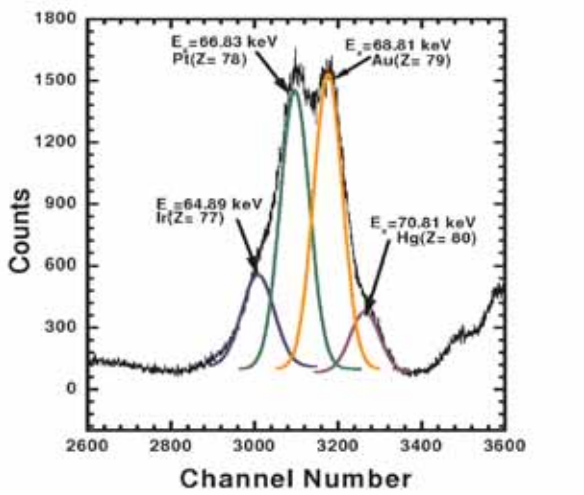

Fig.1. X-ray spectrum observed in the decay of reaction products in 16O+181Ta reaction

From the decay curves the residues ^{193}Pt, ^{195}Au, ^{195}Hg and ^{195,197}Tl have been identified. All the above residues decay predominantly by EC respectively to ^{193}Ir, ^{195}Pt, ^{195}Au and ^{195,197}Hg. It may however be noted that from the X-ray spectra there is no isotopic selection as X-rays emitted by different isotopes of a given element gave a cumulative peak. In order to separate the contribution of various isotopes, the observed X-ray spectrum has been fitted by Gaussian peaks and the X-ray intensity of the peak has been plotted as a function of time. The analysis of the decay curve gave the contribution of individual channels. Further, in order to have the complementary analysis, EF's for several reactions have also been measured using the intensity of the characteristic γ-lines. The γ-ray analysis has indicated a significant contribution of ICF process in some α-emission channels. In order to obtain the relative contribution of CF and ICF channels experiment for recoil range distribution (RRD) has also been carried out at 100, 94, and 85 MeV energies. The analysis of the data is in process.

(The project is partially supported by UGC-Emeritus Fellowship)

REFERENCES

[1] P. R. S. Gomes et. al., Phys. Rev. C73, 064606(2006).

[2] Manoj Kumar Sharma et al., Nuclear Physics A774-4, 83(2006).

[3] Manoj Kumar Sharma et al., Phys. Rev. C75, 064608(2007).

[4] Manoj Kumar Sharma et al., Phys. Rev. C70, 044606(2004).

[5] Pushpendra P. Singh et al., Euro. Phys. J. A34, 29(2007).

5.2 MATERIALS SCIENCE

There have been a large number of experiments in materials science with energetic ion beams, on various types of materials such as polymers, metals, semiconductors, oxide materials, magnetic materials etc. The problems related to electronic sputtering, ion beam mixing, nanostructuring of the materials, surface modifications, materials modifications, ion beam induced epitaxial crystallization etc. were investigated.

On-line ERDA using large area position sensitive detector was used for a study on the electronic sputtering dependence on the strain in LiF thin films. The observations were qualitatively explained by thermal spike model assumptions. The ion beam mixing experiments in Ti/Si, Fe/Bi and metal/polymer, Ni_3N/Si systems were performed. From the ion beam mixing experiments performed at IUAC this year and previous years, it appears that ion beam mixing occurs if the ion beam creates track in one of the two systems/layers. However, if the heat of mixing of the system is not favorable, the ion beam mixing does not take place even if both the components of the bi-layer have track creation by ion-beam as observed in Fe/Bi case.

Formation of Ge nanocrystals in SHI irradiated Ge atom embedded in silica matrix was observed. The amorphous TiO_2 film was shown to get transformed to nanocrystalline as a result of swift heavy ion irradiation. Phase transformation from amorphous TiO_2 to a mixed rutile and anatase phase was observed by ion irradiation. The nanostructures appears at the surface of semiconducting oxide thin film of SnO_2 after swift heavy ion irradiation. There were indications of elongation of ZnS nanoparticles by high energy heavy ion irradiation. The signature of nanoscale magnetic domains was noticed in the swift heavy ion irradiated GeO_x thin film. The role of microstructure of CdTe thin film was studied for the swift heavy ion beam induced modifications. The defect creation as well as the defect annealing were observed (by ion irradiation) depending on the initial microstructure of the film.

SHI induced modifications were studied in NiO, doped NiO thin films, Al_2O_3, YBCO, Zinc ferrite nanoparticles, silica glass, borosilicate glass, metal polymer nanocomposite, polypropylene, polyethylene tetraphelate (PET) etc. Free volume studies by positron annihilation technique were performed in pristine and irradiated conducting poly ethylene oxide polymers. Li ion irradiation was shown to create holes in a ten micrometer thick polycarbonate film on Au deposited GaAS substrate, without any chemical etching. A large number of experiments on the straggling and energy loss measurements were performed in mylar, polypropylene, polycarbonate and kapton. The electrical characterization studies of the pristine and irradiated high speed NPN power transitions were carried out. Deep level defects were studied in the ion irradiated bipolar junction transistors. The electronic circuits for devices in spacecraft were tested for radiation damage, to stimulate the space radiation.

5.2.1 An Evidence of Strain Induced Increase in Electronic Sputtering Yield of LiF Thin Films

Manvendra Kumar[1], A. C. Pandey[1], S. K. Srivastava[2], S. A. Khan[3] and D. K. Avasthi[3]

[1]Department of Physics, University of Allahabad, Allahabad 211 002

[2]Department of Physics and Meteorology, IIT, Kharagpur-721 302

[3]Inter-University Accelerator Centre, Post Box -10502, New Delhi - 67

The electronic sputtering from LiF thin films as a function of film thickness (10-265 nm thick) and grain size (10-34 nm) is investigated using 120 MeV Ag^{25+} ions in equilibrium charge state as projectiles. The observed sputtering yield is ~ 10^6 atoms/ion. A reduction in sputter yield is observed with increasing thickness/grain size [1-2] as shown in figure 1. Smaller grain size and lower thickness of the films restrict the motion of excited electrons (i.e. reduction in mean diffusion length) resulting in better confinement of the deposited energy, which finally enhances the temperature and duration of temperature spike, resulting in higher sputtering yield. Numerical calculation of the expected common sputtering yield for thickest film under normal ion incidence has been performed using the thermal spike code [1]. The calculated value (~7000 atoms/ion) is less than 1/3rd even of the minimum observed sputtering yield (for the thickest film) i.e. a discrepancy is observed in the experimental and simulated sputtering yields. The rapid increase of the yield with decreasing film thickness, however, still remains subtle.

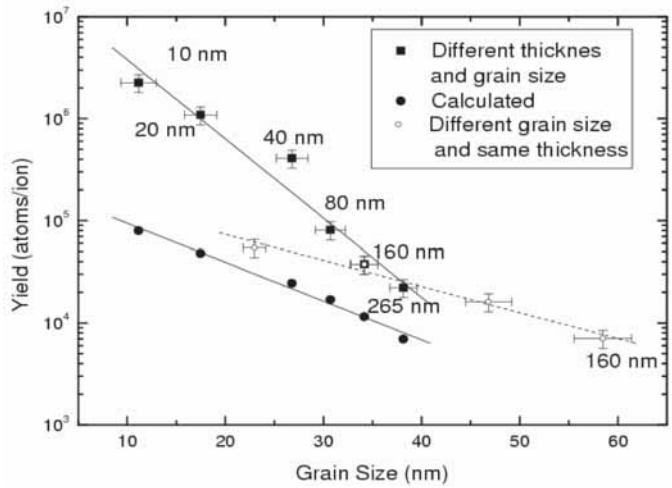

Fig. 1. Experimental and calculated sputter yields

These lattice imperfections induce strain in the lattice since the relative atomic positions related to the imperfections are different from the crystal lattice parameter. The strain present in each film is calculated and it is clearly evident that the strain (the amount of crystal imperfection) in the as-deposited films themselves increases rapidly with decreasing thickness (figure 2). The crystal imperfections must also reveal themselves as an increase in the electrical resistivity of the films. It was observed that the resistivity of the film increases with reduction in the film thickness. Interesting

results were obtained when natural logarithm of the measured resistivity was plotted with the calculated strain, which showed a linearly increasing trend of (ln ρ. with ε, as expected as shown in inset (a) of figure 2.

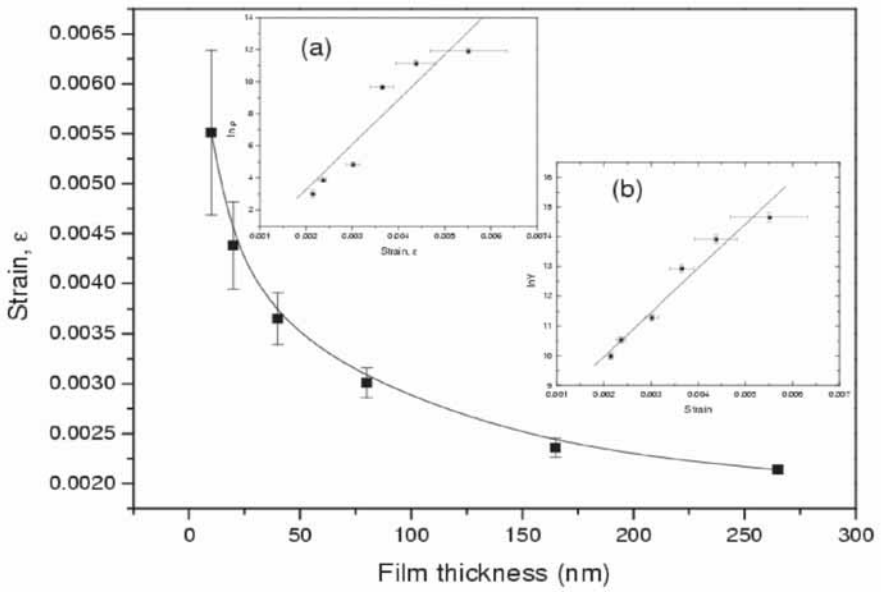

Fig. 2. Increase in strain with reduction in film thickness. Inset (a) shows variation of (ln ρ) with strain, while inset (b) shows linear increase in logarithm of sputtering yield with strain

The XRD and resistivity results, thus, verify that the as-deposited films inherit lattice imperfections; the imperfections increase with decreasing thickness. These lattice imperfections are also responsible for the reduction of λ which in turn, enhances the sputtering yield. A part of the difference between the calculated yield for a perfect crystal and the experimental yield even for the thickest film, thus, arises from the (small) strain possessed by the film. At this point, it is quite intriguing to see how the experimental sputtering yield varies with the calculated strain. The natural log of the yield is, therefore, plotted against the strain, and it turns out to follow a straight line, i.e., the sputtering yield increases exponentially with increasing lattice strain/crystal imperfections as shown in inset (b) of figure 2.

REFERENCES

[1] Manvendra Kumar et al., J. Appl. Phys. 102 (2007) 083510.

[2] M. Kumar et al., Nucl. Instrum. and Methods B 256 (2007) 328.

5.2.2 Study of swift heavy ion induced mixing Ti/Si using X-ray standing waves

Parasmani Rajput[1], Ajay Gupta[1], Vasant Sathe[1], and D. K. Avasthi[2]

[1]UGC-DAE Consortium for Scientific Research, Indore, 452 017
[2]Inter-University Accelerator Centre, Aruna Asaf Ali Marg, New Delhi - 67

High-energy heavy-ion beams are well established as powerful tool for modifying the surface and interfaces at nanometer scale. X-ray fluorescence measurement under standing wave condition has been shown to be a powerful technique for elemental depth profiling. The depth resolution of the technique can be further improved by making use of x-ray waveguide structure [1,2]. In the present work, we have used x-ray waveguide in order to study swift heavy ion induced intermixing in Si/Ti/Si tri-layer with different thicknesses of Ti layer.

Two multilayers having structure: substrate (float glass)/ Pt (50 nm)/Si (15.4 nm)/Ti (2 nm)/Ti (9.0 nm)/Pt (3.5 nm), designated as Ti2, and substrate (float glass)/ Pt (50 nm)/Si (14.7 nm)/ Ti (5.8 nm)/ Si (8.7 nm)/Pt (3 nm), designated as Ti6, have been prepared using ion beam sputtering. Two Pt layers form the walls of the planar waveguide, while the tri-layer Si/Ti/Si forms the cavity of the planar waveguide. Waveguide modes can be excited in the cavity, whenever the following condition is satisfied, i.e. $D = n\lambda/2 \sin\theta$, where θ is the wavelength of the x-rays, θ is the angle of incidence of the x-rays, D is the thickness of the waveguide cavity, and n is the order of the mode. X-ray reflectivity and x-ray fluorescence measurements were done using Bruker AXS D8 Discover diffractometer using Cu K_α radiation. Reflected x-rays were collected using a scintillation detector, while the Ti fluorescence from the sample was measured using an Amptek XR100T PIN diode detector (with an energy resolution of 250 eV) kept vertically above the sample. Raman measurements were performed on a Horiba JY HR800 micro-Raman system using an 488 nm Argon laser as an excitation source and a CCD detector. Samples were irradiated with 120 MeV Au^{7+} ions to fluences of 1×10^{13} and 2×10^{13} ions cm^{-2} using the 15UD Pelletron at Inter-University Accelerator Centre , New Delhi, India.

Figure 1 shows the x-ray reflectivity and Ti fluorescence of Ti2 and Ti6 pristine sample as well as irradiated samples to a fluences of 1×10^{13} ions /cm^2 as a function of scattering vector $q = 4\pi \sin\theta/\lambda$, θ being the scattering angle, λ being the wavelength of the radiation. Sharp dips in the x-ray reflectivity pattern below the critical angle for total reflection from the Pt, signals the excitation of waveguide modes. At the corresponding q values Ti fluorescence exhibits well defined peaks due to resonance enhancement of x-ray intensity inside the cavity whenever a waveguide mode is excited. Figure 2 gives the normalized Raman spectra of Ti2 and Ti6 pristine and irradiated films in the spectral range 100–700 cm^{-1}. In Raman spectra, the broad peak comes at 465 cm^{-1} due to amorphous Si in the pristine samples of Ti2 and Ti6. With increasing irradiation fluence, the height of the Si peak at 465 cm^{-1} keeps on decreasing, indicating intermixing of Si with Ti. The concentration profile of the Ti marker layer in Ti2 and Ti6 pristine as well as irradiated samples as obtained from the fitting of the x-ray reflectivity and fluorescence data are shown in fig. 3. One may note that in both the cases the concentration profile gets broadened as a result of irradiation. In the case of 2nm thick Ti layer intermixing is stronger as compared to 6nm Ti film, which can be understood in terms of a stronger confinement of the dissipated energy in the Ti layer due to increased interface scattering of δ-electrons in the case of 2nm thick Ti layer. In 6nm thick Ti layer, intermixing is asymmetric at the two interfaces, which may be due to a possible asymmetry in the interface structure in the as deposited film itself.

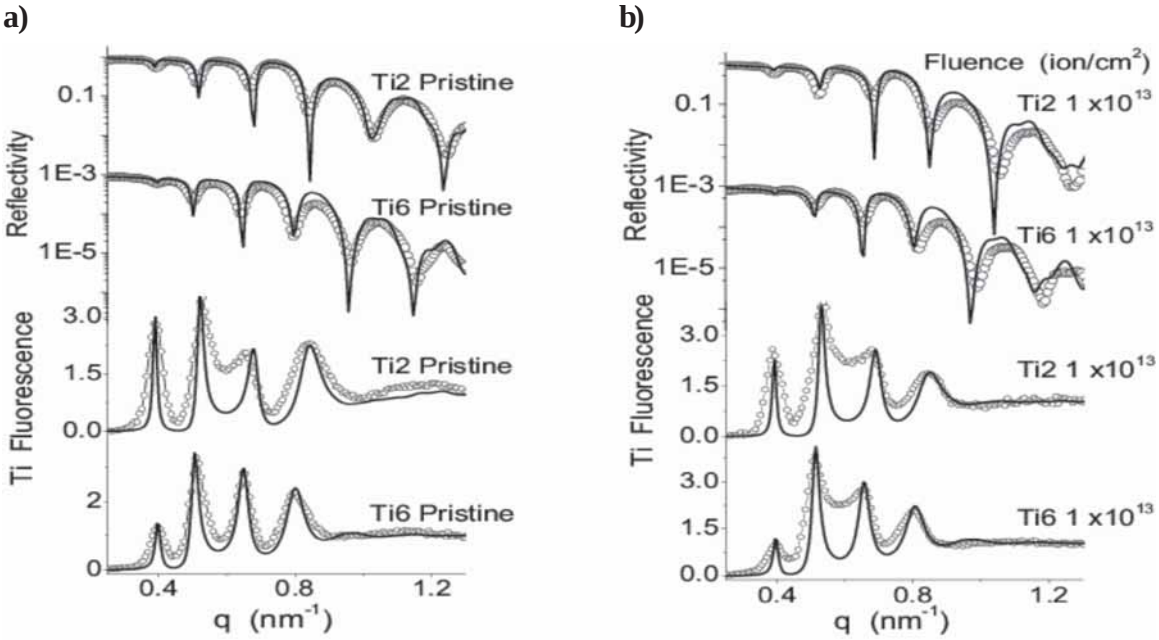

Fig. 1. X-ray reflectivity and Ti fluorescence of Ti2 and Ti6 a) pristine samples b) after an irradiation fluence of 1x10^{13} ions/cm^2 as a function of scattering vector q

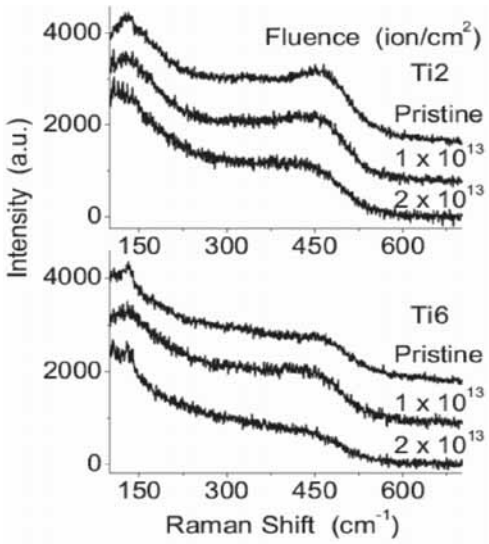

Fig. 2. Raman spectra of Ti2 and Ti6 pristine and irradiated samples

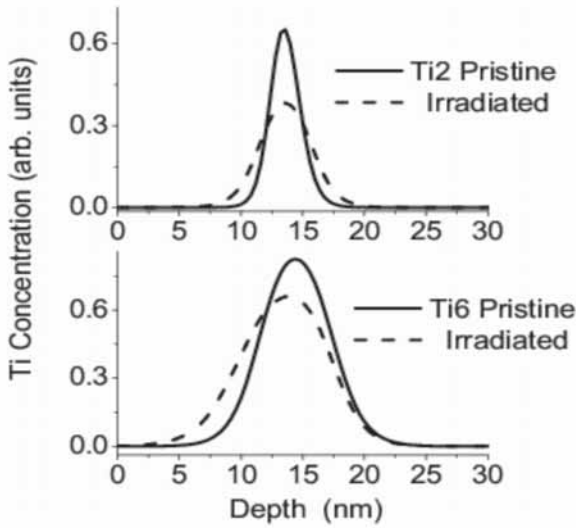

Fig. 3. The concentration profile of the Ti marker layer in pristine as well as irradiated samples, as obtained from simultaneous fitting of the x-ray reflectivity and fluorescence data

REFERENCES

[1] A. Gupta, P. Rajput, A. Saraiya, V. R. Reddy, M. Gupta, S. Bernstorff, and H. Amenitsch, Phys. Rev. B 72 (2005) 075436.

[2] P. Rajput, A. Gupta, V. R. Reddy, V. Sathe, D. K. Avasthi, J. Phys.: Condens. Matter 19 (2007) 036221.

5.2.3 Smoothening, Roughening and Sputtering: The Complex Evolution of Immiscible Fe/Bi Bilayer System

A. Gupta[1], S. Kumar[2], D. C. Agarwal[1], S. A.Khan[3], A.Tripathi[3], D. Kabiraj[3], S. Mohapatra[3], T. Som[4], D. K. Avasthi[3] and R. S. Chauhan[1]

[1]Department of Physics, R. B. S. College, Agra, 282 002

[2]Department of ASH (Physics), CITM, Aravali Hills, Sector-43, Faridabad

[3]Inter-University Accelerator Centre, Post Box-10502, New Delhi - 67

[4]Institute of Physics, Sachivalaya Marg, Bhubaneswar, 751005

The formation of non equilibrium solid phases, including amorphous and metastable crystalline phases, in binary metal systems with negative heat of mixing ($\Delta H_{mix}<0$) by ion beam mixing and solid state reaction of multiple metal layers, has been extensively studied over the last two decades by experiments as well as by theoretical approaches based on the thermodynamics of solid and growth kinetics [1,2]. In contrast, the formation mechanism of various metastable phases in the system with positive heat of mixing ($\Delta H_{mix}>0$) has not been thoroughly studied and is not yet well understood [3]. To the best of our knowledge, the immiscible Fe/Bi bilayer system has not been studied previously by swift heavy ions (SHI). Therefore, it is of interest to investigate the possibility of mixing in immiscible bilayer system by SHI. In this work, we present the first experimental evidence of surface smoothening, roughening and sputtering of immiscible Fe/Bi bilayer system by swift heavy ion irradiation SHI.

A typical RBS spectrum of pristine and irradiated Fe/Bi bilayer samples at different fluences is shown in Fig.1. A detailed analysis showed that the Bi peak in pristine sample could not be fitted accurately because of large tail, which could be attributed either to the interface roughness or to the asymmetric granular nature of the Bi film. In fact, RBS spectra of the pristine sample exhibited a long tail at the low energy edge of the Bi peak, which indicates an extreme roughness with a non-Gaussian height distribution. RBS analysis revealed that steepness of the low energy edge of the Bi signal increases at the fluence of 3×10^{13} ions cm^{-2} and beyond this fluence slope of rear edge increases with fluence. The increased steepness is due to smoothening induced at low fluence, however, the increase in rear edge beyond 3×10^{13} ions cm^{-2} fluence shows broadening in lower energy edge of Bi. The broadening at higher fluences may be the result of interface mixing, surface roughening and/or the effect of both. To confirm this we characterized our samples by AFM. We have extracted the value of surface roughness using AFM and investigated the effect of surface roughening on interface broadening in RBS spectra.

The results obtained in the present work from RBS and AFM analysis of Fe/Bi bilayers strongly support this interpretation. As mentioned in the literature [4], the broadening obtained from RBS measurements, $\Delta\sigma^2_{RBS}$ may contain two contributions: Interface mixing and surface roughening. When comparing the quantities $\Delta\sigma^2_{RBS}$ and $\Delta\sigma^2_{AFM}$ obtained for Au-irradiated Fe/Bi bilayers, it turns out that the broadening observed with RBS is to a large extent due to an increasing

surface roughness, The difference $\Delta\sigma^2_{RBS} - \Delta\sigma^2_{AFM}$ can be regarded as a direct measure of the interface mixing or surface roughening effect and is plotted in Fig. 2 versus fluence. It is clear from Fig. 2 that interface broadening in the RBS spectra is due to the surface roughening induced by ion beam.

In essence, we have investigated SHI irradiation effects: surface smoothening, roughening and sputtering in case of immiscible Fe/Bi bilayer system. We didn't observe any mixing in this system, although Fe and Bi are both known to be sensitive to high electronic energy deposition by SHI. We conclude from RBS and AFM results that SHI irradiation induced the surface smoothening, roughening and sputtering instead of mixing. This can be explained on the basis of positive heat of mixing which prevent the interdiffusion across the interface during the transient thermal spike.

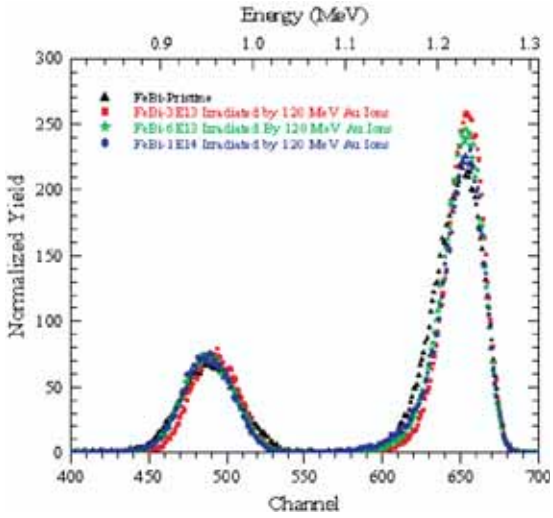

Fig. 1. RBS spectra of Fe/Bi film on Si (100) substrate after being irradiated with 120 MeV Au ions of different fluences at RT and inset is showing the variance σ^2 of the depth profiles and interface broadening $\Delta\sigma^2$extracted from the RBS data versus the fluence

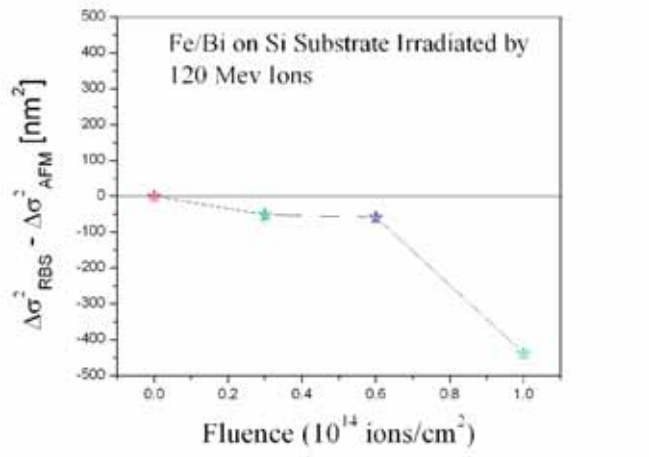

Fig.2. Variation of effective mixing ($\Delta\sigma^2_{RBS} = \Delta\sigma^2_{d} + \Delta\sigma^2_{mix}$) versus ion fluence using 120 MeVAu ions

REFERENCES

[1] Z. G. Wang, C. Dufour, S. Euphrasie, M. Toulemonde, Nucl. Instr. and Meth. B. 209, 194 (2003)

[2] Ajay Gupta, Suneel Pandita, D. K. Avasthi, G. S. Lodha, R. V. Nandedkar, Nucl. Instr. and Meth. B. 144, 265 (1998)

[3] J. Teillet, F. Richomme and A. Finidiki, Phys. Rev. B 55, 11560 (1997).

[4] A. Crespo-Soa. P. Schaaf, W. Bolse, K-P. Lieb, M. Gimbel, U. Geyer, C. Tosello, Phys. Rev. B 53 14795 (1996).

5.2.4 Swift Heavy ion induced modifications in Metal/polymer system

Jai Prakash[1], A. Tripathi[4], S. A. Khan[4], P. Kulriya[4], F. Singh[4], Sarvesh Kumar[2],V. K. Mittal[3], D.K Avasthi[4] and Jalaj Tripathi[1]

[1]Department of Chemistry, M.M.H (P.G) College, Ghaziabad –201 001

[2]Department of ASH (Physics), CITM, Aravali Hill, Sector-43, Faridabad-121 001

[3]Department of Physics , Punjabi University, Patiala-147 002

[4]Inter-University Accelerator Center, Aruna Asaf Ali Marg, New Delhi - 67

Ion beam mixing is a versatile method to prepare novel compounds/phases that are unattainable by conventional methods. The study of metal/polymer interface is interesting not only from fundamental point of view, it also plays a vital role in applications such as synthesis of metallized polymers. Metallized polymers are used in various technologies for a wide range of applications [1,2]. It has been shown that using SHI, mixing at metal/polymer interface can be achieved which improves the adhesion [3]. The present investigation primarily deals with the ion induced sputtering in Ni/PET system using on-line Elastic Recoil Detection Analysis (ERDA). To study the changes in the polymer structure and phase formation at the interface XRD study has been performed. Further investigations are going on to study interface mixing and adhesion. Commercially available (from Good Fellow, Cambridge Ltd., England) PET film of thickness 0.35 mm (1x1 cm^2) was used as a substrate. 100nm thin Ni layer was deposited on these using electron beam evaporation technique in UHV chamber (~10^{-7} torr) with a deposition rate of 0.4-0.5 Å/s. Samples were irradiated with 80 MeV Br ions and 100 MeV Ag ions were used for online ERDA at IUAC, New Delhi. Sample was tilted at an angle of 20° with respect to the beam direction and the recoils generated ion beam were recorded at an angle of 45°. Irradiated samples were characterized by X-ray diffraction (XRD) technique with Cu K_α radiation (λ = 1.54 Å) using Brucker D8 advance X-ray diffractometer in the scan range of 2q between 20° to 50° with a scan speed of 1 deg./min.

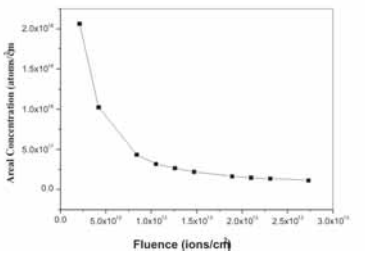

Fig.1. Areal concentration of Ni film vs fluence

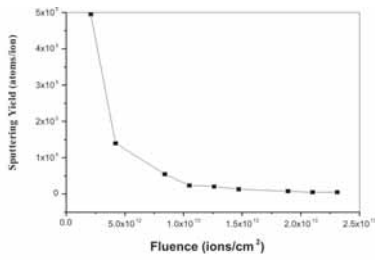

Fig.2. Sputtering yield vs ion fluence

From on-line ERDA, a consistent reduction in areal concentration (N_c) of Ni has been observed with increase in ion fluence which indicates sputtering of Ni film. The areal concentrations were determined from the counts, *y*, of the recoil spectra using formula [4]

$$N_c = \frac{y \sin\alpha}{N_p (\partial\sigma / \partial\Omega)\Omega}$$

where N_p is the number of incident ions, Ω ($5x10^{-3}$msr) is the solid angle subtended by detector, $\alpha = 20^{\circ}$ is the tilt angle of the sample surface to the beam direction and ($\partial\sigma/\partial\Omega$is the recoil cross section. The reduction of areal concentration of Ni versus ion fluence is plotted in Fig.1 Sputtering yield is determined from the difference in areal concentration at two consequent fluences divided by the corresponding difference in the fluences. Fig.2 shows the plot of sputtering yield versus ion fluence. It shows that the sputtering yield decreases with increasing ion fluence. The sputtering yield is of the order of 10^5 atoms/ion upto the fluence ~$8x10^{12}$ ions/cm^2. Thereafter it has negligible variation with fluence. Similar behavior has been reported in case of polymers [5] where hydrogen loss cross-section has different values at either side of over-lapping fluence.

REFERENCES

[1] G. N. Tew, J. Am. Chem. Soc. 128 (2006) 3104.

[2] S. Shongtong, G. S. Ferguson, J. Am. Chem. Soc. 124 (2002) 7254.

[3] D. M. Ruck, Nucl. Instr. and Meth. B 166-187 (2000) 602.

[4] D. P. Gupta et al., Radiation effect and defect in solids 161 (2006) 331.

[5] V. K. Mittal, Radiation effect and defect in solids (1999)

5.2.5 Au irradiation at Ni_3N/Si bilayers: Surface roughening and interface mixing

Renu Dhunna[1], Chhagan Lal[1], V.Ganesan[2] and I.P. Jain[1]

[1] Centre for Non-Conventional Energy Resources, University of Rajasthan, Jaipur

[2] UGC- DAE Consortium of Scientific Research, University Campus, Indore.

Ion beam mixing [1-4] in elemental metal/metal and metal/semiconductor bilayers and multilayer systems has been investigated in order to understand the ion induced atom transport processes and the formation of intermetallic phases at the interface. The relative importance of various mixing mechanisms such as ballistic mixing, thermal spike mixing and radiation-enhanced diffusion, has been established. The transition between these various scenarios concerning the ion parameters (mass, energy and fluence) and thermodynamic properties and temperature of the samples are being debated.

Binary nitrides are an interesting set of compounds that display a wide range of properties such as thermal stability or electrical conductivity. Technologically important compounds are BN,

AlN, Si_3N_4, WN, TiN and NbN, which have been well characterized. On the other hand, less known but potentially important a number of covalent metal nitrides of limited thermal stability are Sn_3N_4, Cu_3N and Ni_3N. These nitrides decompose into the elements, thus suggesting possible uses in metallization reactions, which could be of importance for the electronic industry. Sputtering at low deposition rate and power density can generate crystalline nitrides of tin, copper and nickel. In the present work a more comprehensive study of Ni_3N/Si bilayers irradiated with Au ions was designed to combine analytical methods sensitive to surface roughness and phase formation.

The irradiation effects in Ni_3N/Si bilayers induced by 100 MeV Au ions using 15 UD Pelletron Accelerator at IUAC, New Delhi at fluences up to $1.5x10^{14}$ ions/cm^2 were investigated at room temperature. To investigate the mixing process in more detail, a bilayers system was formed by 90 nm of Ni_3N on Si (110). The deposition was made by Ion beam sputtering at vacuum $1.2x10^{-4}$ Torr at IUC, Indore.

GIXRD measurements were performed using CuKα (λ=1.54060 Å) radiation and irradiation effect on the surface morphology of the Ni_3N/Si was been undertaken with the help of Atomic Force Microscope in contact mode in IUC, Indore. The observed dissociation and preferential sputtering of Ni_3N followed by nitrogen out-diffusion were related to small binding energy of this compound. The diffraction pattern of the pristine Ni_3N/Si bilayers system and giving separate crystalline peaks corresponding to Ni_3N (111), (300) and (113), which shows the hexagonal structure of Ni_3N. At $1.5x10^{-14}$ ion fluences of Au ions, the formation of $NiSi_2$ and Si_3N_4 phases at the interface was found.

Morphological changes of surface during irradiation have been investigated by AFM in contact mode. Scan various sizes from 1x1 μm^2 were recorded on pristine and irradiated samples, and were found to be 0.34 nm and 1.8 nm respectively.

REFERENCES

[1] W. Bolse, Mater. Sci. Eng., R. 12, 53 (1994)[OpenURL]; Mater. Sci. Eng., A A253, 194 (1998).

[2] J. Desimoni and A. Traverse, Phys. Rev. B 48, 13 266 (1993).

[3] S. Dhar, Y. N. Mohapatra, and V. N. Kulkarni, Phys. Rev. B 54, 5769 (1996).

[4] Nastasi and J. W. Mayer, Mater. Sci. Eng., R. 12, 1 (1994).

5.2.6 Cross-sectional TEM study of ion beam synthesized SiC

Y.S. Katharria[1], Sandeep Kumar[1], J. Ghatak[2], Umananda[2], P. V. Satyam[2] and D. Kanjilal[1]

[1]Inter-University Accelerator Centre, Aruna Asaf Ali Marg, New Delhi - 67
[2]Institute of Physics, Sachivalaya Marg, Bhubaneswar-751 005, India

The buried continuous β-SiC layers are promising candidates for application in microelectronics. Self-standing stable β-SiC membranes may be obtained using a selective Si

etching step. These surface layers could also be used as seeds for growing β-SiC on Si using other techniques such as chemical vapor deposition, molecular beam epitaxy etc. Ion beam induced epitaxial crystallization (IBIEC) is known to result in defect free crystalline layers from initial amorphous layers in Si at temperature far below than that required for its solid-phase epitaxial growth. The requirement of very high temperature (~800°C) as reported in [1] to initiate crystallization of SiC in C implanted Si still makes the process of IBIEC speculative and further studies employing lower temperatures are highly desired. In the present study, we used 110 MeV Ni ions irradiation at 350°C to look for IBIEC effect in C implanted Si. Si (100) substrates were implanted at room temperature with 100 keV C^+ ions to an ion fluence (f) of $6\times10^{17}cm^{-2}$. One of the implanted samples was annealed at 1000°C for 2 hrs under ($Ar+H_2$) environment.

Fig.1 shows the XTEM images of C implanted Si (100) samples after annealing at 1000 °C. Implantation of 100 keV C^+ ions results in amorphization of Si up to the end of the range (EoR) lying at a depth ~475 nm. When the samples are annealed, the thickness of amorphous (a-) layer decreases to ~350 nm indicating the recrystallization of Si, which start at the amorphous-to-crystalline Si interface. A thick silicon oxide layer of 65 nm thickness was formed during annealing due to the oxygen impurity in the $Ar+H_2$ gas. As shown in Fig.1(a), a five-layer structure consisting of top oxide layer followed by a-Si, β-SiC, a-Si and the base Si layers is formed after annealing. The interface between oxide and Si layer below it is shown in Fig.1(b). The formation of β-SiC precipitates is also confirmed by some other studies [2]. These SiC precipitates do not occur with a well-defined shape. A lattice image of one such β-SiC precipitate is shown in Fig.1(c). The lattice spacing of 2.19 Å found for these precipitates matches closely with spacing (2.18 Å) of (200) planes of β-SiC. Another plane of these precipitates that could be seen is (111) plane having a lattice spacing of 2.51 Å. The SiC precipitates are surrounded by a-Si as could be seen from Fig.1(c). The transformation of crystalline (c-) Si in SiC could be regarded as a topotactic transformation. An almost 20% lattice mismatch between β-SiC (lattice constant=4.36 Å) and Si (5.43 Å) leads to a high interfacial energy, resulting usually in a defects rich SiC/Si interface. Conversion of a given volume of Si in β-SiC does not involve a large change in Si atomic density $r_{Si,}$ as Si density in β-SiC is only 3.4 % less than r_{Si} in Si. Therefore, it is mainly the addition of sufficient number of C atoms accompanied emission of Si self-interstitials and rearrangement of atoms during annealing, which is required for SiC formation. Thermal annealing above 600 °C also tends to recrystallize Si layer damaged by C^+ ions. However, a complete recovery of C implanted Si lattice is achieved only at annealing temperatures of ~1200 °C for sufficient durations. At lower temperatures, a high density of defects is usually seen near the EoR. Some of these defects such as missing planes, twin boundaries, and dislocations which are formed, could be clearly seen from Fig.1(d).

In an attempt to observe IBIEC in high dose C implanted Si at relatively low temperatures, SHI irradiation with 110 MeV Ni ions at 350 °C was performed. However, ion irradiation at 350°C does not result in any significant structural change, suggesting the ineffectiveness of ion irradiation in crystallizing SiC from a solid solution of Si and C up to 350°C. The process of IBIEC is explained mainly on the basis of thermal spike model of ion energy loss inside a material. During ion passage, a molted zone is created along ion path due to the energy transfer of the ion to the material and electron-phonon coupling of the material. The strength of this energy transfer depends

primarily on electron-phonon coupling constant. Though this constant is expected to increase in ion amorphized Si, a huge increase in Si melting point due to C incorporation may be one of the possible reason for the ineffectiveness of Ni ion irradiation in IBIEC of C implanted Si in present study. A similar behavior of C implanted layer in Si under ion irradiation is also shown in our earlier report [3].

In summary, MeV ion irradiation could not be used as an effective tool to recrystallize

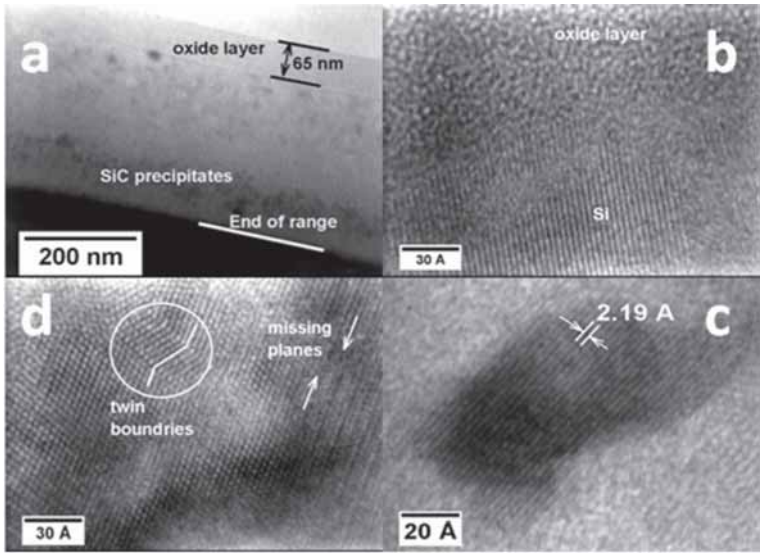

Fig.1: XTEM images of 100 keV C^+ implanted Si; (a) after annealing treatment at 1000°C, (b) SiO_2-Si interface, (c) β-SiC crystallite, and (d) defected Si lattice near EoR of C ions.

buried SiC layers formed by C implantation in Si upto an irradiation temperature of 350°C, Further studies utilizing higher substrate temperature could be useful and are, therefore, required to be done.

REFERENCES

[1] S. Intarasiri et al., J. Appl. Phys. 101, 084311 (2007).

[2] Y. S. Katharria, et al., J. Phys. D: Appl. Phys. 39, 3969 (2006).

[3] Y. S. Katharria et al., Nucl. Instrum. Meth. B 260, 563 (2007).

5.2.7 Elastic recoil detection analysis of as deposited and rapid thermal annealed SiN_x:H Films

Sarab Preet Singh[1], P. Srivastava[1], S. Ghosh[1], S A Khan[2]

[1] Department of Physics, IIT Delhi, Hauz Khas, New Delhi – 110016
[2] Inter- University Accelerator Centre, Aruna Asaf Ali Marg, New Delhi - 67

Silicon nitride (SiN_x) and silicon oxynitride (SiN_xO_y) thin films owing to their widely tunable properties are used in various microelectronics related applications. Generally, these films are deposited by different chemical vapor deposition (CVD) techniques in which silane (SiH_4) and ammonia (NH_3) are used as precursor gases. Therefore, the incorporation of hydrogen is an inherent feature of the resulting films causing thermal instability in physical and electrical properties [1, 2], which can be overcome by post deposition annealing. In addition to this, hydrogen is deliberately introduced in Si- solar cell by post deposition annealing to passivate defect and thereby increase the minority carrier lifetime [3]. Various attempts [4, 5] have been made to examine the post annealing effects on these films. Presence of hydrogen is detrimental or useful from the device point of view is still inconclusive. It is therefore necessary to study the content of hydrogen or its distribution in the silicon nitride films (both as deposited and annealed) by a sensitive technique such as Elastic Recoil Detection Analysis (ERDA).

Hydrogenated amorphous silicon nitride films (a-SiN_x:H) were deposited by Photo-CVD on n-type <100> silicon wafer using silane (2% in argon) and ammonia as reactant gases. The details and the basic Photo-CVD reaction sequence are described elsewhere [6]. Flow rate ratio 'R' (SiH_4/NH_3) was varied in order to deposit films with different hydrogen content. The refractive index 'n' and thickness 't' of the films were measured at 6328Å using ellipsometer. Rapid thermal annealing (RTA) was done in nitrogen ambient at 945 ^oC for 10sec. The ERDA measurements have been carried out with 100MeV Ag^{7+} beam at Inter-University Accelerator Centre, New Delhi. The samples were mounted on metal ladder in a scattering chamber, which was evacuated with a ion pump based pumping system to achieve a pressure of 4.5×10^{-6} mbar. A collimated beam of silver ions with a spot size of 1×1 mm^2 was made incident on the as deposited and RTA samples. The tilt angle of the samples with respect to the beam direction was kept 20^o. The hydrogen recoils from the films were detected in a silicon surface barrier detector kept at 30^o whereas, nitrogen and oxygen recoils were detected by ΔE-E telescope detector kept at 45^o with respect to the beam direction. A polypropylene film of whose thickness was estimated using SRIM was kept before silicon surface barrier detector to stop all the recoils except for hydrogen. Areal concentration (at/cm^2) of H, N and O of the films have been calculated using standard formulation of ERDA [7]

Film compaction (~20%) and increase in refractive index (~17%) was observed after RTA. ERDA analysis shows that the areal concentration of hydrogen changes with increase in ion fluence (Fig.1) with two different slopes. This is because of hydrogen loss and eventual modifications due to ion irradiation [7]. From the plot of 'R' versus ratio of hydrogen/nitrogen concentration (Fig.2), it is obvious that for the as deposited films the hydrogen concentration increases for higher 'R' values. It can be understood from the fact that for high 'R' values silane flow rate was increased keeping ammonia flow rate constant during deposition. In contrast to it in rapid thermal annealed samples hydrogen concentration is decreased by an order of magnitude, which implies out diffusion of hydrogen. Moreover nitrogen and oxygen concentration was found to be more in RTA films than in the as deposited. The presence of oxygen is due to the formation of oxide layer after film deposition or post heat treatment (RTA). Compaction of the films and enhancement of refractive index has thus occurred partly due to out diffusion of hydrogen and partly due to rearrangement of

chemical bonding. It is proposed that the presence of hydrogen in films after RTA could be due to incomplete out diffusion of H and it's in diffusion towards the film substrate interface leading towards the passivation of interfacial charge tarps.

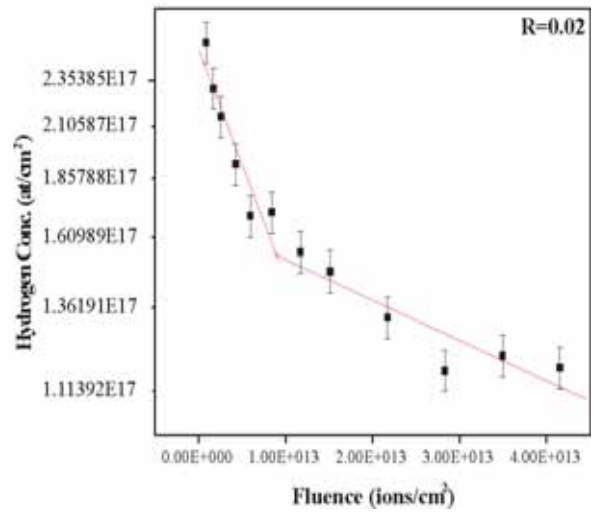

Fig. 1. Areal concentration (at/cm^2) of H versus fluence (ions/cm^2) for 100MeV Ag^{7+}

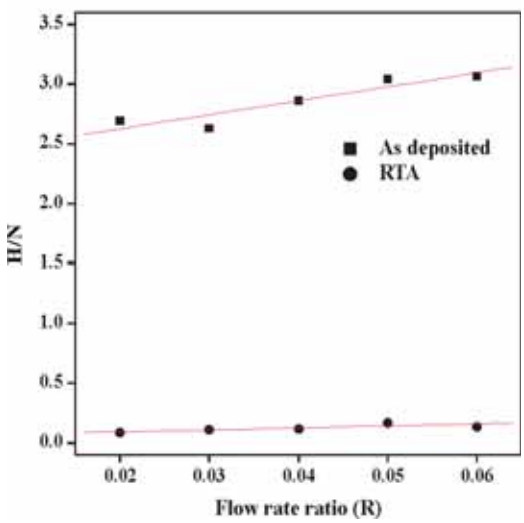

Fig. 2. Hydrogen/Nitrogen vs flow rate ratio (R)

REFERENCES

[1] D. Schalch, A. Scharmann and R. Wolfrat, Thin Solid Films 124 (1985) 301.

[2] A. E.T. Kuiper, M. F.C. Willemsen and L.J. van IJzendoorn, Appl. Phys. Lett. 53 (1988) 2149.

[3] A. G. Aberle, Sol. Energy Mater. Sol. Cells 65 (2001) 239.

[4] Fan Jiang, Michael Stavola, A. Rohatgi, D. Kim, J. Holt, H. Atwater, J. Kalejs, Appl. Phys. Lett 83 (2003) 931.

[5] P. Szöllõsi, P. Basa, Cs. Dücsõ, B. Máté, M. Ádám, T. Lohner, P. Petrik, B. Pécz, L. Tóth, L. Dobos, L. Dózsa and Zs.J. Horváth, 6 (2006)179.

[6] O. P. Agnihotri, S. C. Jain, J. Poortmans, J. Szlufcik, G. Beaucarne, J. Nijs, and R. Mertens, Semicond.Sci. Technol. 15 (2000) R29.

[7] V. K. Mittal, S. Lotha and D. K. Avasthi, Radiat. Eff. Defect. Solids 147 (1999) 199.

5.2.8 High energy irradiation studies on II-VI nanocrystalline thin films and I- III-VI$_2$ chalopyrites

R. Dhanasekaran[1] and D. Kanjilal[2]

[1]Crystal Growth Centre, Anna University, Chennai – 600 025

[2]Inter University Accelerator Centre, Aruna Asaf Ali Marg , New Delhi - 67

Swift heavy ion (SHI) beams play a vital role in the field of modifications of the properties of II-VI and I-II-VI_2 compounds [1-2]. In the present investigation, the effect of ion beam irradiation on the properties of II-VI nanocrystalline thin films such as CdSe, CdS deposited using Chemical Bath Deposition (CBD) and $AgGaS_2$ single crystal grown by Chemical Vapor Transport (CVT) method has been studied. The thin films and single crystal were irradiated with 120 MeV Ag^{9+} ions with fluences of 1 $x10^{13}$, 5 $x10^{12}$ ions/cm^2 at room temperature (RT) of 300K and 5 $x10^{13}$ ions/cm^2 at liquid nitrogen Temperature (LNT) of 77K. During irradiation the ion beam current is maintained constant around one particle nano ampere (pnA). An electro-magnetic scanner focuses the ion beam on the sample surface of having scanned area of 1x1cm^2.

The optical absorption spectra of as grown and irradiated CdS thin films have been recorded at room temperature using a Shimadzu UV-1061 spectrophotometer. There is no significant change in the band edge due to the irradiation but the absorption increases in the visible region. In the case of CdSe thin films, the structural characterization using X-ray diffraction is recorded using a Philips XPERT-PRO (PW3040) X-ray diffractometer with $CuK_{\alpha 1}$ radiation having wavelength 1.5406A°. The CdSe is having zinc blende structure. For the pristine sample, the 2θ values are matched with ICDD data's and their corresponding orientations are 25.7 (111), 42.7 (200), 50.4 (311). LNT irradiated film has only one orientation (111) corresponding to two theta value of 25.7. But the peak has been widened. This may be due to the defect formed on the lattice due to the bombardment of heavy ions with the lattice. The RT irradiated sample is fully amorphous in nature. When the high-energy ions interact with the target, a part of energy will transform into heat. This heat amorphises the surface of the samples.

The glancing angle X-ray diffraction (GAXRD) analysis reveals a huge lattice disorder in $AgGaS_2$ single crystal due to RT irradiation. This is observed form the increase in the full width at half maximum (FWHM) and decrease in the intensity of the AGS (112) peak. Also, AGS (303) peak is not observed for the samples irradiated with the fluences of 5$x10^{13}$ and 1$x10^{13}$ ions/cm^2 at RT conditions. The GAXRD results show the decrease in degree of crystallinity upon ion irradiation at RT while there is no degradation in crystallinity upon ion irradiation at LNT. Atomic force microscope (AFM) studies show that the roughness of AGS increases on increasing the ion fluences. AFM studies indicate the increase in the surface defects with fluences of Ag^{9+} ion irradiation when compared to pristine AGS. The photoluminescence (PL) spectra were analyzed as a function of irradiation ion fluences in the AGS crystals at RT. It has been found that the emission intensities of band-to-band transition decrease with increase of ion fluences. UV-visible transmission spectra shows that the percentage of transmission and band gap energy decrease with increasing ion fluences and also that the peaks are broadened.

REFERENCES

[1] Chandramohan S, Sathymoorthy R, Sudhagar P, Kanjilal D, Kabiraj D and Asokan K 2007 Nucl. Instrum. Methods B 254 236

[2] Soundeswaran S, Senthil Kumar O, Ramasamy P, Kabiraj D, Avasthi D.K and Dhanasekaran R 2005 Pysica B 355 222

5.2.9 Ion beam induced phase separation and formation of silicon nanocrystals embedded in silicon oxide matrix

Nupur Saxena[1], Avinash Agarwal[1], D. Kabiraj[2]and D. Kanjilal[2]

[1] Department of Physics, Bareilly College, Bareilly – 243005.

[2] Inter University Accelerator Center, Aruna Asaf Ali Marg, New Delhi - 67

Swift heavy ion induced synthesis of silicon nanocrystals embedded in silicon oxide is investigated. Silicon nanocrystals embedded in an insulating matrix are of great interest due to its stability, charge retention, optoelectronic property and above all full compatibility with existing silicon technology. Ion beam induced formation leads to the chemically pure and stable nanocrystals as well as good control over the size and size distribution.

There are mainly two techniques of synthesis of nanoparticles viz. top to bottom and bottom to top but none of these two approaches is able to form consistently sub-10 nm silicon quantum dots which can show the effect of quantum confinement [1]. The most applicable processes in this stream are nucleation, growth due to phase separation of suboxide films by some activation [2,3]. We report the phase separation of high vacuum evaporated silicon suboxide films by swift heavy ion beam irradiation. Commercially available silicon monoxide (in the form of chunks) was evaporated in a high vacuum (~ 10^{-6} mbar) chamber by resistive heating method. The substrates used were thoroughly cleaned silicon (111) and quartz. The thickness of the film was 200 nm. These films were irradiated with 120 MeV ^{58}Ni beam at various fluences. The electronic energy loss, nuclear energy loss and projected range of these ions are calculated by SRIM 2006 and the values are 6.122 keV/nm, 9.513x10^{-3} keV/nm and 27.04 μm respectively.

Swift heavy ion beam deposits a large amount of energy in the films through electronic energy loss and causes the decomposition of nanocrystalline silicon and silicon dioxide. Phase separation of SiO_x is due to the fact that this suboxide fulfills the condition for spinodal decomposition. This phase separation due to spinodal decomposition is not due to transport of macroscopic matter by diffusion, but it is due to the local fluctuations in the concentration of the constituents. These transitions occur out of thermodynamic equilibrium or athermal annealing i.e. by swift heavy ion beam. In this case there is no creation of an interface and hence there is no nucleation at all. Spinodal is a region of metastable state outside which the physical system becomes unstable. Swift heavy ion beam quenches the material to the spinodal region with very high quenching rate ~ 10^5 K/s, where the local fluctuations trigger the transition and the material is separated into two phases without any nucleation.

The irradiated films are characterized for their structural modification and optical properties by FTIR, Raman, photoluminescence and UV-Visible absorption spectroscopy. The FTIR results indicate the shift of Si-O-Si asymmetric stretching mode to higher frequency after the irradiation. This feature of FTIR spectrum indicates the structural modification in the film and the formation of SiO_2 after irradiation.

The photoluminescence spectra exhibit two peaks one at 525 nm and second between 650 nm and 700 nm. The peak position of first peak is unaffected by the irradiation and is attributed to the defects in the material whereas the peak position of second peak is shifted towards the blue region as the fluence is increased [4]. Similar observations are found in UV-Visible spectroscopy. The estimated band gaps are given in table1.

Table 1

Ion Fluence	Band gap (eV)
$1x10^{12}$ ions/cm^2	1.8
$1x10^{13}$ ions/cm^2	2.2
$5x10^{13}$ ions/cm^2	2.5

These observations indicate that the size of the nanoparticles thus formed can be controlled by the fluence of the ion beam. These are our preliminary observations. More experiments are planned to develop the clear understanding of the phenomena and to find properties of the nanocrystals thus formed.

REFERENCES

[1] P. F. Trwoga A. J. Kenyon and C. W. Pitt, J. Appl. Phys. 83 (7) 3789-3794 (1998)

[2] W. M. Arnodbik, N. Tomozeiu, E. D. van Hattum, R. W. Lof, A. M. Vredenberg and F.H.P.M. Habraken, Phys. Rev. B 71, 125329 (2005).

[3] W.M. Arnoldbik, D. Knoesen, N. Tomozeiu and F.H.P.M. Habraken NIM B, 258, (1), 2007, 199-204.

[4] Daria Riabinina, Christrophe Durand, Mohamed Chaker and Federico Rosci, Appl. Phys. Lett. 88, 073105 (2006)

5.2.10 Novel effect of 100 MeV Ni^{+7} ion on Silica coated ZnS quantum dots

S S Nath[1], D Chakdar[1], G Gope[1], R Das[1] and D K Avasthi[2]

[1] Dept of Physics, NIT Silchar, Assam

[2] Inter University Accelerator Center, Aruna Asaf Ali Marg, New Delhi - 67

We report synthesis, optical absorption and luminescence spectroscopy of ion irradiated SiO_2 coated ZnS semiconductor quantum dots embedded in PVA matrix. 100MeV Ni ion was selected for the irradiation experiment with different fluences of 1×10^{11}, 3×10^{11}, 1×10^{12}, 3×10^{12} and 10^{13} ions/cm^2. With an increase in fluence, the optical absorption edge of irradiated quantum dots reveal negligible red shift with respect to that of unirradiated (virgin) quantum dots. This phenomenon clearly indicates no significant change in particle size under ion irradiation which is confirmed from high resolution transmission electron microscope (HRTEM) images and the particle

sizes remain within 11 nm. It has been observed that like virgin samples, irradiated quantum dots produces similar kind of green luminescence[3] (Photoluminescence) but the emission intensity increases remarkably after irradiation due to creation of Zn vacancies[2] by ion irradiation.

8wt% D/D water solution of PVOH is prepared and treated in the similar way as in case of CdS quantum dots. Next 1.36wt% aqueous solution of $ZnCl_2$, 1wt% solution of SiO_2 and 0.75wt% solution of Na_2S are prepared. The solutions of PVA, $ZnCl_2$ and SiO_2 are mixed in the molecular weight ratio of 1:1:0.5 and then stirred at 250 rpm at 60^0C while with dropping funnel, Na_2S solution is put into it, until the whole solution appears completely milky. Finally, the solution is cast over glass substrate and then dried in oven at 40^0C. The sample sizes of 1×1 cm^2 were cut for ion irradiation experiment.

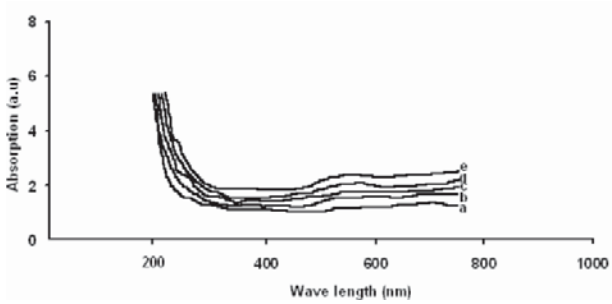

Fig. 1. UV/VIS absorption spectra of ZnS specimens. a, b, c, d, and e stand for virgin sample and samples irradiated by 1st, 2nd , 3rd , and 4th dose respectively

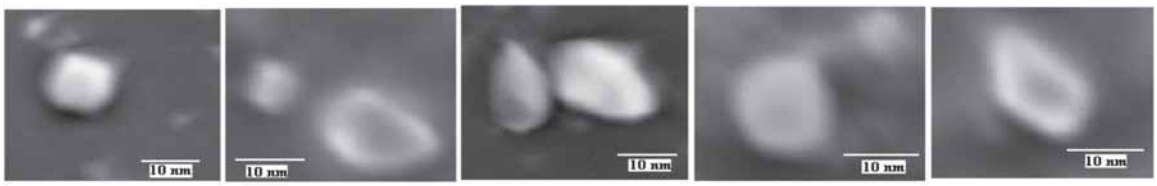

Fig. 2. HRTEM image of ZnS specimens. a, b, c, d, and e stand for virgin sample and samples irradiated by 1st, 2nd , 3rd , and 4th fluence respectively

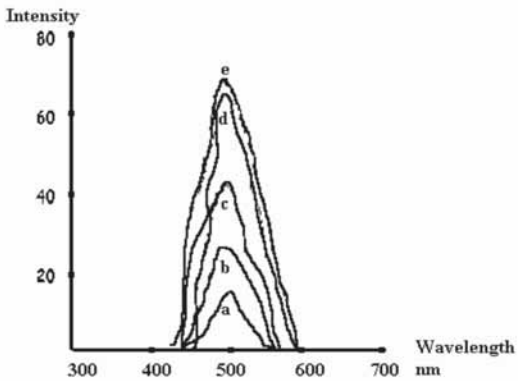

Fig. 3. PL spectra of ZnS samples a, b, c, d and e stand for virgin sample and samples irradiated by 1st, 2nd, 3rd and 4th fluence respectively

REFERENCES

[1] S S Nath et al , Nanotrends-A journal of nanotechnology and its application, ,Vol 02, Issue 03,2007.

[2] S S Nath et al, JDST, 30 (2009) 4, (in press).

[3] S S Nath et al, Intr. Journal of Nanotechnology, Vol 1, No 2, 2008.

5.2.11 HI-ERDA Studies of Ion-beam Synthesized Buried Silicon Oxynitride Layers

A. D. Yadav[1], S. K. Dubey[1], Rucha H. Polji[1] and Saif A. Khan[2]

[1] Department of Physics, University of Mumbai, Vidyanagari campus, Santacruz (E), Mumbai

[2] Inter University Accelerator Centre, Aruna Asaf Ali Marg, New Delhi - 67

The silicon-on-insulator (SOI) technology has much attraction for device fabrication. It offers many advantages over bulk silicon such as radiation hardness, higher operating temperature, low parasitic capacitance and high packing density. The synthesis of buried insulating layers to produce SOI structures by SIMONI (separation by implanted oxygen-nitrogen) process using high fluence ($\geq 1\times10^{16}$ cm^{-2}) oxygen-nitrogen ion implantation into silicon has scope of potential applications in semiconductor technology. In the present experiment, buried silicon oxynitride ($Si_xO_yN_z$) insulating layers were synthesized by 150 keV nitrogen ($^{14}N^+$) and oxygen ($^{16}O^+$) ion implantation into single crystal silicon wafers using low energy ion beam facility (LEIBF) at the Inter University Accelerator Center (IUAC), New Delhi. The samples were implanted to total ion-fluence levels of $1x10^{17}$, $2.5x10^{17}$ and $5x10^{17}$ cm^{-2}. The annealing treatment to the samples was given at 500 and 800 ^{0}C for 30 min in the flow of dry nitrogen gas. The compositional depth profile analysis of the formed structures was carried out with heavy-ion elastic recoil detection analysis (HI-ERDA) using 15 UD Pelletron accelerator facility at Inter University Accelerator Centre, New Delhi. The ERDA spectra were transformed into depth versus concentration profile using the SIMNRA simulation code.

Fig.1 shows two dimensional energy loss versus total energy ΔE1-E (total) ERDA spectrum of the sample implanted with fluence $1x\ 10^{17}$ cm^{-2}. The spectrum clearly shows silicon, oxygen, nitrogen and carbon (impurity) bands. The concentration vs. depth profile for as implanted and annealed samples is shown in Fig. 2(a) and 2(b). For the as implanted samples, both nitrogen and oxygen concentration peaks lie at depth 383 nm, close to the theoretical SRIM projected range 356 nm (of nitrogen) and 340 nm (of oxygen) at 150 keV in silicon. After annealing at 500 ^{0}C, no change in the peak position was observed but redistribution of both nitrogen and oxygen concentration was found at the interface near the surface. On further annealing at 800 ^{0}C, the redistribution of nitrogen and oxygen towards the surface is observed to be prominent as seen from Fig. 2 (b) and the peak concentration is found to have a flat plateau like region towards the surface. Since the implantation damage profile is maximum near the surface [1], a mixed oxynitride phase will be nucleated and grow by gettering free oxygen and nitrogen from the buried layer towards near surface region [2] in this energetic environment.

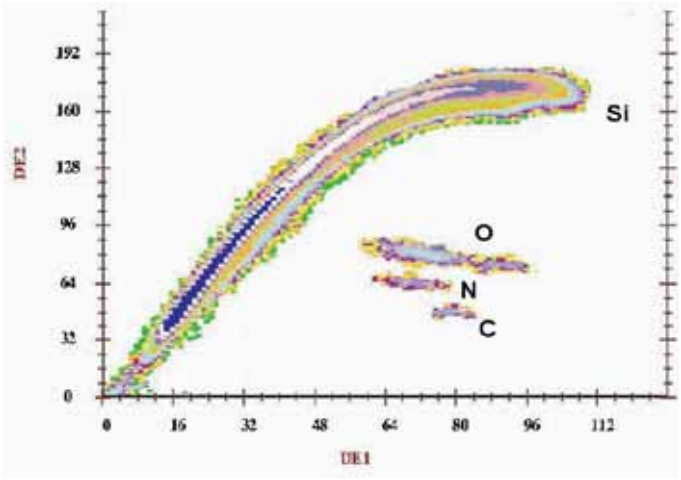

Fig.1. HI-ERDA spectra of silicon sample implanted with N: O ratio 1: 1 at total fluence 1x10^{17} cm^{-2}

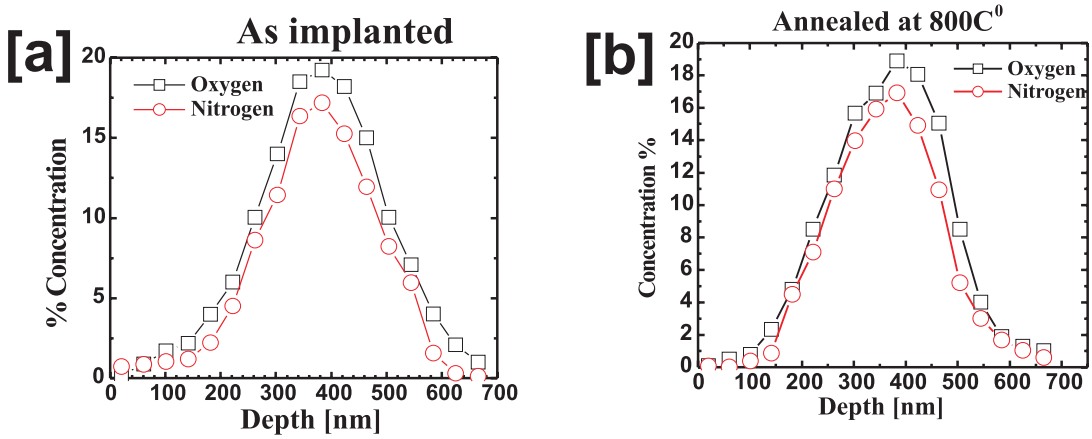

Fig.2. [(a) & (b)] Annealing behavior of silicon sample implanted with N: O ratio 1: 1

From the Hi-ERDA studies, it is observed that both nitrogen and oxygen redistribute near surface side of the silicon promoting the formation of continuous buried layer after annealing at 800 ^{0}C.

REFERENCES

[1] J. P. de Souza, Yu. Suprun-Belevich, H. Boudinov C. A. Cima, J. Appl. Phys. 89 (2001) 42.

[2] K.J. Reeson, P.L.F. Hemment, C. D. Meekison, C. Marsh, G. R. Booker, J.R. Davis, R.J. Chater, J.A. Kilner, Nucl. Instr. And Meth. B 32 (1988) 427.

5.2.12 Fast ion irradiation of ultra thin bulk pellets of some electronically important oxide semiconductors

Kriti Ranjan Sahu[1], S. Asad Ali[2], Rajesh Kumar[2], Rajendra Prasad[2], Pawan K Kulriya[3], Fouran Singh[3] and Udayan De[4]

[1] Physics Dept., ESSB College, Egra 721429, Purba Medinipur, West Bengal

[2] Dept of Appl Physics, Z. H. College of Engg & Techn, Aligarh Muslim University, Aligarh

[3] Inter-University Acclerator Centre, Aruna Asaf Ali Marg, New Delhi - 67

[4] Variable Energy Cyclotron Centre, DAE, 1/AF Bidhannagar, Kolkata-700064

Three II-VI materials, Cd-oxide (IIb-VIa), Mg-oxide (IIa-VIa) and Zn-oxide (IIb-VIa), have been taken up for fast ion irradiation in suitable bulk forms, ultra thin bulk pellets. These materials have electronic and optical applications, and the present work focuses on preparation and 50 MeV Li^{3+} ion irradiation [1] of bulk samples, ~ 200 μm thick CdO & ZnO and ~ 400 μm thick MgO. According to TRIM calculations, these thicknesses allow the ion beam to pass through the samples as needed for studying radiation damage without any implantation.

The well known advantage of thin film samples in terms of more easily achievable lower sample thickness and hence a choice of heavier ions has led to some such thin film experiments at IUAC and elsewhere. Here, we note that often there is a significant difference in properties for thin films and bulks. So, results of radiation damage investigations in films are related to but likely to be different from such investigations in the bulk. Here, we carry out a feasibility study of making such radiation damage in the bulk state with available facilities.

In search of longer ion range, Li-ion has been chosen and 50 MeV, the highest energy [1] available at present in IUAC. Pellets of 10mm diameter and different thicknesses were made under the same palletizing load of 6 ton, from Cadmium Oxide (Ma Teck GmbH 99.99+%), Zinc Oxide (Ma Teck GmbH 99.999%), Magnesium Oxide (Ma Teck GmbH 99.99%). Extreme care was needed in handling these delicately thin pellets. These and thicker pellets were heat treated at 800 °C or other temperatures in air for 36 hours [2] in a Carbolite Furnace with PID temperature controller to prepare the final samples for ion irradiations. But, curving of these ultra thin pellets on simple heat treatment (sintering) has been blocking further progress. Finally, it was found [2] that putting the pellets under a pressure of $12.1\times10^4 N/m^2$) during firing, slow cooling after the 36 hour firing and taking the samples out of the furnace only below 50°C gave flat ultra thin pellets.

Doping of II-VI semiconductors like ZnO with a 3rd element is now a hot topic for electronic industry for p-n junction fabrication. However, self-doping possible by non-stoichiometry in these oxides has been largely unnoticed. Large non-stoichiometry due to heat treatment at different temperatures has been observed [3] by us. Here, CdO_120 & CdO_800 imply cadmium oxide after 120°C & 800°C firing for 36 hours. Latter is found to be ~ 10 times more conducting than the former, and so damage studies in both have been planned. Difference in response to ion irradiation due to difference in the initial state of the unirradiated sample has thus been studied here by irradiating differently heat-treated CdO, ZnO and MgO samples. XRD in the Bruker Diffractometer at IUAC showed the correct phase in each sample.

20 flat and ultra-thin pellets of Cadmium, Zinc and Magnesium Oxides were thus prepared and put on three faces of the all copper IUAC Target Holder (called Ladder). Beam Current for

the 50 MeV Li^{3+} irradiation was never allowed to exceed 3 nA to avoid beam heating of the sample. A current integrator measured the charge collected by the sample. This gave the irradiation fluence. Irradiations were done for fluences up to $5x10^{13}$ Li^{3+}/cm^2 only, and targeted maximum fluence of ~ $1x10^{15}$ Li^{3+}/cm^2 could not be achieved.

XRD of all the irradiated samples have been done and optical & XPS characterizations started for a full analysis of the results. There is a need for irradiation to higher fluences. Irradiation induced re-distribution of the intensities of the XRD peaks, observed for CdO_120 and CdO_800 samples, for example, implies some atomic re-arrangements. It is clear that with suitable sample preparation and careful mounting into the ladder, pure radiation damage in bulk samples of the oxides of Cd, Zn and Mg can be studied with IUAC facilities.

REFERENCES

[1] A. Sarkar, Udayan De, D. Sanyal, Ravi Kumar & D. Banerjee, Nuclear Instru. & Methods in Phys. Res. B156 (1999) 50

[2] Kriti Ranjan Sahu[1], Rajesh Kumar[2], Rajendra Prasad[2] Pawan K Kulriya[3], and Udayan De[4], Condensed Matter Days 2007, NIIT, Rourkella (India)

[3] Udayan De, M.K. Chattopadhya, S. Chaudhury, A. Sarkar, D. Sanyal & T.K. Dey, J. Phys. & Chem. of Solids 61 (2000) 1955; K.C. Verma and Udayan De, Ind. J Phys. 79 (2005) 1075

[4] "XPS & RBS study of thermally induced oxygen non-stoichiometry in Zn & Cd Oxides", Udayan De, Rajesh Kumar, Dipak Paramanik, Sikha Verma and Rajendra Prasad, International Conference on Atomic Collisions in Solids (ICACS) 2006, Berlin, 21st-26th of July 2006; "Atomic defects in differently fired Magnesium Oxide", Udayan De, Dipak Paramanik, Rajesh Kumar, Rajendra Prasad , P.K. Kulriya and Sikha Verma.

5.2.13 Structural and optical characterisation of Swift Heavy Ion Irradiated GaN Epitaxial Layers

N Sathish[1], S Dhamodaran[1], A P Pathak[1], S A Khan[2] and D K Avasthi[2]

[1] School of Physics, University of Hyderabad, Central University (P.O), Hyderabad – 500 046

[2] Inter University Accelerator Centre, Aruna Asaf Ali Marg, New Delhi – 110 067, India.

III- Nitride semiconductors are novel class of materials for optoelectronics, high power and high temperature device applications. A wide range of optical devices from Blue Light Emitting Diode (LED) to violet laser diode (LD), UV photo detectors and High Electron Mobility Transistors (HEMTs) are possible. These devices were demonstrated for high frequency, power handling and wide operation range of temperature. The recent developments in epitaxial growth by MBE and MOCVD, processing of materials, relevant device fabrication and possible future trends have been reviewed extensively in the literature [1]. The main problems in III-Nitride device technology are material quality, difficulties in p-type doping and interface roughness. The possibility of material reconstruction and interface smoothening has been demonstrated using ion beams [2]. In this work we are reporting the effects of Swift heavy ion in the GaN bulk epitaxial layers.

Samples studied are 2 mm thick GaN layers grown on c-plane sapphire by MOCVD. Samples are irradiated with 150 MeV Ag^{12+} ions at a fluence of 5 x 10^{12} ions/cm^2. These ions penetrate to depths of approximately 11.03 μm and 11.13 μm in GaN and Sapphire respectively, and lose energy at the rate of 24.79 keV/nm in GaN and 22 keV/nm in Sapphire, through electronic interactions. Surface morphology of the samples are studied by contact mode Atomic Force Microscopy (AFM). GaN layer thicknesses are measured by Rutherford Backscattering Spectrometry (RBS). High resolution X-Ray Diffraction (HRXRD) experiments are carried out using a Philips MRD diffractometer. The ω–2θ scan on (0002) direction are done on all the samples. Optical transmission and reflectance spectra are recorded from 190 to 2000 nm wave length region, keeping standard samples in reference beam. Band gaps are calculated from $(\theta E)^2$ Vs E plot.

As grown samples show surface morphology having larger hillock sizes varying from 200 to 1700 nm which are commonly observed in GaN films. Ending of threading screw dislocation at the surface normally results in this kind of morphology [3]. In our samples, as a result of irradiation, both hillocks and deep holes are observed in A4. But in A6 there are no hillocks only deep holes are formed, and their sizes are of the order of hillock sizes present in as grown samples. We have not observed any qualitative changes before and after irradiation in RE48 as in A4 and A6; but the sizes of the pinned steps have reduced after irradiation. A4 and A6 samples show different morphologies, showing hillocks and deep holes after irradiation. In RE48, it has thin AlN layer on the top of the GaN. Strain energy in the AlN/GaN interface prevents any change in the surface morphology.

FWHM of XRD peaks of all the samples increased after irradiation which shows that the samples are damaged after irradiation. In the sample RE48, increase in FWHM is less compared to the other samples. In A4, increase in FWHM is less when compared to that of A6, indicating that the damage caused in A6 is more compared to all other samples. In all the as grown samples both Lorentzian and Gaussian broadenings are observed, which shows that both kinds of defects are present in these samples i.e., dislocations as well as point defects. The layer quality along the perpendicular direction to the substrate surface is limited by mixed dislocations which causes Lorentzian broadening [4]. FWHM of all the samples increased after irradiation which shows that the samples are damaged after irradiation. In the sample with AlN cap layer, increase in FWHM is less compared to the other samples.

The spectral transmittance curves show sharp absorption edge for as grown samples. This is generally observed in MOCVD grown GaN in spite of high defect density. GaN has very high absorption coefficient of the order of 10^5 cm^{-1} and hence transmittance is very less [5]. Here our sapphire substrate is single side polished so we have only 6-8 % transmittance and the spectra is normalised to the blank sapphire spectra. After irradiation band edge absorption increases exponentially instead of sharp increase. This kind of behaviour is observed in highly defected samples or at high doping level. From $(\alpha E)^2$ vs hn plots band edges are calculated. In the as grown samples measured band gap are 3.39, 3.39 and 3.38 eV for RE48U, A4U and A6U respectively. After irradiation the calculated band gap values are decreased to 3.34, 3.24 and 3.29 eV for

RE48I, A4I and A6I respectively. This kind of broadening of near band edge absorption may be due to irradiation induced point defects and locally strained regions or relaxed extended defects.

In conclusion, Damage creation in GaN by Swift Heavy Ions (SHI) is a complex process. The high energy deposited by the ion to the lattice, results in two kinds of damage creation in GaN. One is N loss and Ga rich regions, as confirmed by the Gaussian broadening of X-Ray peak widths and small shoulder peaks. Broadening of the optical band-edge absorption also confirms this. AlN cap layer can be used to reduce the N loss due to irradiation. The second damage is dissociation and movement of the stable dislocations due to energy deposited by the energetic ion. This may be confirmed by Lorentzian broadening of the x-ray peak width and from the AFM surface morphologies. Also the initial defect configuration plays major role in the damage creation by swift heavy ion irradiation.

REFERENCES

[1] SC Jain, M. Willander, J. Narayan and R. Van Overstraeten,.Journal Appl Phys. 87, (2000) 965

[2] S. O. Kucheyev, M. Toth, M. R. Phillips, J. S. Williams, C. Jagadish, and G. Li, J.Appl.Phys. 91 (2002) 3940

[3] B. Heying, XH Wu, S. Keller, Y. Li, D. Kapolnek, SP Denbaars, and. JS Speck. Appl. Phys. Lett. 68 (1996) 643.

[4] T. Metzger, R. Hoepler, E. Born, O. Ambacher, M. Stutzmann, R. Stoemmer, M. Schuster, H. Goebel, S. Christiansen, M. Albrecht and H. P. Strunk. Phil. Magz. A 77 (1998) 1013

[5] JF Muth, JH Lee, IK Shmagin, RM Kolbas, HC Casey, BP Keller, UK Mishira, and SP Den Baars, Appl. Phys. Lett. 71 (1997) 2572.

5.2.14 RBS/Channeling, HRXRD and AFM studies on swift heavy ion irradiated AlGaN/GaN heterostructures

N Sathish[1], S Dhamodaran[1], A P Pathak[1],S A Khan[2] and D K Avasthi[2]

[1] School of Physics, University of Hyderabad, Hyderabad 500 046, India

[2] Inter-University Accelerator Centre, Aruna Asaf Ali Marg, New Delhi - 67

As emphasized in the accompanying report, III- Nitride semiconductors are a novel class of materials for various applications in optoelectronics. Here we report complimentary work on AlGaN/GaN heterostructures.

Samples studied in this work are (50 nm) $Al_{0.2}Ga_{0.8}N$ / (1 nm) AlN / (1 μm) GaN / (0.1 μ m) AlN on SI 4H-SiC irradiated with 150 MeV Ag ion at fluence of $5x10^{12}$ ion/cm^2. Irradiation was performed at room temperature using NEC 15 MV pelletron accelerator at IUAC, New Delhi. Surface morphology of the samples are studied by contact mode Atomic Force Microscopy (AFM). Strain measurements and defects characterization on irradiated and unirradiated samples were carried out by RBS/Channeling. The dechannelling parameter is calculated from the normalized back scattering yield to see the energy dependence for defect analysis. High resolution

XRD experiments have been performed using the Philips X'Pert system. Reciprocal space mapping has been carried on 0002 direction in triple crystal mode. w and ω-2θ scans were extracted from the map.

Surface morphology of AlGaN/GaN heterostructures shows pinned steps or hillocks and craters. The size of hillocks ranges from 10 to 100 nms [1]. In the irradiated samples we observe similar morphology as in the unirradiated ones but with surface blistering. This may be due to the surface mass transport induced by the swift heavy ions. Apart from this we did not observe any other changes on the surface; this may be due to stronger nature of AlGaN layer to irradiation.

ω Scans and ω-2θ scans of AlGaN/GaN heterostructures were extracted from the reciprocal space map of 0002 direction. These scans were fitted using Pseudo-Viogt function. Lateral Correlation length ($L_{\|}$), Lorentzian shape function (h) and defect density (N_D) were calculated from the parameters extracted from the fit and all the values are given in the Table 1. FWHM of unirradiated GaN layer was 0.168° and Lorentzian shape function is 0.739. This shows that GaN has many defects and the broadening is mainly due to dislocations. $L_{\|}$ of GaN layer is 191 nm shows that the layer is having many defects; calculated defect density is $9.3x10^7$ cm^{-2}. AlGaN layer has a FWHM of 0.204° and Lorentzian shape function is 0.597, which implies that the defects from the GaN layers are travelling across interface to AlGaN layer. Lateral correlation length of 172 nm shows that the layer has more defects than the GaN layer. It may be due to strain relaxation that adds more dislocations in the AlGaN layer with a calculated defect density of $2.3x10^8$ cm^{-2}[2].

Sample	Lateral Correlation Length (L_{II})	Defect Density (N_D) HRXRD	Tetragonal distortion Stain (ε_t)	Defect density (N_D) RBS/C
Unirradiated GaN Layer	191.51 nm	$9.3933x10^7$ cm^{-2}		$2.1414x10^8$ cm^{-2}
Unirradiated AlGaN Layer	172.24 nm	$2.3518x10^8$ cm^{-2}	0.55 %	$1.9917x10^8$ cm^{-2}
Irradiated GaN Layer	275.78 nm	$5.002x10^8$ cm^{-2}		$3.6832x10^8$ cm^{-2}
Irradiated AlGaN Layer	166.63 nm	$2.8505x10^8$ cm^{-2}	0.76%	$3.2010x10^8$ cm^{-2}

Table.1. Lateral Correlation Length, Defect density and strain obtained from HRXRD and RBS/Channelling

After irradiation, the thick GaN layer shows an increase in FWHM to 0.207° and reduction in Lorentzian shape function to 0.345 which clearly indicates increase in defects. Lateral correlation length is increased to 275 nm. Irradiation gives enough energy to dislocations to move laterally. As a result, these dislocations cluster and the lateral correlation length increases even though the defect density increases to $5x10^8$ cm^{-2}. Irradiation introduces point defects also in the GaN layers, this is evident from the decrease in the Lorentzian shape function, and the diffraction curve has more Gaussian broadening. In AlGaN layer, FWHM increases to 0.223°, Lorentzian shape function doesn't change and defect density of $2.8x10^8$ cm^{-2}. FWHM increase is mainly due to the defects

created at the interface by the strain induced in the layer and point defects introduced by the swift heavy ions [3].

The Channelling strain measurement shows that unirradiated sample has a small residual compressive strain, and it increases after irradiation. Increase of defect density due to irradiation in the AlGaN and GaN layers were calculated. AFM surface morphology shows there is a clustering of the defects at the surface after irradiation. This complements the increase in lateral correlation length from HRXRD measurements. In conclusion Swift heavy ion induces more defects in GaN than AlGaN layer and the AlGaN layer compressive strain is induced by the process of self dynamic annealing.

REFERENCES

[1] B Heying, E J Tarsa, C R Elsass, P Fini, S P DenBaara and J S Speck, Jour Appl Phys, 85 (1999) 6470.

[2] T. Metzger, R. Hoepler, E. Born, O. Ambacher, M. Stutzmann, R. Stoemmer, M. Schuster, H. Goebel, S. Christiansen, M. Albrecht and H. P. Strunk. Phil. Magz. A 77 (1998) 1013

[3] S. O. Kucheyev, H. Timmers, J. Zou, J. S. Williams, C. Jagadish, G. Li, J. Appl. Phys. **95** (2004) 5360

5.2.15 Structural studies of Ge nanocrystals embedded in SiO_2 matrix

N Srinivasa Rao[1], S Dhamodaran[1], A P Pathak[1*], P K Kulriya[2], Y K Mishra[2], F Singh[2], D Kabiraj[2], J C Pivin[3] and D K Avasthi[2]

[1] School of Physics, University of Hyderabad, Central University (P.O), Hyderabad 500 046.

[2] Inter University Accelerator Centre, Aruna Asaf Ali Marg, New Delhi - 67

[3] CSNSM, IN2P3-CNRS, Batiment 108, F-91405 Orsay Campus, France.

Si and Ge nano crystals (nc-Ge, nc-Si) embedded in SiO_2 have recently attracted much attention due to their possible applications in integrated optoelectronic devices. Although porous Si is expected to be the most promising Si-based light emitting material, Ge nano crystalline (nc-Ge) embedded in Silica glasses have their own advantages. These Ge dots are useful in infrared detectors. Ge has smaller electron and hole effective masses and larger dielectric constant than Si. The effective Bohr radius of the exciton in Ge is larger than that in Si. Hence Ge is much easier to change the electronic structure around the band gap than Si due to its larger exciton Bohr radius. The present study concentrates on the structural characterization of the films prepared by Atom Beam Sputtering as a function of annealing temperature and ion irradiation induced crystallization.

The samples were prepared by fast Atom Beam Sputtering (ABS) method where small pieces of high purity Ge pieces were placed on a SiO_2 target by varying Ge concentration and they were co-sputtered by Argon atom source. The annealing of the samples was performed at 973 and 1073 K in quartz tube furnace in Ar + H_2 (5%) reducing atmosphere. We also irradiated the as-deposited films by 100 MeV Au^{8+} ions with $1x10^{13}$ ions/cm^2 fluence and compared with the

results of annealing. We have investigated the effects of annealing and high energy ion irradiation using Raman, XRD, FTIR and RBS.

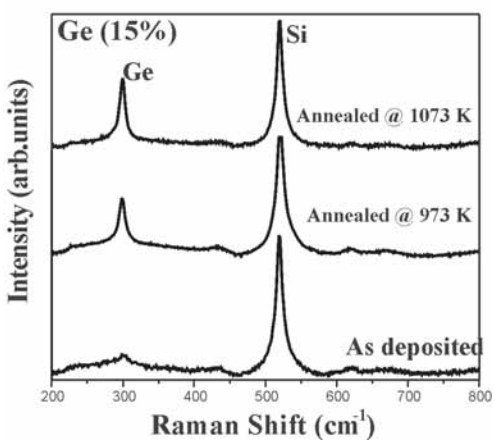

Fig. 1a

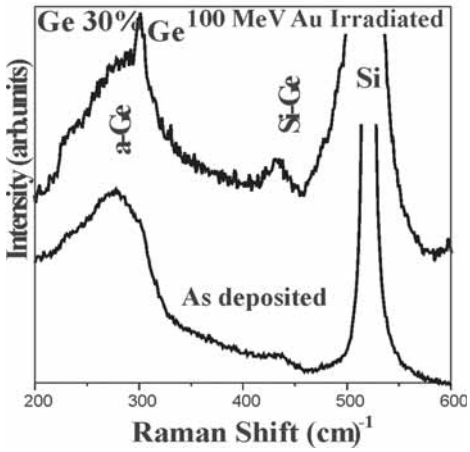

Fig. 1b

The peak around 300 cm^{-1} from annealed films appears asymmetric in the low-frequency region which is due to the smaller size of the Ge particles. The irradiated sample shows a sharp peak around 300 cm^{-1} together with a shoulder at low frequency (~270 cm^{-1}), corresponding to the crystalline Ge and amorphous Ge respectively (Fig 1 a, b). This is in contrast to the annealing results where only sharp crystalline Ge mode was seen and no signal of amorphous Ge was observed [1]. The energy loss of high energy ions is mainly through electronic stopping mechanism (in the present case ~ 17 keV/nm) and hence the irradiation results in local heating of the samples limited to nm dimensions, within a nanometric track. The material within the ion tracks is molten for a short duration of time 10^{-12} s if the input energy is large enough. The obtained result indicates that the heating is sufficient for promising short range rearrangements leading to Ge crystallization. No Ge peak is observed from the as-deposited films while high temperature annealing results in a broad Ge (311) peak at 54.5^0. From the FTIR spectra the structure of amorphous GeO_2 can be described as Ge-Ge_yO_{4-y} tetrahedral connected by bridging oxygen atoms. The asymmetric stretching vibration mode of Ge-O-Ge in stoichiometric GeO_2 is at 885cm^{-1}.

REFERENCE

[1] N. Srinivasa Rao, S. Dhamodaran , A.P. Pathak , P.K. Kulriya , Y.K.Mishra , F. Singh, D. Kabiraj , J.C. Pivin , D.K. Avasthi. Nucl. Inst. Meth B 264 (2007) 249–253.

5.2.16 Swift heavy ion induced modifications in $AgInSe_2$ films

Dinesh Pathak[1], R.K.Bedi[1], Davinder Kaur[2] and Ravi Kumar[3]

[1] Material Science Lab, Department of Physics, G.N.D.U.,Amritsar

[2] Department of Physics and center of Nanotechnology, I.I.T. Roorkee

[3] Inter University Accelerator Center, Aruna asaf Ali Marg, New Delhi -67

Swift heavy ions lose energy in the target mainly via inelastic collision leading to the excitation of the target electron. The electronic energy loss has been found to create various modifications in the target material, which include creation of point defects, latent tracks formation, sputtering and intermixing of interfaces. The material modification using swift heavy ion irradiation has been studied quite extensibly.

$AgInSe_2$ alloy has been synthesized by mixing the constituents in stochiometric amount. The $AgInSe_2$ films were grown on glass and Si substrate kept in temperature range 30^0-500^0C. The films prepared on Si substrate are found to be more textured as compared to those prepared on glass. This may possibly due to the lattice matching between Si (5.45 A^0) and $AgInSe_2$ (a=6.10 and c=11.6 A^0). It has been observed that chalcopyrite (112) phase dominates up to Ts 300^0C in case of films deposited on glass and Si. $AgIn_5Se_8$ phase appears to dominate on increasing substrate temperature. The films prepared by thermal evaporation on Glass and Si were irradiated with 200 MeV Ag beam with dose 5 x 10^{11} ions/cm^2 using 15 UD Pelletron. XRD, AFM, FESEM and EDAX techniques are employed for their characterization. Irradiation induced crystallization is observed for the films prepared on glass kept at Ts 30^0C and 200^0 C. However for the films prepared on Si substrates, the damage of structure is noticed as evident from X-Ray diffraction data. Also rod like growth is observed in some parts of FESEM images of irradiated films prepared on Silicon substrates. Detailed investigations are in progress.

5.2.17 Formation of nanostructures using swift heavy ion beam

Madhavi Thakudesai[1], A Mahadkar[2], P.K.Kulariya[3], Varsha Bhattacharyya[1] and D Kanjilal[3]

[1] Department of Physics, University of Mumbai, Vidyanagri, Mumbai – 400 098

[2]Tata Institute of Fundamental Research, Homi Bhabha Road Mumbai – 400 005

[3] Inter University Accelerator Centre, Aruna Asaf Ali Marg, New Delhi – 67

In the present investigation, TiO_2 nanostructures are formed using swift heavy ion (SHI) beam. For this purpose, Ti metal target is evaporated by e-beam evaporation method. Films of thickness 100 nm are deposited on fused silica substrates. These films are subsequently annealed in flowing oxygen in a tube furnace. The samples are annealed at temperature 800°C for two hours. These films are irradiated by 100 MeV Au^{7+} ion beam. The irradiation fluence is varied between 1×10^{11} and 1×10^{13} ions.cm^{-2}. Both the as-deposited and irradiated films are characterized by GAXRD and UV-VIS spectroscopy.

Fig.1 shows the GAXRD spectra of as-deposited and irradiated films**.** The GAXRD spectrum of as-deposited film shows mostly amorphous nature. After irradiation at a fluence of 1×10^{11}ions.cm^{-2} the crystallinity of the film increases along with structural phase transformation. Rutile phase of TiO_2 is formed after irradiation. The particle size estimated using Scherrer's formula

(FWHM = 0.71-0.58) is 19-23 nm. When the irradiation fluence is increased to 1×10^{12} ions.cm^{-2}, a rutile phase mixed with brookite phase is formed. The particle size estimated using Scherrer's formula (FWHM 0.85) is 16 nm. This amorphous to crystalline phase transition observed during irradiation can be attributed to SHI induced athermal annealing. Amount of deposited energy increases with increasing fluence leading to increase in crystallinity. When irradiation fluence is still increased further to 1×10^{13} ions.cm^{-2} again the amorphous phase is formed. At this fluence as number of impinging ions is more and closely spaced latent tracks are formed. Formation of amorphous phase is due to overlapping of tracks. (Not shown in Fig. 1).

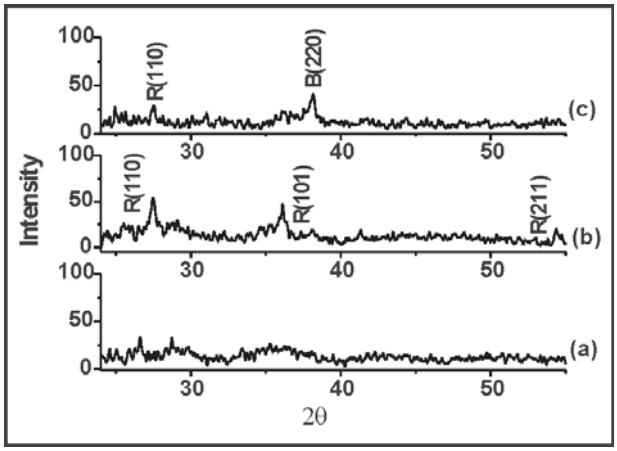

Fig. 1. GAXRD spectrum of 100 nm thick amorphous TiO_2 film

(a) as-deposited
(b) irradiated by 100 MeV Au ion beam at a fluence of 1×10^{11}ions.cm^{-2}
(c) irradiated by 100 MeV Au ion beam at a fluence of 1×10^{12}ions.cm^{-2}

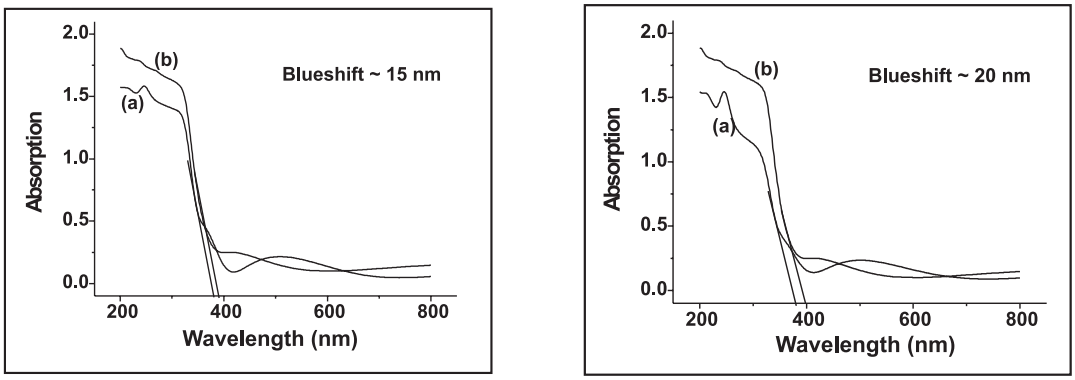

Fig. 2. UV-VIS absorption spectra of 100 nm thick TiO_2

(a) (a) as-deposited film and (b) film irradiated by 100 MeV Au ion beam at a fluence of 1×10^{11}ions.cm^{-2}

(b) (a) as-deposited film and (b) film irradiated by 100 MeV Au ion beam at a fluence of 1×10^{12}ions.cm^{-2}

Fig 2 (a) and (b) show absorption spectra of as-deposited and irradiated films. The blue shift of 15 nm and 20 nm is observed in absorption band edge of the film irradiated at a fluence of 1×10^{11} ions.cm^{-2} and 1×10^{12} ions.cm^{-2} respectively. The observed blue shift is due to quantum confinement of nanostructures formed after irradiation. The absorption band edge of the film irradiated at a fluence of 1×10^{13} ions.cm^{-2} remains unchanged as amorphous phase of this film is not changed after irradiation.

We conclude that nanocrystallisation is induced in TiO_2 films deposited by e-beam evaporation method by Au ion beams. The nanophase formation is observed upto irradiation fluence of 1×10^{12} ions.cm^{-2}. Nanostructure formation can also be inferred from blue shift observed in UV-VIS absorption spectra.

5.2.18 Irradiation led nanoarray patterning for binary semiconductor nanoparticles

U. Das[1], D. Mohanta[1], A.Choudhury[1,2], F. Singh[3], A. Tripathi[3] , D. K. Avasthi[3] and G. Stanciu[4]

[1]Nanoscience Laboratory, Department of Physics, Tezpur University, Sonitpur, Assam

[2]Gauhati University, Gopinath Bordoloi Nagar, Guwahati, Assam-781 014, India

[3]Inter-University Accelerator Centre, Aruna Asaf Ali Marg, New Delhi - 67

[4]Department of Physics, University "Politehnica" of Bucharest, 313 Splaiul Independentei str., sector 6, 060032 Bucharest, Romania

Recently, elongated nanostructures (nanowires, nanorods or nanoneedles etc.) are gaining importance owing to a number of interesting properties. The asymmetric morphology of these nanostructures has great advantage compared to spherical nanoparticles. These 1-dimensional nanostructures can display polarized light emission [1], lasing with lower gain threshold [2], suppressed non-radiative Auger-recombination [3] and improved photo-voltaic efficiency [4]. There is opportunity in fabricating stable elongated nanostructures using swift heavy ion irradiation on embedded nanostructured systems, if ion, energy and fluence are selected efficiently.

As a starting material CdS:Mn nanoparticles were grown in styrene butadiene rubber matrix. Previously, we have reported that 80 MeV oxygen ion irradiation led to formation of CdS:Mn elongated nanostructures which were characterized by scanning probe microscopy (SPM) and photoluminescence spectroscopy [5].

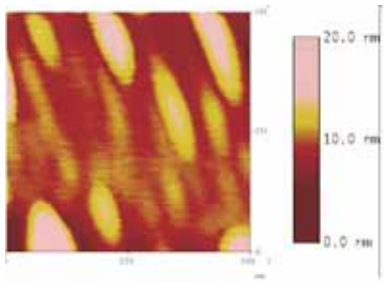

Fig. 1. Elongated ZnS nanostructures due to irradiation

Next, 150 MeV titanium ion irradiation experiment was performed on undoped and transition metal doped ZnS nanoparticles embedded in a rigid and atactic polymer matrix (polyvinyl alcohol-PVOH) [6]. Structural modification in the form of elongation (oblate and flat shaped nanostructures) was observed along the direction perpendicular to the ion beam path (Fig.1). We speculate that the selection of heavy ion has something to do with push-in (pressure) effect which might alter the shape of the nanoparticles before allowing them to coalesce along the beam direction. Electron microscopic studies have revealed that these nanostructures have fluence dependent nanoparticle growth where as photoluminescence studies display luminescence quenching with increasing fluence (Fig.2). The detailed mechanism has been published elsewhere [6,7].

Also, we had considered irradiation with light ions. 100-MeV chlorine ion bombardment on ZnS nanoparticles in PVOH matrix reveals nanoparticle growth along the direction of the beam which is consistent to our earlier prediction [5]. The atomic force microscopy (AFM) images revealed elongated nanostructures. Light ion has less pressure effect while impinging into the sample allowing nanoparticle growth along the direction of ion-passage. The theoretical considerations that might help in understanding such experimental observation are in progress.

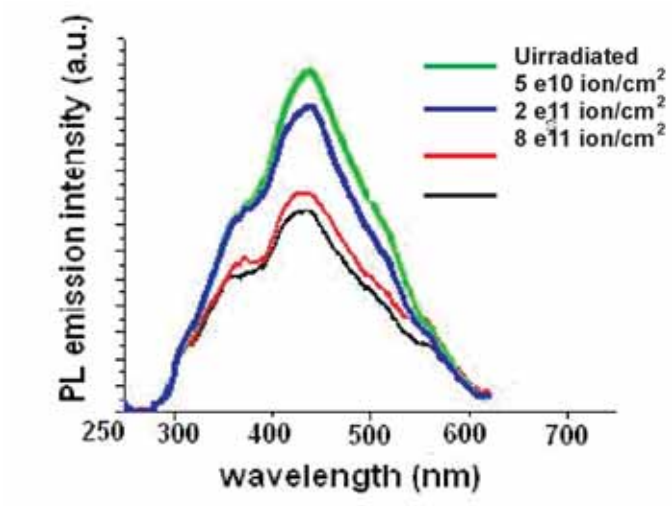

Fig. 2. PL of unirradiated and irradiated nanostructures

REFERENCES

[1] J. Hu, L. Li, W. Yang, L. Manna, L. Wang & A.P. Alivisatos, Science 292 (2001) 2060.

[2] M. Kazes, D.Y. Lewis, Y. Ebenstein, T. Mokari, U. Banin, Adv. Mater. 14 (2002) 317.

[3] H. Htoon, J.A. Hollingworth, A.V. Malko, R. Dickerson, V.I. Klimov, Appl. Phys. Lett. 82 (2003), 4776.

[4] W.V. Huynth J.J. Dittmer, A.P. Alivisatos, Science 295 (2002) 2425.

[5] D. Mohanta, G.A. Ahmed, A. Choudhury, F. Singh, D.K. Avasthi, G. Boyer & G.A. Stanciu, EPJ: Appl. Phys. 35 (2006) 29-36.

[6] U. Das, D. Mohanta G.A. Ahmed A. Choudhury F. Singh D.K. Avasthi, Ind. J. Phys., 81 (2007), 155-159

[7] U. Das, D. Mohanta, G.A. Ahmed, A. Choudhury, F. Singh , D.K. Avasthi, Ind. J. Phys., 82 (*In press*, February-2008)

5.2.19 Nanotrack Formation on MOCVD Grown Gallium Nitride Epilayers using Ni Ions Irradiation

V. Suresh Kumar[1], J. Kumar[1], S. Munawar Basha[1], P. Puviarasu[1], D. Kanjilal[2], F. Singh[2], A. Tripathi[2] and K. Asokan[2]

[1] Crystal Growth Centre, Anna University, Chennai – 600 025

[2] Inter-University Accelerator Centre, Aruna Asaf Ali Marg, New Delhi – 67

Metal organic chemical vapour deposition (MOCVD) grown Gallium nitride (GaN) epilayers were irradiated with 100 MeV Ni^{9+} ions and of fluence 1×10^{12}, 1×10^{13} and 5×10^{13} ions/cm^2 at room temperature and low temperature. Figure 1 shows the AFM image of GaN irradiated at room temperature to a fluence of 5×10^{13} ions/cm^2. The observed rms roughness value increases with increasing ion fluences, which are 1.4, 1.7 and 5.8 nm. It is observed that nano tracks are produced by Ni^{9+} ions upon irradiation at higher fluences. The total number of the tracks are varying by fluences [1,2]. The dimensions of the tracks are around 60 nm.

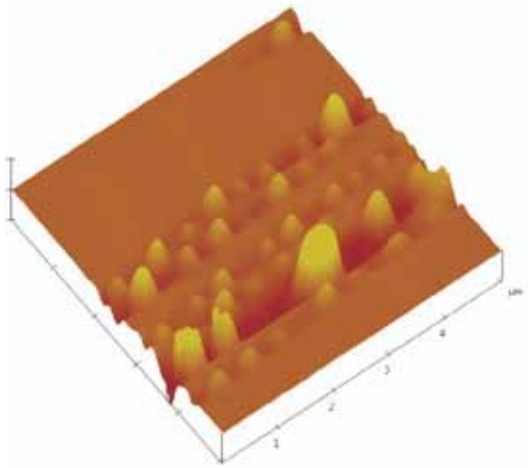

Fig. 2. PL spectrum of (a) pure GaN and irradiated with 100 MeV Ni $^{9+}$ions at a fluence of (b) 1×10^{12}, (b)1×10^{12} and (d)1×10^{12} ions/cm^2

XRD results reveal the Ga_2O_3 formation after Ni ions irradiation on GaN. This results is matched with the reported literatures [3]. Figure 2 shows the PL spectra of unirradiated GaN and Ni^{9+} ions irradiated samples recorded at room temperature. The pristine GaN exhibits a near band-edge emission peak at 3.4 eV and a broad yellow band centered at 2.38 eV. It is observed that after irradiation the yellow emission shifts towards the blue band side centered at 3.7 eV. This shift is due to the nitrogen vacancy creation after ion irradiation [4] and luminescence and band edge emission decrease after irradiation. The high energy radiation induced defects are responsible for the observed change in PL spectra. At higher fluence, there is no luminescence observed.

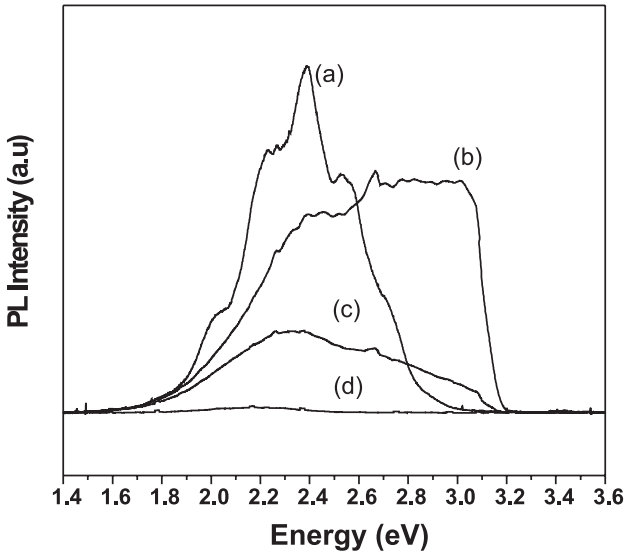

Fig. 2. PL spectrum of (a) pure GaN and irradiated with 100 MeV Ni $^{9+}$ions at a fluence of (b) 1×10^{12}, (b)1×10^{12} and (d)1×10^{12} ions/cm^2

REFERENCES

[1] T. Mohanty, N.C. Mishra, F. Singh, U. Tiwari and D. Kanjilal. 212 (2003) 179.

[2] S.O Kucheyev, H.J. Timmers Zou, J.S. Williams, C Jagadish and G. Li. 95 (2004) 5360.

[3] V. Suresh Kumar, M. Senthil Kumar, T. Mohanty, A. Tripathi, D. Kanjilal, K. Asokan and P.K. Kulyria 162 (2007) 229.

[4] S. Dhara. Solid State Mat. Sci., 32 (2006) 1.

5.2.20 Swift heavy ion irradiation induced modification of semiconducting oxide nanostructures

T. Mohanty[1], A. Tripathi[2] and D. Kanjilal[3]

[1]School of Physical Sciences, J.N.U, New Delhi, India-110 067

[2]Inter University accelerator Centre, Aruna Asaf Ali Marg, New Delhi - 67

Nanostructured oxide materials are currently attracting increasing attention due to the possibility of their applications in solar cells, sensors, photo detectors, field effect transistors and microelectronics. Among metal oxide thin films tin oxide (SnO_2) thin films are stable large band gap semiconductors which have excellent photoelectric properties, gas sensitivities and superior chemical stability. Studies of structural, morphological and optical properties of SnO_2 nanocrystalline films are necessary in order to fabricate high efficiency devices. In this work, modification of tin oxide nanocrystalline thin films grown on transparent substrates were carried out by energetic ion bombardment. Energetic ions create Frenkel pairs deep within a crystalline solid which typically have high mobilities, thereby accelerating structural reorganization. Nanostructured thin films of SnO_2 were grown by e-beam evaporation on both amorphous (quartz) as well as crystalline

(sapphire) substrates. Morphology of as-deposited films analyzed by AFM studies shows wide variation in size. These films were bombarded by 150 MeV silver (Ag) beams. Ion bombarded films as well as as-deposited films were characterized by GAXRD, AFM and UV/Visible absorption techniques for structural, morphological and optical characterizations. Shifting of optical absorption band edge after ion bombardment shows the effect of quantum confinement in these nanostructured thin films. Changes in the size and structure of nanocrystalline grains by few nanometers induced by ion bombardment are analyzed. Uniformity in nanocrystalline grain size is achieved after ion bombardment in thin films grown on different substrates. Effect of substrate and fluence on grain size modification is studied in detail.

With increase of fluence from $1x\ 10^{11}$ to $5 x\ 10^{11}$, observation of mass flow towards one direction is observed. This phenomenon is more observed in quartz substrates. It is expected that ion bombardment had induced surface diffusion of atoms and had affected the morphology of nanostructures.

REFERENCES

[1] T. Mohanty, P.V. Satyam and D. Kanjilal, J. of Nanosci. and Nanotechnol, 6 (2006) 2554

[2] T. Mohanty, Y. Batra, A. Tripathi and D. Kanjilal, J. of Nanosci. and Nanotechnol. 7 (2007) 2036

5.2.21 Role of microstructure in determining the energy relaxation processes of swift heavy ions in semiconductors

V V Ison[1,4], A Ranga Rao[1], V Dutta[1], P K Kulriya[2], D K Avasthi[2] and S K Tripathi[3]

[1] Photovoltaic Laboratory, CES, IIT Delhi, Hauz Khas, New Delhi 110016

[2] Inter University Accelerator Center, Aruna Asaf Ali Marg, New Delhi - 67

[3] Department of Physics, Panjab University, Chandigarh 160014

[4] Department of Physics, St. Thomas College, Pala, Arunapuram 686574

The data on swift heavy ion irradiation in semiconductors show that the energy relaxation processes are influenced not only by the electronic energy deposition, but also by several material properties. A combination of material characteristics will be contributing to the ion beam induced changes that make the interaction mechanism extremely complex [1,2]. A quantitative picture of the material characteristics that decide the energy relaxation mechanism of swift heavy ions will also help in preparing a material that can be engineered properly for its applications. This study highlights the role of film microstructure in determining the energy relaxation processes of heavy ions in semiconductors. Two sets of CdTe polycrystalline thin films prepared using vacuum evaporation and spray pyrolysis that differ in their microstructure are irradiated with with 100 MeV Ag^{7+} ions using 15 UD Pelletron accelerator at fluences 3×10^{10}, 1×10^{11}, 3×10^{11}, 1×10^{12}, 3×10^{12} and 1×10^{13} ions/cm^2. The differences are noticed in the response of the two sets of films to the beam are correlated with the differences in their microstructure.

The evaporated films exhibit an annealing of defects at lower fluences indicated by an increase of peak intensity and grain size. At higher fluences, being the energy deposited is very high, a partial loss of zinc-blende structure is seen due to the creation of point defects, defect clusters etc. An increase of lattice constant with fluence is observed for these films due to an increase of tensile strain within and between the grains. The interplay between the defect annealing and defect generation noticed in the evaporated films is not seen in spray deposited films. The crystallinity of these films follows a continuously decreasing trend with irradiation fluence. The lattice constant remains constant with irradiation, as there is no variation for the strain in the film. The pressure accumulated in the grains during irradiation may be easily transported away due to the presence of large voids in these films. The effects due to defect annealing if at all present in spray deposited films is completely overshadowed by the effects of defect creation at all fluences [3,4]. A decreasing trend observed for the bandgap of the two sets of films shows that by suitable adjusting the ion fluence, we may introduce defect levels in the materials band structure in a controlled way [5].

REFERENCES

[1] W. Wesch, A. Kamarou,E. Wendler, Nucl. Instrum. Methods. B 225 (2004) 111

[2] S.O. Kucheyev, H. Timmers, J. Zou, J.S. Williams, C. Jagadish, G. Li, J. Appl. Phys. 95 (2004) 5360

[3] A. Benyagoub, Nucl. Instrum. Methods. B 225 (2004) 88

[4] Y.S. Chaudhary, S.A. Khan, R. Shrivastav, V.R. Satsangi, S. Prakash, D.K. Avasthi, S. Dass Nucl. Instrum. Methods. B 225 (2004) 291

[5] P.M. Ratheesh Kumar, T.T. John, C. Sudha Kartha, K.P. Vijayakumar K P, Nucl. Instrum. Methods. B 244 (2006) 171

5.2.22 Structural evolution of TiO_2 thin film by Thermal Annealing and Swift Heavy Ion Irradiation

H.Rath[1], S. Ananda[2], M. Mohapatra[2], P.Dash[1], T. Som[3], P.V. Satyam[3,] U.P. Singh[4] and N.C. Mishra[1]

[1]Department of Physics, Utkal University, Bhubaneswar 751 004

[2]Institute of Minerals and Materials Technology, Bhubaneswar 751 013

[3]Institute of Physics, Bhubaneswar 751 005

[4]KIIT University, Bhubaneswar 751024

Nano-crystalline titanium dioxide (TiO_2) is one of the extensively investigated material in thin film form because of its applications [1]. It exists in nature in three major crystalline structures: rutile, anatase, and brookite. In the present study, we probe into the structural phase transition from anatase to rutile in nanocrystalline thin films under thermal annealing and swift heavy ion (SHI) irradiation. TiO_2 thin films were prepared through chemical route using sol-gel and spin coating techniques on silicon (100) substrates. Films were characterized by X-ray diffractometer (Bruker-D8) in a grazing incidence mode with Cu K_α radiation and Micro-Raman Spectrometer (Renishaw-

INVIA).We show that annealing of the film leads to crystallization in the anatase structure above 400° C and partial conversion to rutile phase above 700° C. Annealing the films at 1000° C does not lead to complete conversion from anatase to rutile phase. This observation is in conformity with earlier observations of the lack of complete conversion to rutile phase in films annealed even up to 1100° C [2]. Irradiating the 1000° C annealed films by 200 MeV Ag ions however led to formation of pure rutile phase at a fluence of 3×10^{12} ions.cm^{-2}. Other phases like the tetragonal dTiO and the hexagonal phases of TiO evolve at intermediate fluences (Fig.1a). At the highest fluence (3×10^{12} ion.cm^{-2}) of irradiation however, the peak due to rutile phase is most intense and that due to all other phases are suppressed. Raman spectra (Fig.1b) also indicate complete phase transformation from anatase to rutile phase in films irradiated at the fluence of 3×10^{12} ion/cm^2. Though thermal annealing could not lead to complete conversion from anatase to rutile phase, irradiation by 200 MeV Ag ions resulted in complete conversion to rutile phase.

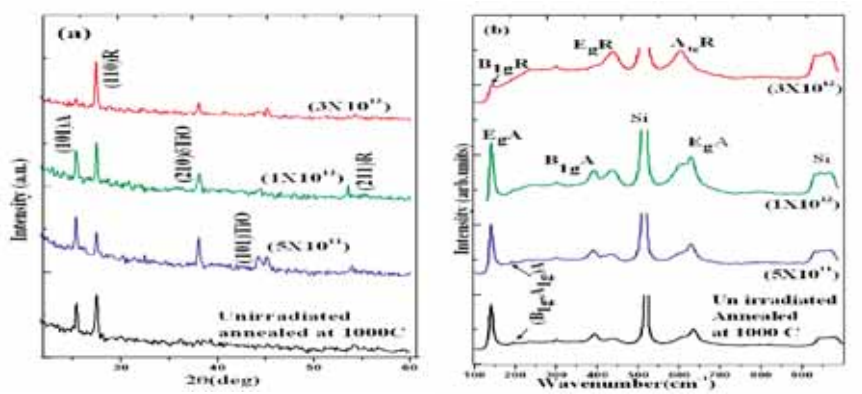

Fig. 1. Evolution of (a) GAXRD and (b) Raman spectra of TiO_2 thin film with 200 MeV Ag ion irradiation

REFERENCES

[1] Z. W. Zhao, B. K. Tay, J Electroceram 16 (2006) 489

[2] S. Yamamoto, T. Yamaki, H. Naramoto, S. Tanaka, Nucl. Instr and Meth. B 206 (2003) 268

5.2.23 In-situ XRD studies on $YBa_2Cu_3O_{7-x}$ thin films with SHI irradiation at low temperature

R Biswal[1], J John[2], P K Kulriya[3] and N C Mishra[1]

[1]Department of Physics, Utkal University, Bhubaneswar 751004, India

[2]Tata Institute of Fundamental Research, Mumbai 400005, India

[3]Inter University Accelerator Center, Aruna Asaf Ali Marg, New Delhi 110067, India

The epitaxial YBCO thin films of thickness ~ 150nm were deposited by pulsed laser deposition technique on single crystal $LaAlO_3$ substrate using KrF Excimer pulsed laser (248nm wavelength) in oxygen atmosphere. The films were irradiated at 89 K with 200 MeV Ag ions using the 15 MV tandem Pelletron accelerator at the IUAC, New Delhi. The XRD data were collected

in-situ at different fluences of irradiation at 89 K using Cu K_α radiation from Brucker X-ray diffractometer (Model D8) under identical conditions. The irradiation fluence, Φ was varied from 1×10^{10} ions cm^{-2} to 2×10^{13} ions cm^{-2}. The ion beam was magnetically scanned over the complete sample surface for uniform irradiation. The scan patterns of the films show the sharp $(00l)$ peaks (l= 2 to 7) indicating grain orientation along c-axis. Figure 1a presents some X-ray spectra after irradiation with different fluences of 200 MeV Ag ions. The spectra exhibit a noticeable reduction in peak intensity of with irradiation, which is an indication of amorphization of the sample along the ion path. Along with intensity reduction, the shifting of peak towards lower angle (i.e. increase of lattice parameter 'c') is shown in figure 1b. This shifting can arise due to the concentration of point defects after irradiation around the ion path at LT, where the defect diffusion is restricted and to the strain field imposed by the amorphized track on the surrounding medium. The former process can arise due to SHI induced secondary electrons [1, 2]. These defects are stabilized at LT, which anneal out on warming the sample to room temperature (RT). We have also done in-situ XRD at RT on an identical film at several increasing fluences for comparison. The c- axis lattice parameter shows 0.6% increase with increasing fluence up to ions cm^{-2} at RT, while it is 1.3% for LT irradiated film. This result reveals possibility of point defect creation at LT that provides the extra contribution to c-axis increase.

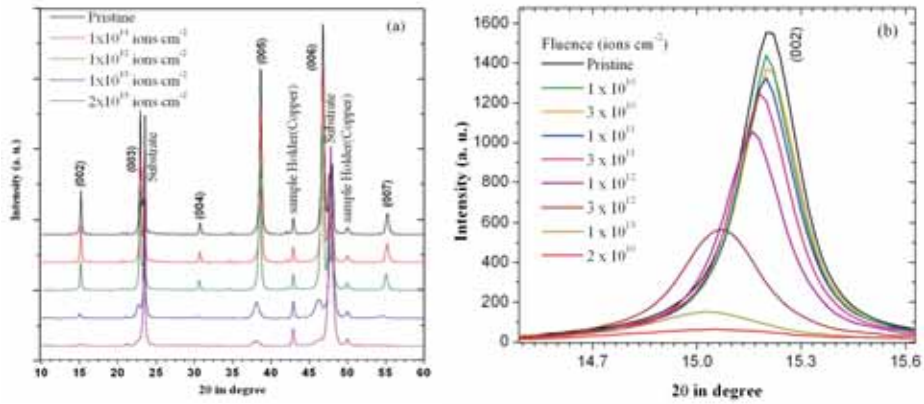

Fig. 1. In-situ X-ray 2θ diffraction pattern of (a) YBCO thin film at various fluences and (b) (002) peak only

REFERENCES

[1] D. Behera, T. Mohanty, S. K. Dash, T. Banerjee, D. Kanjilal, N.C. Mishra, Radiation Measurements 36 (2003) 125.

[2] R. Biswal, J. John, D. Behera, P. Mallick, S. Kumar, D. Kanjilal, N.C. Mishra, Indian J. Phys. 82 (2008) 109.

5.2.24 Influence of 100 MeV oxygen ion irradiation on Ni/n-Si (100) Schottky barrier characteristics

Sandeep Kumar, Y. S. Katharria and D. Kanjilal

Inter-University Accelerator Centre, Aruna Asaf Ali Marg, New Delhi – 67

Controlling the metal-semiconductor (MS) interface properties is a crucial issue in device fabrication. Ion implantation has found universal acceptance for this process because of its ability to introduce dopants with precise concentration profiles. The practical consequence of this constraint is the necessary dopant activation after implantation, which requires a relatively high-temperature thermal annealing step. High-temperature annealing results in dopant redistribution and hence partial loss of Schottky barrier height control. Any attempt to reduce dopant redistribution by lowering the thermal cycling would result in incomplete activation of the dopant as well as residual damage that could manifest itself as an increase in the leakage current and noise. Therefore, new reliable processes for a better control of the properties of Ni/n-Si are required. The aim of present work is examine the possibilities of using high energy swift heavy ions (when velocity of ion comparable to Bohr velocity of electron) to tailor the characteristics of Ni/n-Si Schottky barrier. In this paper, we report the effects of 100MeV O^{+8} ion irradiation on Ni/n-Si Schottky barrier as a function of ion fluence. It is shown that irradiation by high energy oxygen ions results in an improved value of Schottky barrier height accompanied by a decrease in the value of ideality factor.

Schottky diodes were fabricated on *n*-type Si (100) wafer. First a silicon dioxide layer (1 μm thick) was deposited on the wafer front side. The Ohmic contact on the highly doped side was formed by sintering of a 200 nm thick Ti/Au film. The Schottky contact was formed by thermal evaporation of about 150 nm thick Ni film. The ion irradiation was performed at room temperature by 100 MeV O^{+8} ion beam using the 15UD Pelletron accelerator facility at Inter-University Accelerator Centre, New Delhi. 100 MeV O^{+8} ions have a mean projected range of 95.2μm inside the silicon after crossing the interface with $(S_e/S_n) \sim 1800$ at the interface. The ion fluence was varied from 1×10^{9} to 1×10^{13} ions cm^{-2}. The electrical properties of the Ni/n-Si Schottky barrier were investigated by *in situ* current voltage (*I–V*) measurements of the diodes carried out using a Keithley 2400 source meter unit.

As prepared metal-semiconductor contacts usually exhibit non-ideal current-voltage characteristics. In case of a moderately doped semiconductor, thermionic emission is the dominant current transport mechanism across the barrier at room temperature [1]. From a fit of linear region of the forward bias *I-V* characteristics, the values of ideality factor and Schottky barrier height were determined.

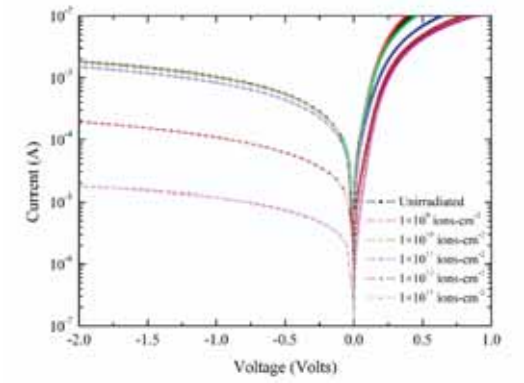

Fig. 1

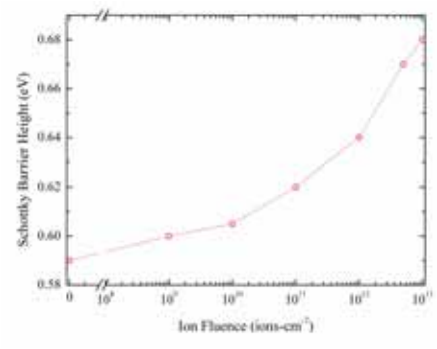

Fig. 2

For the unirradiated diode the barrier height is 0.59eV. Interestingly, the SHI irradiation results in an increase of the Schottky barrier height until Φ_B reaches the value of 0.68 eV after irradiation at fluence of 1×10^{13} ions-cm^{-2}. The variation of barrier height with the irradiation fluence is shown in Fig.2. The ideality factor decreases from a value of 1.3 to 1.1 after ion irradiation. It is noteworthy that, compared to traditional implantation and heavy ion irradiation studies on n-Si, irradiation by 100MeV O^{8+} shows reverse effects on modifying Schottky rectification characteristics. Irradiation by oxygen ions at 100 MeV has led to significant increase in barrier height and about two order of magnitude reduction in leakage current. The increase in the value of the Schottky barrier height is connected to a decrease of the leakage current with increasing irradiation fluence (Fig.1). Change in barrier height indicates a change in electrical properties of the MS interface. An increase in series resistance was found for all irradiation fluences, indicating that the product of the mobility and carrier concentration has reduced. The reduction in mobility is due to the introduction of defect centers on irradiation, which act as scattering centers. The capacitance decreases as the ion irradiation fluence increases. Decrease in capacitance implies a widening in the semiconductor depletion width. Since the charge neutrality condition at the interface should be satisfied, widening of the depletion width results from a reduction of the ionized donor concentration (N_D). One of the possible mechanisms is that ion irradiation produces defects with energy levels below the Fermi level in n-type material. These defects will capture electrons from the conduction band and reduce the equilibrium electron concentration. The carrier concentration decreases from a value of 1.9×10^{16} cm^{-3} for unirradiated diode to 6.3×10^{15} cm^{-3} after an irradiation fluence of 1×10^{13} ions-cm^{-2}. These defects result in the compensation of the positive shallow donors in the depletion region so that the effective net ionized-donor concentration is decreased. The barrier thickness depends on N_D through the depletion width ($\propto N_D^{-1/2}$); in this case, a dopant deactivation at near MS interface determines an increase of the Schottky barrier thickness (d), which contributes to the decrease of the leakage current in reverse bias. As a consequence of the dopant deactivation after ion irradiation a modification of the potential and electric field distribution will occur at near-interface region that can be a reason for the increase of the barrier height.

In this work the effect of 100 MeV O^{+8} ion irradiation on Ni/n-Si (100) Schottky barrier using i*n-situ* current-voltage characterization as a function of irradiation fluence has been studied. A significant increase of Schottky barrier height from a value of 0.59 eV for unirradiated diode to 0.68 eV is achieved after irradiation at a fluence of 1×10^{13} ions/cm^2. Current-voltage characteristics reveal that with an optimal choice of the irradiation parameters these results could find useful applications in the control of the Schottky barrier height of Ni/n-Si (100) structures.

REFERENCES

[1] E. H. Rhoderick, R. H. Williams. *Metal-semiconductor contacts*, 2nd ed. (Claredon, Oxford, 1988.)

5.2.25 Growth of nano-pillars and nano-dots on the surface of copper sulphide thin film using 100 MeV Au ion irradiation

Abhay A. Sagade[1], Y. G. Gudage[1], Ramphal Sharma[1], F. Singh[2], A. Tripathi[2] and Neeti Tripathi[2]

[1] Thin Film and Nanotechnology Laboratory, Department of Physics, Dr. Babasaheb Ambedkar Marathwada University, Aurangabad- 431004, Maharashtra

[2] Inter-university Accelerator Centre, Aruna Asaf Ali Marg, New Delhi – 67

Recently, there are number of reports on the ion beam pattering on the surface of solids using heavy ions (SHI) of energies in MeV's [1, 2]. In this study, of CuS thin films were prepared by using solution growth technique at room temperature (298 K) on glass substrates. The post deposition treatment of ion beam irradiation was performed on 200 nm thick and 1×1 cm^2 targets using 15 UD tandem Pelletron accelerator at Inter-University Accelerator Center (IUAC), New Delhi, India. The sample resistivity was 100 Ω-cm. The irradiation was performed at a 90° angle of incidence with respect to the surface. Ion beam was scanned on the sample surface by magnetic scanner for uniform irradiation. During irradiation the temperature of the samples was maintained at 300 K. The chamber pressure during irradiation was 1.2×10^{-6} torr. Four samples were loaded on the target ladder and irradiated at fluence values of 10^{11}, 5×10^{11}, 10^{12} and 5×10^{12} ions/cm^2. Scanning probe microscope (SPM) Nanoscope IIIA from Veeco was used to image the irradiated sample surfaces with a silicon nitride cantilever and tip radius of 20 nm operated in tapping mode. Images ranging from 0.5 to 5 μm^2 were obtained. The photoluminescence (PL) measurements were performed by using 320 nm LASER from Cd-He source. The experiments were performed in dark room and local software is used for the acquisition of data.

The surface topography of as-deposited (pristine) and SHI irradiated films is first observed through AFM. The AFM image of pristine surface is featureless and smooth surface. Ion beam induced growth of CuS nanostructure starts from first fluence of 10^{11} ions/cm^2. Irradiating with 5×10^{11} ions/cm^2 fluence, the small nanostructures are converted into very well separated big and vertical nano-pillars. Further, at fluence of 10^{12} ions/cm^2 the number of heavy ions coming at the surface of film increases and hence the nano-pillars gets coalesce to form appended pillars.

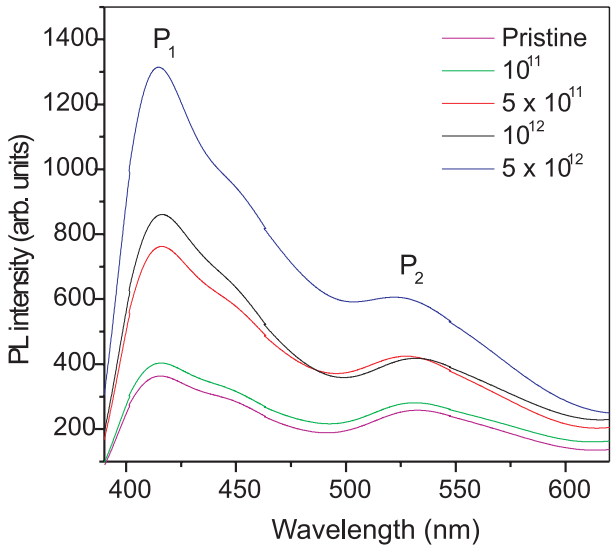

Fig. 1. PL of the Pristin and irradiated samples

The PL measurements carried out at room temperature is shown in Fig. 1. There are two peaks namely P_1 and P_2 from CuS surface. The second peak P_2 is attributed to band edge emission at 533 nm for pristine sample. This P_2 peak is blue shifted from 533 nm for pristine sample to 526 nm for the fluence of 5×10^{12} ions/cm^2, which is manifestation of formation of nanostructure. The other peak P_1 is assigned to excitonic emission [3]. Here, intensity of P_1 peak increases with fluence indicating that emission is from highly co-ordinated nanostructure grown on the surface of CuS thin film.

REFERENCES

[1] E.M. Bringa, R.E. Johnson and R.M. Papaleo Phys. Rev. B 65 (2002) 094113; D. Pramanik and S. Varma Nucl. Instr. And Meth. B 244 (2006) 81.

[2] Abhay A. Sagade *et al* Rad. Eff. Defects Solids 16 (2007) 77; R. R. Ahire, Abhay A. Sagade *et al* J. Phys. D: Appl. Phys. 40 (2007) 4850.

[3] P. Roy and S.K. Srivastava Crys. Growth and Design 6 (2006) 1921.

5.2.26 Swift Heavy Ion Induced Recrystallization of SOI Structures

A. D. Yadav[1], S. K. Dubey[1], Rucha H. Polji[1] and Saif A. Khan[2]

[1] Department of Physics, University of Mumbai, Vidyanagari campus, Santacruz (E), Mumbai

[2] Inter University Accelerator Centre, Aruna Asaf Ali Marg, New Delhi - 67

Silicon on insulator (SOI) structures have attracted significant research interest for future nanometer scale devices. The SOI substrates can be obtained by high fluence ($\geq 10^{17}$–10^{18} cm^{-2}) ion implantation of nitrogen and / or oxygen ions into silicon (Si) at 100–200 keV energy. The annealing is essential step to remove the implantation induced damage to recover the crystallinity of the silicon. The ion-beam-induced epitaxial crystallization (IBIEC) is of current interest as an alternative method for damage recovery of ion-implanted materials. Swift heavy ion (SHI) irradiation through an amorphous/crystalline interface causes solid phase epitaxy or layer by layer crystallization. IBIEC has been shown to take place in silicon and other materials at considerably lower target temperatures than necessary for thermal annealing when performed under irradiation. In the present work, SHI induced recrystallization effects in silicon oxynitride layers, synthesized by N and O implantation in silicon are studied. The recrystallization of the silicon is investigated using Fourier transform infrared (FTIR) spectroscopy.

In the present experiment, buried silicon oxynitride ($Si_xO_yN_z$) insulating layers were synthesized by 150 keV nitrogen ($^{14}N^+$) and oxygen ($^{16}O^+$) ion implantation into single crystal silicon wafers using low energy ion beam facility (LEIBF) at the Inter University Accelerator Center (IUAC), New Delhi. For SHI induced recrystallization of silicon the as implanted SOI wafers were irradiated by 60 MeV Ni^{+5} ions to a fluence of $1x10^{14}$ cm^{-2} in a vacuum of $4.9x10^{-7}$ mbar. The temperature of the sample was held at 270 ^{0}C during the irradiation process. The irradiation

was carried out using the beam from 15 UD Pelletron accelerator at Inter University Accelerator Center, New Delhi. The total fluence of $1x10^{14}$ cm^{-2} was estimated by integrating the total charge by current integrator.

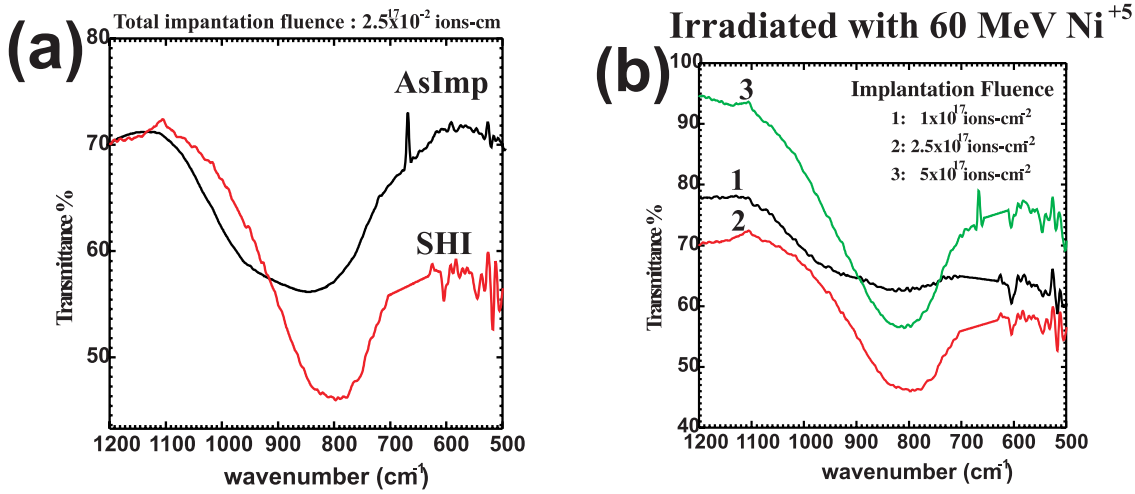

Fig. 1: FTIR spectrum of silicon sample implanted with nitrogen and oxygen

(a) As implanted sample (implantation fluence $2.5x10^{17}$ cm^{-2}) before and after irradiation with 60 MeV Ni^{+5}

(b) Comparative study of FTIR spectra for different implantation fluences

The silicon sample implanted with nitrogen and oxygen at 150 keV with fluence $2.5x10^{17}$ cm^{-2} was characterized by the FTIR spectroscopy before and after SHI irradiation as shown in Fig. 1(a). The as implanted sample shows a single absorption band in the range 1200-600 cm^{-1} which is attributed to the formation of silicon oxynitride structures [1]. The broad absorption spectrum is associated with the amorphous nature of the oxynitride layer formed after implantation. After irradiation with 60 MeV Ni^{+5}, it is observed that the peak position shifts towards lower wavenumber. The peak position at 830 cm^{-1} resembles Si-N stretching vibration mode [1,2]. The sharpening of peak indicates the formation of more ordered oxynitride compound. The recrystallization of the layer is also evidenced by decrease in the FWHM of the FTIR absorption spectra.

Since nitrogen is having lower solubility in silicon, the deposition of energy through electronic energy loss phenomenon leads to the rearrangement of nitrogen atoms more effectively [3, 4]. This results in the structural phase change in the buried layer. For higher fluence of implantation structural changes after irradiation are found to be more prominent Fig. 1(b).

REFERENCES

[1] J.A. Diniz, A.P. Sotero, G.S. Lujan, P.J. Tatsch, J.W. Swart Nucl. Instr. and Meth. B 166 (2000) 64.

[2] D. V. Tsu, G. Lucovsky, M. J. Mantini. S. S. Chao, J. Vac. Sci. Technol. A, 5 (1987) 1998.

[3] Prajakta S. Chaudhari , Tejashree M. Bhave, Renu Pasricha , Fouran Singh, D. Kanjilal, S.V. Bhoraskar, Nucl. Instr. and Meth. B 239 (2005) 185.

[4] A. I. Belogorokhov, V. T. Bublik, K. D. Scherbachev, Yu. N. Parkhomenko, V. V. Makarov, A.B. Danilin, Nucl. Instr. and Meth. B 147 (1999) 320.

5.2.27 Defect Characterization and Its Correlation with the Transport and Magnetic Property of ZnO Based Dilute Magnetic Semiconductor

Soubhik Chattopadhyay[1], A. Banerjee[1], S. Bandyopadhyay[1], D. Jana[1], S. Chattopadhyay[2], A. Sarkar[3] and R. Kumar[4]

[1]Department of Physics, University of Calcutta, 92 A.P.C. Road, Kolkata 700009
[2]Department of Physics, Taki Government College, Taki 743429
[3]Department of Physics, Bangabasi Morning College, 19 R.C. Sarani, Kolkata 700009
[4]Inter University Accelerator Center, Aruna Asaf Ali Marg, New Delhi - 67

Mn doped ZnO has potential application as room temperature dilute magnetic semiconductor (DMS) as predicted by Dietl et al. [1]. We prepared Mn doped ZnO ($Zn_{1-x}Mn_xO$) through conventional solid-state reaction method [2] and characterized them using XRD, UV-Visible absorption spectroscopy, room temperature PAL spectroscopy and room temperature resistivity measurement. Ferromagnetism particularly in this type of DMS samples is mainly carrier mediated. In ZnO samples controlled production of defect states by ion beam irradiation might favor in achieving ferromagnetism through carrier generation. Ion beam irradiation might also be very much useful for single-phase formation [3]. So the studies of effect of ion beam irradiation on the structural, transport, magnetic and optical properties are important.

In this report we mainly present our systematic plans to study the irradiation induced structural modification and physical properties of the system of 2 & 4 at% Mn doped ZnO samples (prepared at 96 hour mixing). These two sets of samples were irradiated by 50 MeV Li^{3+} ions with different fluence of 1×10^{12}, 1×10^{13}, 5×10^{13} and 1×10^{14} ions/cm^2 using the Pelletron accelerator at Inter-University Acceleration Centre (IUAC), New Delhi.

After irradiation the low temperature resistivity measurement of the 2at% Mn doped samples have been done at IUAC. From resistivity data we find that the resistivity has decreased with respect to the unirradiated sample and shows a semiconductor to metal transition, the transition temperature shifted towards the lower temperature with increasing fluence as shown in Fig 1.

REFERENCES

[1] Dietl et. al., Science 287 (2000) 1019

[2] P Sharma et. al., Nature materials 2 (2003) 673

[3] Ravi Kumar et al, Appl. Phys. Lett. 88 (2006) 142502

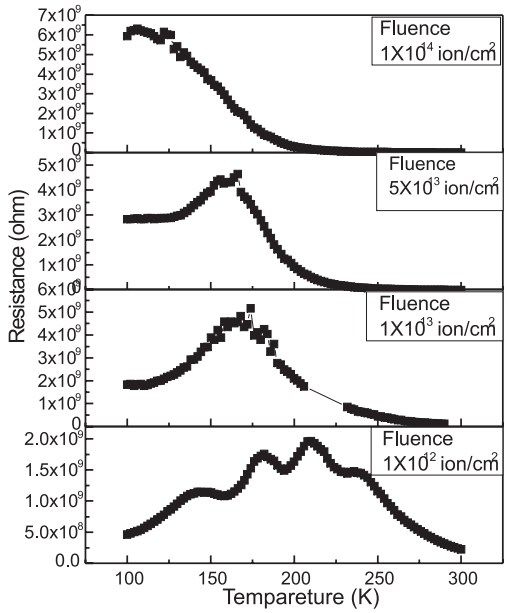

Fig. 1. Variation of resistance of 2 at% Mn doped ZnO at different fluence with temperature

5.2.28 Formation of nanoscale magnetic domains in swift-heavy-ion irradiated GeO_x thin films

Y. Batra, D. Kabiraj, A. Tripathi and D. Kanjilal

Inter University Accelerator Centre, Aruna Asaf Ali Marg, New Delhi - 67

Room temperature magnetism in non-magnetic metallic nanoparticles and carbon nanostructures has been reported by various research groups. We demonstrated the formation of nanoscale magnetic domains in ion irradiated GeO_x thin films. Magnetic force microscopy (MFM) was employed to study the magnetic domain structure in the films. Transmission electron microscopy (TEM) reveals the formation of Ge nanostructures in the irradiated films, which is supported by our micro-Raman results. We explain the formation of magnetic domains in the irradiated films as due to the presence of Ge nanostructures, which are formed as a result of phase separation in the films. GeO_2 was deposited on Si substrates by electron beam evaporation under high vacuum conditions. The thickness of the film was 100 nm, which was measured by calibrated quartz crystal monitor during deposition. The films were irradiated at room temperature for different fluences starting from $1x10^{10}$ ions/cm^2 to $1x10^{13}$ ions/cm^2. The ion beam was scanned over an area of 1 cm^2 for homogeneous irradiation. The electronic energy loss, nuclear energy loss and range of 200 MeV Ag ions in GeO_x are 12.3 keV/nm, 0.032 keV/nm and 26.1 μm respectively, as calculated by SRIM-2006.02. The range of the ions was greater than the film thickness, so no ion was implanted in the films and modifications were expected only due to passage of ion through the films. Pristine as well as irradiated films were characterized by various characterization techniques. MFM studies are carried out by Nanoscope-IIIa atomic force microscope with a magnetized MESP tip.

Fig 1 shows the MFM images of pristine as well as irradiated films of GeO_x at various fluences. Pristine GeO_x thin film (Fig 1(a)) doesn't show any contrast indicating the non-magnetic nature of the films. On the other hand, films irradiated at various fluences show magnetic ordering. Images were taken at various lift heights (distance between tip and sample surface) in order to ensure that the contrast appeared in magnetic images is not purely of topographical origin.

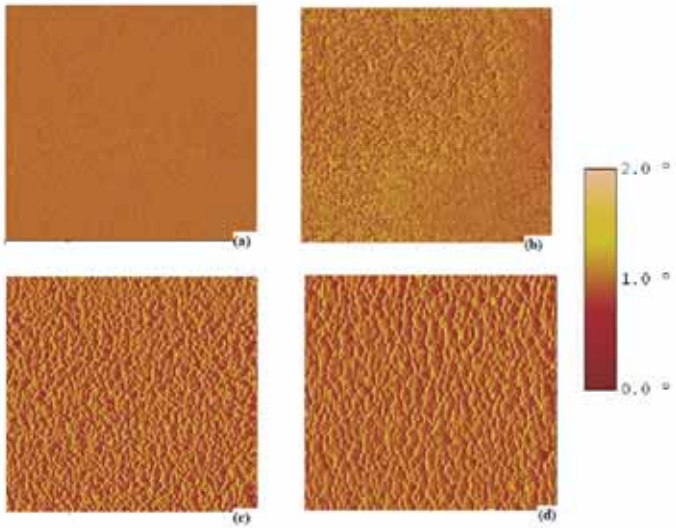

Fig. 1. MFM images (1 μm × 1 μm) of GeO_x thin films (a) pristine (b) irradiated at 1×10^{11} ions/cm^2 (c) irradiated at 1×10^{12} ions/cm^2 (d) irradiated at 1×10^{13} ions/cm^2

In conclusion, we have demonstrated controlled formation of nanoscale magnetic domains in ion irradiated thin films of GeO_x. MFM studies revealed the existence of sharp magnetic contrast in the irradiated films. This type of irradiation induced formation of Ge nanostructure without conventional thermal annealing has the advantage of control over the pattern and depth of formation without appreciable diffusion.

5.2.29 100 MeV Ag^{+7} ion irradiation effects on electrical properties of Li doped NiO thin films

U.S. Joshi[1], P.A. Joshi[1], S.J. Trivedi[1], U.N. Trivedi[2], S.A. Khan[3], D.K. Avasthi[3] and B.M. Arora[4]

[1]Department of Physics, School of Sciences, Gujarat University, Ahmedabad-380 009

[2]Vishwakarma Govt. Engineering College, Chandkheda, Gandhinagar-382 424

[3]Inter University Accelerator Centre, Aruna Asaf Ali Marg, New Delhi - 67

[4]Department of Condensed Matter Physics & Material Sciences, T.I.F.R., Mumbai-400 005

Resistive random access memory (RRAM) is one of the candidate technologies for the promising next generation non-volatile memories with fast switching speed, low power consumption and nondestructive read out. The switching phenomena have been observed in various perovskite

and binary oxides such as $Pr_{1-x}Ca_xMnO_3$ (PCMO) [1], Cr-doped $SrTiO_3$ [2], NiO [3] etc. Among these oxides, polycrystalline NiO has triggered a lot of interest due to its remarkable properties such as simple structure and non-polar switching, that is, the resistance switching is independent of bias polarity [3], while resistance switching in most of the other oxides is caused by the polarity of voltages [1-2]. The observed repetitive resistance switching in ternary and binary oxide thin films is attributed various mechanisms, such as filamentary model, Schottky barrier model, interface model, defect state model and so on. However, the exact mechanism governing the R-switching still remains an open question.

We have investigated the effect of SHI irradiation on the structural and electrical properties of *p*-type wide band gap semiconductor $Li_{0.1}Ni_{0.9}O$ thin films; grown on SiO_2 substrates by chemical solution deposition technique.

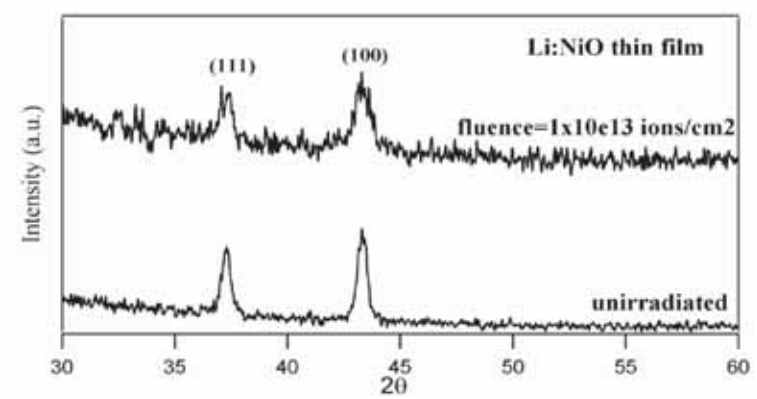

Fig. 1. XRD patterns of $Li_{0.1}Ni_{0.9}O$ thin films before and after 100 MeV Ag^{+7}SHI irradiation

Transparent and semiconducting thin films of Li:NiO were irradiated by 100 MeV Ag^{+7} ions with a dose of $1x10^{13}$ ions/cm^2. Fig. 1 shows the XRD patterns of Li:NiO thin films. Single cubic rock salt NiO structure is observed, even after Ag^{+7} SHI irradiation of high fluence, such as$1x10^{13}$ ions/cm^2. Average crystallite size were estimated from the XRD is found to be in the range of 20-30 nm.

I-V properties were recorded by four probe technique on Ag/Li:NiO/Ag planner geometry at room temperature using Keithley 4200 Semiconductor Characterization System and results are displayed in Fig. 2.

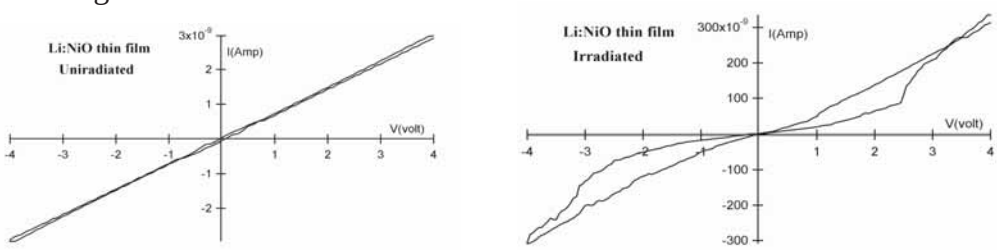

Fig. 2. I-V curves of Li:NiO thin films (a) before and (b) after 100 MeV Ag^{+7} SHI ions irradiation

Linear I-V characteristics have been observed for unirradiated Li:NiO thin films. On the other hand, well defined hysteresis in the I-V curves for the sample irradiated by $1x10^{13}$ ions/cm^2 Ag^{+7} SHI is observed. This suggest the low resistance state (LRS) and high resistance state (HRS) in the film. Symmetrical resistance ratio (R_{high}/R_{low}) of the order of ~ 220% at ± 2.4 V has been observed. The observed results may be attributed to SHI induced defect states in the band gap. Our findings support the defect state model of observed RRAM behaviour. Further investigations are on.

REFERENCES

[1] A. Sawa, T. Fujii, M. Kawasaki and Y. Tokura, Appl. Phys. Lett. 85 (2004) 4073.

[2] Y. Watanabe, J. G. Bedonorz, A. Bietsch, Ch. Gwrber, D. Widmer, A. Beck and S. J. Wind, Appl. Phys. Lett. 78 (2001) 3738.

[3] I. G. Baek, M. S. Lee, S. O. Park, H. S. Kim, U-In Chung, S. Seo, M. J. Lee, D. H. Seo, D. -S. Suh, J. C. Park, I. K. Yoo and J. T. Moon, 2004 IEDM Technical Digest, December, 2004, pp. 587-590.

5.2.30 Observation grain growth in SHI irradiated NiO thin films

P. Mallick[1], Chandana Rath[2], D.C. Agarwal[3], R. Biswal[4], D. Behera[5], D. Kanjilal[6], A. Tripathi[6], P.V. Satyam[7] and N.C. Mishra[4]

[1] Department of Physics, North Orissa University, Baripada 757 003

[2] School of Material Science & Technology, IT, BHU, Varanasi 221 005

[3] Department of Physics, R.B.S. College, Agra 282 002

[4] Department of Physics, Utkal University, Bhubaneswar 751 004

[5]Department of Physics, National Institute of Technology, Rourkela 769 008

[6]Inter-University Accelerator Center, Aruna Asaf Ali Marg, New Delhi - 67

[7]Institute of Physics, Bhubaneswar 751005, India

NiO is known to behave differently as compared to many other oxides to SHI irradiation. Atomic and collective mass transport during the excited phase of the ion track is known to occur this system [1]. The NiO thin films on Si (100) were prepared by e-beam evaporation method, annealed at 700 ^{0}C for half an hour and irradiated with 120 MeV Au ions at IUAC, New Delhi. Since the electronic energy loss (31.7 keV.nm^{-1}) of 120 MeV Au in NiO exceeds the threshold (~30 keV.nm^{-1}) [2] for track formation, SHI irradiation should suppress crystallinity. We however observed improvement of crystallinity and grain growth at some fluence of irradiation. The total integrated area, A_T under the two XRD peaks represents the amount of crystallinity in the films at different fluences of irradiation (Fig. 1 a). The films showed a decrease of A_T at a fluence of 3×10^{11} ions.cm^{-2}. Further irradiation led to increase of A_T up to a fluence of 1×10^{13} ions.cm^{-2} and then decrease at higher fluence. The improvement of crystallinity at the fluence of 3×10^{12} ions.cm^{-2} as compared to the pristine film is indicated from the higher value of A_T than that of the pristine. The SHI induced grain growth is also supported by the increased grain size as seen in the AFM micrograph (Fig. 1 b, c) at the same fluence of irradiation.

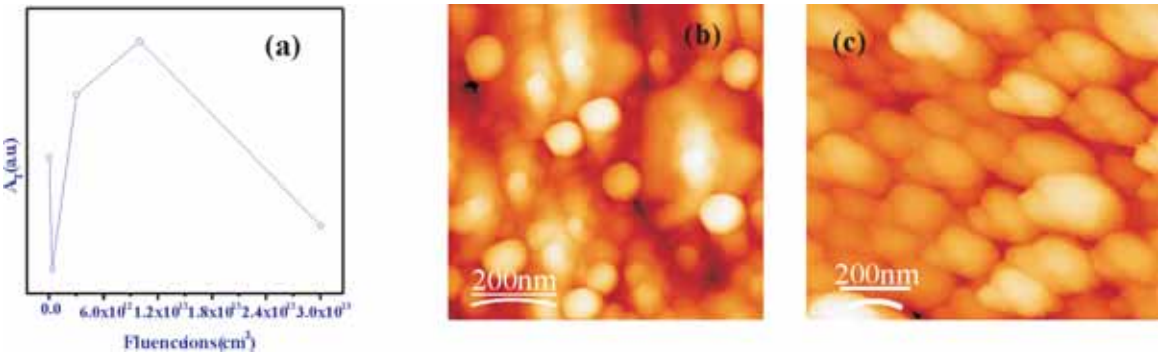

Fig. 1. (a) Variation of sum of the area under the XRD peaks, A_T with fluence for NiO films deposited on Si (100) and sintered at 700 ^{0}C, 1μm×μm AFM image of NiO/Si (b) pristine film and (c) irradiated with 3×10^{12} ions.cm^{-2}

REFERENCES

[1] W. Bolse, Nuclear Instruments and Methods in Physics Research B 244 (2006) 8.

[2] B Schattat, W Bolse, S Klaumunzer, I Zizak & R Scholz, Appl. Phys. Lett. 87 (2005) 173110.

5.2.31 Swift Heavy Ion Induced Modification in Zinc Ferrite Nanoparticles

Jitendra Pal Singh[1], R. C. Srivastava[1], H. M. Agrawal[1], Ravi Kumar[2] and Prem Chand[3]

[1]Department of Physics,G. B. Pant Univ. of Ag. & Tech., Pantnagar, Uttarakhand-263145
[2]Inter University Accelerator Centre,Aruna Asaf Ali Marg, New Delhi - 67.
[3]Department of Physics, Indian Institute of Technology, Kanpur-208016.

The study on the investigation of the change in the properties of nanoferrites irradiated by swift heavy ion is a field of great interest now-a-days. In the present investigation we have used the 100 MeV oxygen beam (O^{7+}) to observe the irradiation induced effects in zinc ferrite nanoparticles of different size. The zinc ferrite nanoparticles were synthesized by the chemical route [1]. The precursor was sintered at various temperatures for 1 hr ranging from 300^{o}C to 1000^{o}C . The particle size for the sintered sample, estimated from Scherrer's formula varies from 10-62 nm. The electronic stopping and nuclear stopping values for oxygen beam are calculated by using the SRIM-2006. For 100 MeV oxygen beam the parameters are: S_e = 1.09 keV/nm, S_n = 0.618 eV/nm and projected range is = 65 μm. The threshold electronic stopping value for producing the columnar defects in zinc ferrite is ~ 13 keV/nm [2]. Hence, we expect only the point/cluster of defects in this material. We irradiated samples with fluence of 1×10^{13} ions/cm^2 and 5×10^{13} ions/cm^2 in order to observe the effect of fluence on the nanoparticles of various sizes. The crystallographic phase and particle size of the irradiated samples were determined by the XRD. EPR and UV-VIS spectra at room temperature were also recorded.

Fig 1 shows the XRD spectrum of the irradiated and pristine sample having particle size 12 nm. The observed peaks are corresponding to the cubic spinel phase of the material. The peak

(200) appears in all the irradiated samples. It has been observed that the peaks get broadened and it increases with the increase in fluence. This may be attributed to the decrease in the particle size and increase in strain. This type of behavior is also observed for the Ni-Zn and Mn-Zn ferrite irradiated by 190 Mev Ag^{15+} ion beams [3]. Fig 2 shows the UV-VIS spectra of the sample having particle size 12 nm at various fluences. The pristine sample shows the strong absorption in the UV region. We have also recorded the EPR spectra of the pristine and irradiated sample having particle size 12 nm. Table 1 shows the various parameters estimated from the EPR spectra at room temperature for the sample. The estimated values of optical band gap from Tauc relation has also been colloted in Table 1. The pristine sample shows higher value of band gap in comparison to bulk zinc ferrite (E_g ~1.9 eV). The optical band-gap decreases after the irradiation. The detailed analysis of the data for rest of the samples is in progress.

Table 1: EPR and UV-Vis Parameters for the Sample (12 nm)

Fluence (ions/cm^2)	EPR Parameters		UV-Vis Parameter
	g-value	Peak to peak line width (Gauss)	Band-gap (eV)
Pristine	2.02	375	4.1
5×10^{13}	2.05	400	3.5

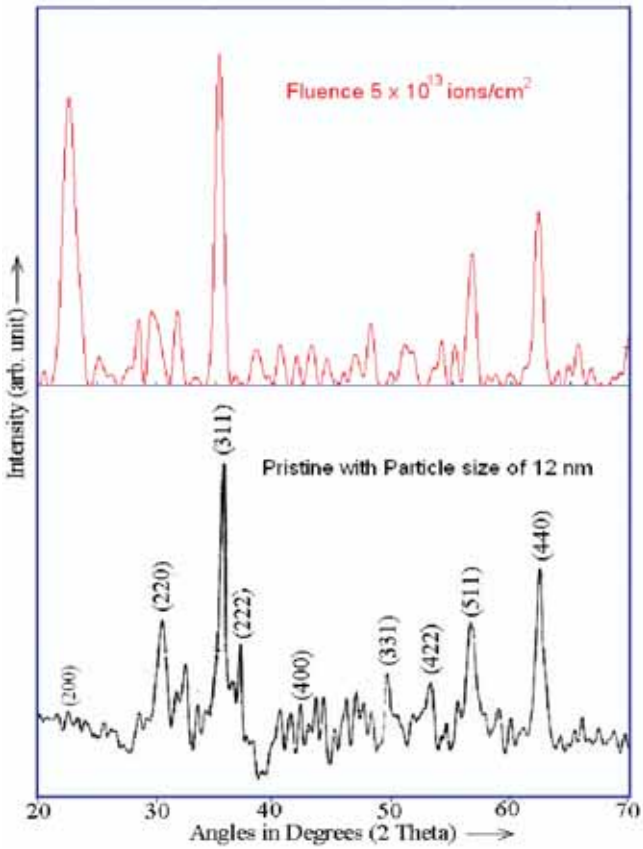

Fig.1. XRD spectra of the pristine and irradiated sample (12 nm)

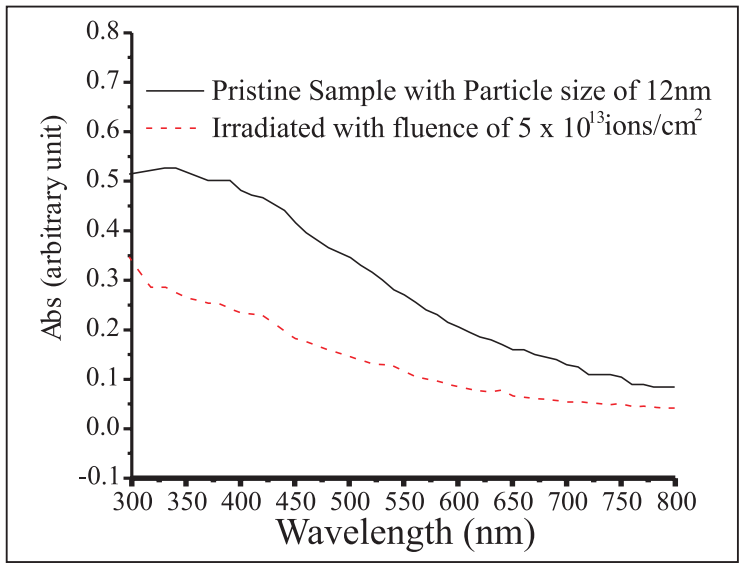

Fig.2. UV-VIS spectra of the pristine and irradiated sample (12 nm)

REFERENCES

[1] J. P. Singh, R. C. Srivastava, H. M. Agrawal, R. P. S. Kushwaha, P. Chand and Ravi Kumar, International Journal of Nanoscience, (in press).

[2] Ravi Kumar, S. K. Sharma, A. Dogra, V. V. Shivakumar, S. N. Dolia, A. Gupta, M. Knobel and M. Singh, Hyperfine Interaction, 160, (2005) 143.

[3] B. P. Rao, K. H. Rao, P.S.V. Subba Rao, A. M. Kumar, Y. L. N. Murthy, K. Ashokan, V. V. Siva Kumar, Ravi Kumar, N. S. Gajbhiye, O. F. Caltum, Nuclear Instruments and Methods in Physics Research B, 244 (2006) 27.

5.2.32 Swift heavy ion irradiation induced modified surface and optical properties of nanostructured titania thin films derived from $TiCl_4$ solutions

S.J. Trivedi[1], P.A. Joshi[1], U.S. Joshi[1], U.V. Chhaya[2] and S.A. Khan[3]

[1]Department of Physics, School of Sciences, Gujarat University, Ahmedabad-380 009
[2]Physics Department, St. Xavier's College, Ahmedabad-380 009
[3]Inter University Accelerator Centre, Aruna Asaf Ali Marg, New Delhi - 67

Nanostructured titania (TiO_2) thin films have attracted lot of attraction due to its variety of functionalities such as, surface photocatalysis, *n*-type semiconducting nature with wide band gap, diluted magnetic semiconductors and so on. Most of the functionalities of TiO_2 originate from its novel surface chemistry. TiO_2 is one of the most investigated metal oxide surfaces [1-2]. Nevertheless, experimental investigations of the kinetics of the surface growth of anatase TiO_2 are scarce. Here, we report on the 100 MeV Ag^{+7} swift heavy ion (SHI) irradiation induced modifications on the surface and optical properties of nanostructured TiO_2 films.

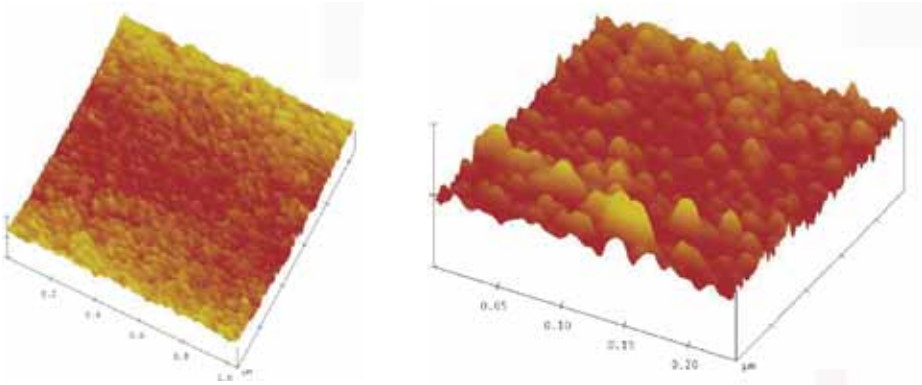

Fig. 1. Three dimensional surface topography of (a) pristine anatase TiO_2 thin films and (b) irradiated by 100 MeV Ag ions with a fluence of $1x10^{13}$ ions/cm^2

High quality thin films of TiO_2 were fabricated on SiO_2 substrate via chemical solution deposition spin coating technique. Fuming solution of $TiCl_4$ was used as starting material, contrary to the most of the reports on titania, where, titanium isopropoxide or butoxides were used. Monodispersed, nanosized titania films with smooth surface morphologies were obtained. The surface properties (parameters, such as size of nanoparticles, surface roughness and morphology) of the films strongly depend on the choice of the compound used. A narrow size distribution of the film particles leads to relatively smooth films. Thermal treatment to 600°C leads to films presenting the anatase diffraction peaks. Fig. 1 (a) shows the AFM image of anatase TiO_2 film. Uniform particle size confirmed about ~ 30 nm by the XRD and AFM analysis, while the RMS surface roughness is ~ 1.078 nm, suggesting an excellent smoothness of the CSD grown surface.

Upon SHI irradiation, a sharp reduction in the particle size i.e., ~10 nm, and surface reconstruction was seen, as shown in Fig. 1 (b). Further, a narrow distribution of crystallite size was also observed as compared to the pristine sample. However, the film roughness was found to increase due to surface atom rearrangements and SHI induced defects [3]. No significant change in the structural and scanning probe properties of the titania films were observed when irradiated by two different set of 100 MeV ions, namely, Ag and Ni, suggesting that the type of swift ion has little role to play for such compound.

Optical measurements show excellent trasmittance of ~80 % in the visible range for pristine TiO_2 thin films as can be seen in the optical spectrographs shown in Fig. 2.

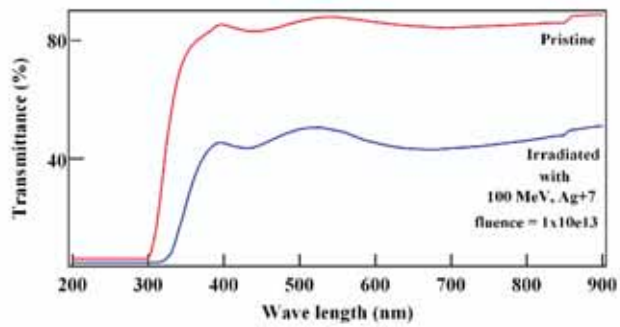

Fig. 2. UV-Vis. transmission spectrographs of pristine and irradiated TiO_2 films grown on SiO_2substrates

However, it was found to decrease down to ~50% upon SHI irradiation due to increased defect states and roughness of the films. The optical band gap values were estimated using Tauc's plot by plotting $(\alpha h\nu)^2$ versus $h\nu$ and extrapolating the linear portion of the absorption edge to find the intercept with energy axis. The calculated band gap values for pristine and SHI irradiated ~80 nm thick, TiO_2 films were 3.98 and 3.73 eV, respectively. This reduction in the band gap clearly suggests the presence of oxygen vacancy and crystallite size reduction of Ti-O atoms.

REFERENCES

[1] U. Diebold, Surf. Sci. Rep. 48 (2003) 53–229

[2] Y. Matsumoto, M. Murakami, T. Shono, T. Hasegawa, T. Fukumura, M. Kawasaki, P. Ahmet, T. Chikyow, S. Koshihara and H. Koinuma. Science 291 (2001) 287

[3] D.C. Agarwal, Amit Kumar, S.A. Khan, D.Kabiraj, F. Singh, A. Tripathi, J.C. Pivin, R.S. Chouhan and D.K. Avasthi, Nucl.Inst. and Meth. B 244 (2006) 136

5.2.33 Effect of SHI irradiation on FeNiCr thin films

Senoy Thomas[1], Ambuj Tripathi[2], D K Avasthi[2] and M R Anantharaman[1]

[1]Cochin University of Science and Technology, Cochin 682022
[2]Inter University Accelerator Centre, Aruna Asaf Ali Marg, New Delhi - 67

FeNi based amorphous alloy thin films are currently of great interest due to their potential applications in the field of sensors, actuators and magnetic recording media. Control of magnetic properties in these materials is essential in order to obtain miniaturized magnetic devices with improved performance characteristics. From a fundamental perspective nanocrystallization and the impact of swift heavy ions on the magnetic and structural properties are also of great interest to scientists.

FeNiCr films were prepared on glass substrates by thermal evaporation of metglas 2826 under controlled conditions and were then irradiated with 108 MeV Ag^{8+} ions using the 15UD Pelletron accelerator facility at Inter University Accelerator Centre, New Delhi. The irradiation was performed at room temperature with fluence ranging from $3x10^{11}$ to $3x10^{13}$ ions/cm^2. These films were then characterised using the Glancing angle XRD facilities at Inter University Accelerator Centre New Delhi. Atomic force microscopy was used to investigate the evolution of thin film roughness with fluence. Vibrating sample magnetometer was used to study the magnetic evolution with the ion beam irradiation. Compositional analysis was performed using XPS and the results are correlated with structural data.

Figure 1 (a) and (b) shows the 3-D view of the surface of the films irradiated at fluences $3x10^{12}$ and $3x10^{13}$ respectively.

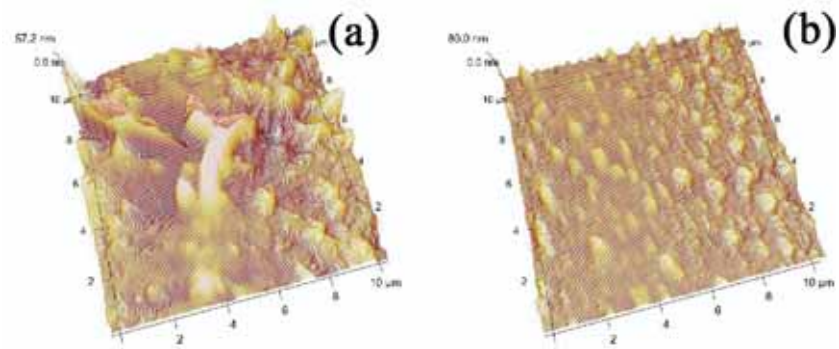

Fig. 1. Three dimensional AFM images of Fe-Ni-Cr thin films irradiated with 108 MeV Ag^{8+} ions at fluences (a) $3x10^{12}$ (b) $3x10^{13}$ ions/cm^2

The statistical analysis indicated that rms roughness increases from 7.49 nm with fluence as shown in figure 2.

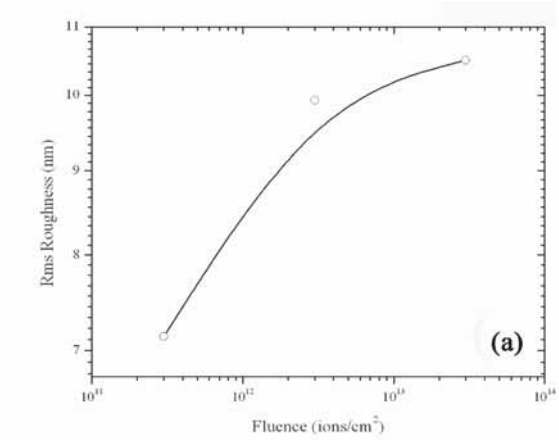

Fig. 2. variation of rms roughness with ion fluence

The room temperature hysteresis loop for pristine as well as irradiated samples is shown in figure 3. There is a clear difference between the coercivity of the pristine and irradiated thin films.

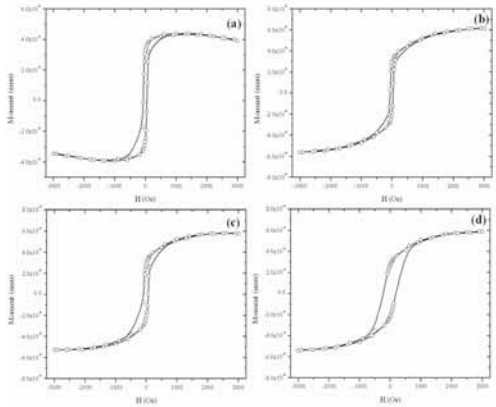

Fig. 3. Room temperature hysterisis loop for Fe-Ni-Cr thin films (a) pristine and irradiated with 108 MeV Ag ions at fluences (b) $3x10^{11}$ (c) $3x10^{12}$ (d) $3x10^{13}$

Further work is in progress to understand ion irradiation induced modifications.

5.2.34 Swift Heavy Ion Induced Thermoluminescence tudies in Pure and Lanthanum Doped Polycrystalline Aluminium Oxide

K.R. Nagabhushana[1], B.N. Lakshminarasappa[1] and Fouran Singh[2]

[1] Department of Physics, Jnanabharathi, Bangalore University, Bangalore-560 056

[2] Inter University Accelerator Centre, Aruna Asaf Ali Marg, New Delhi - 67

Thermoluminescence (TL) is the emission of light from a previously irradiated insulator or semiconductor as a result of thermal stimulation [1]. The TL intensity enhances as a function of certain dose of radiation absorbed by the sample and thus is used in radiation dosimetry [2]. Al_2O_3 is one of the earlier materials studied for its possible application as a radiation dosimeter owing to its superior thermal and chemical stability. Pure and 1 mol% La (lanthanum) doped polycrystalline aluminum oxide was synthesized by combustion technique. Pellets of these compounds of 6 mm diameter are irradiated with 100 MeV Ni^{7+} for the fluence in the range 1×10^{11} ions cm^{-2} to 1×10^{14} ions cm^{-2}. TL measurements were made at a linear heating rate of 5 Ks^{-1} using based TL analyzer (Nucleonix Systems Pvt. Ltd Hyderabad, India).

A prominent and well resolved TL glow with peak at 613 K and unresolved shoulder at 510 K are observed in Ni^{7+} ion irradiated undoped polycrystalline aluminum oxide. The glow peak intensity at 613 K increases with increase in ion fluence up to 1×10^{13} ions cm^{-2} and thereafter it decreases. But, the glow peak intensity at 510 K decrease with increase in ion fluence. However, the shoulder was completely disappearing at fluence 1×10^{14} ions cm^{-2}. This might be due to the annihilation of the defect centers responsible for the TL emission. The glow peak temperature slightly shifts towards lower temperature region with increase in ion fluence. This is one of the properties of the second order kinetics. It is found that the width towards the higher temperature side at half maximum is greater than that towards the lower temperature side. This can be understood from the fact that in the second order reaction significant concentrations of released electrons are retrapped before they recombine, resulting delay in the luminescence emission and spreading out of the emission over a wider temperature range [4]. In the case of lanthanum (1 mol%) doped polycrystalline Al_2O_3 irradiated with 100 MeV Ni^{7+} ions for the fluence in the range 1×10^{11} to 5×10^{13} ions cm^{-2} it shows a single and prominent TL glow with peak at 603 K. It is observed that the TL glow peak intensity decreases with increase in ion fluence and TL intensity is completely absent for the fluence of 5×10^{13} ions cm^{-2}. Further work is in progress.

REFERENCES

[1] J.K Rieke and F. Daniels, J. Phy. Chem. 51. 629 (1957).

[2] C. Lucas and B. K. Lucas, Radiat. Protect. Dosim. 85. 455 (1999).

[3] A.J.J. Bos, Nucl. Instr. Meth. B 184. 3 (2001).

[4] K.R. Nagabhushana, B.N. Lakshminarasappa, Fouran Singh, (In press) Radiat. Meas. (2008).

5.2.35 100 MeV Ni^{8+} ion irradiation of $Mo_{0.98}Fe_{0.02}O_3$ thin films grown by pulsed laser deposition

Devki Chauhan[1], Y. S. Katharria[2], R. J. Choudhary[3], F. Singh[2], Ravi Kumar[2] and Alimuddin[1]

[1]Department of Applied Physics, Aligarh Muslim University, Aligarh-202 002

[2]Inter-University Accelerator Centre, Aruna Asaf Ali Marg, New Delhi - 67

[3]UGC-DAE Consortium for Scientific Research, Khandwa Road, Indore-452 017

Molybdenum oxide is a potential candidate for developing positive alphanumeric display devices, high-density memory devices, optical smart windows, and solid-state microbatteries. It has also found applications in optically switchable coatings, gas sensors, catalysis, and is also used as a diffusion barrier.

We, in the present work, investigate the structural and optical modifications of pulsed laser deposited molybdenum oxide films doped with 2 % of Fe. A KrF laser (λ=248 nm) was used to ablate molybdenum oxide target having 2 % Fe composition. As deposited films usually have a MoO_x (with $2<x<3$) type composition. To remove oxygen deficiency and obtain MoO_3 phase, the films were annealed at 450 °C in oxygen environment for 2 hrs. The films were then irradiated at room temperature with 100 MeV Ni ions with ion fluence (ϕ) varying from 1×10^{12} to 1×10^{14} ions-cm^{-2}. Fig.1 shows the variation of optical band gap of pristine and the ion irradiated films. The previously reported values of band gap of MoO_3 films lie close to 3 eV [1]. However, we obtained a band gap close to 1.8 eV using Tauc's formula for indirect band gap semiconductors. The reason for the reduction of the band gap in the present study may lie in the defects present in the MoO_3 films. These defects introduce energy levels in the forbidden gap of a semiconductor. Due to the transitions from valence band to these levels or from these levels to the conduction band, the band gap of a semiconductor may appear less than the actual value.

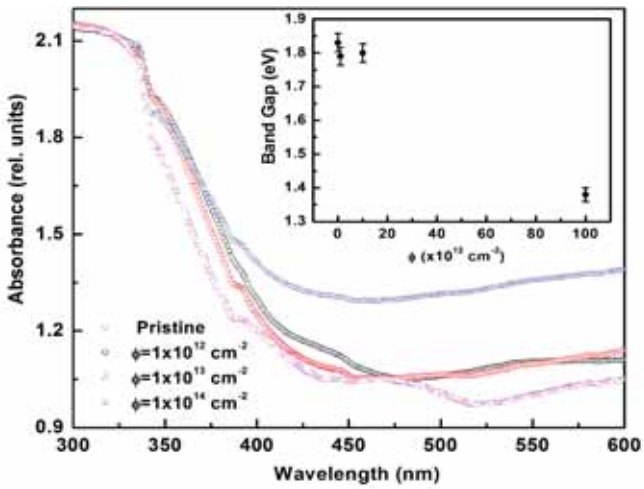

Fig.1. UV-Visible absorption curves and optical band gap (inset) of Ni ion irradiated MoO_3 films

The band gap remains almost constant with Ni irradiation for $\phi < 1\times10^{13}$ ion-cm^{-2}. However, a drastic decrease to a value close to 1.4 eV is observed at $\phi = 1\times10^{14}$ ion-cm^{-2} possibly due to the formation ion beam induced defects.

Fig.2 shows the Fourier transform infrared (FTIR) spectra of MoO_3 films before and after Ni ion irradiation. The dotted lines are drawn to show the positions of IR modes of the films. Absorption bands at 817 cm^{-1} and 968 cm^{-1} correspond to stretching mode vibration of bridging oxygen in Mo-O-Mo and to terminal Mo=O bond vibrations [2]. The presence of these phonon modes indicates that the films have a layered orthorhombic MoO_3 structure. These modes are broadened and finally get disappeared with increasing fluence of 100 MeV Ni ions indicating that the films are structurally damaged by the energy deposition of the incident ions. The FTIR mode at 737 cm^{-1} could not be identified. This mode is also observed in undoped MoO_3 films suggesting that this mode should be related to MoO_3 and not with the doped Fe.

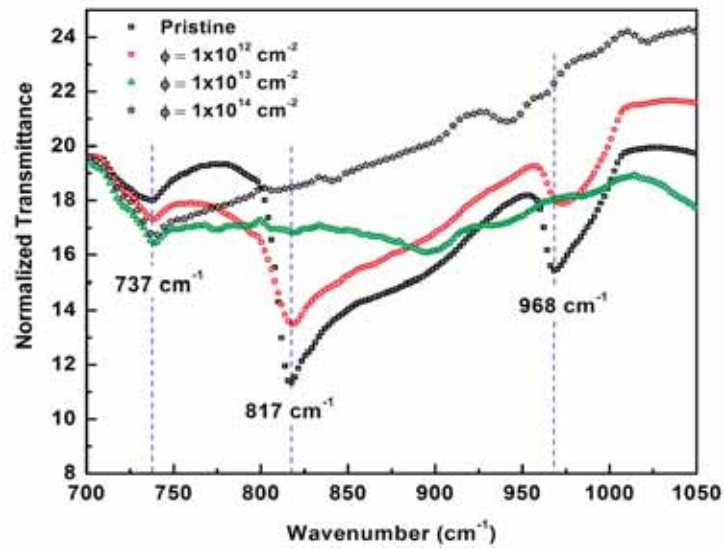

Fig.2. FTIR spectra of Fe doped MoO_3 films irradiated with 100 MeV Ni ions

In summary, a preliminary study of MeV ion irradiation is performed on MoO_3 films. The films would be characterized further to get detailed modifications of electrical and magnetic properties of the films.

REFERENCES

[1] D. Manno, M. D. Giulio, A. Serra, T. Siciliano and G. Micocci J. Phys. D 35 (2002) 228.

[2] T. S. Sian, and G. B. Reddy, Sol. Ene. Sol. Cells 82 (2004) 375.

5.2.36 TL Response of Swift Heavy Ion Irradiated Silica Glass

A. K. Sandhu[1], S. Singh[1], O. P. Pandey[2], F. Singh[3] and S. P. Lochab[3]

[1] Department of Physics, Guru Nanak Dev University, Amritsar-143005

[2] School of Physics and Materials Science, Thapar University, Patiala-147004

[3] Inter University Accelerator Center, Aruna Asaf Ali Marg, New Delhi - 67

The high energy swift heavy ions lose their energy in the target material mainly via inelastic collisions leading to the excitation of the target electrons. The electronic energy loss has been found to create various modifications in the target material, leading to the changes in the structural [1], optical [1-3] and luminescence [1,4] properties of the material.

Glasses are generally made of silica as the basic material with certain additional trace elements as per its intended application. Sand made up of silica has been reported as a thermoluminescence (TL) dosimetric material for high dose and accidental dosimetry [5,6]. TL in common natural materials, e.g., natural quartz present in sand provides a useful method for direct measurement of absorbed radiation [7]. Thermoluminescence produced in the soda-lime silica glass by the impact of MeV ion irradiation is the aim of the present investigation.

The TL glow curves are recorded in the temperature range of 50 to 400 ^{o}C for the silica glass (60% SiO_2, 30% Na_2O, 5% MgO, 5% Al_2O_3 (all in mole %)) irradiated with 60 MeV C^{5+} ions using 15UD Pelletron Accelerator at IUAC, New Delhi in the fluence range of 1 x 10^{12} to 1 x 10^{14} ions/cm^2. TL glow curves recorded at a heating rate of 5 ^{o}Cs^{-1} have one prominent peak at 180 ^{o}C and a less intense peak at 360 ^{o}C (Figure 1). It is observed that the TL intensity of the peak at 180 ^{o}C increases upto a dose of 1 x 10^{13} and thereafter decreases; however, the glow peak at 360 ^{o}C follows exactly opposite trend. The former peak may be attributed to the [AlO_4] hole center former under irradiation from its precursor [AlO_4Na] center as an electron is released and an alkali ion migrates away. The recombination of the electron released by heating on this center leads the appearance of TL peak at 180 ^{o}C. The latter peak may be attributed to the non-bridging oxygens (NBOs) generated by ion irradiation.

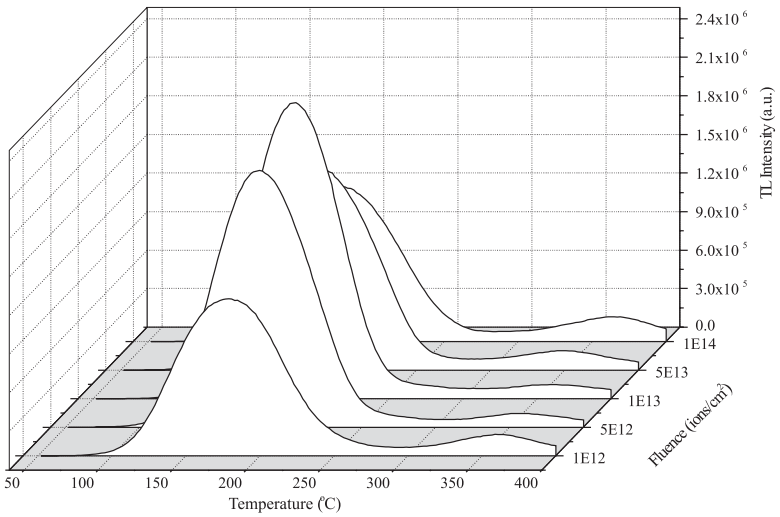

Fig. 1. TL glow curve of silica glass irradiated with C^{5+} ions at different fluences

REFERENCES

[1] T. Mohanty, N. C. Mishra, S. V. Bhat, P. K. Basu and D. Kanjilal, J. Phys. D 36 (2003) 3151.

[2] M. S. Kamboj, R. Thangaraj, D. K. Avasthi and D. Kabiraj, Nucl. Instr. and Meth. B 211 (2003) 369.

[3] M. S. Kamboj, G. Kaur, R. Thangaraj and D. K. Avasthi, J. Phys. D 35 (2002) 477.

[4] B. N. Lakshminarasappa, H. Nagabhushana and F. Singh, Nucl. Instr. and Meth. B 244 (2006) 153.

[5] S. G. Vaijapukar, R. Raman and P. K. Bhatnagar, Radiat. Meas. 29 (1998) 223.

[6] F. A. Balogun, F. O. Ogundare and M. K. Fasai, Nucl. Instr. and Meth. A 505 (2003) 407.

[7] G. Kitis, E. Kaldoudi and S. Charalambous, J. Phys. D 23 (1990) 945.

5.2.37 100 MeV O^{+7} Ion Irradiation effects on Polypyrrole Thin Films

Subhash Chandra[1], J. M. S. Rana[1], R. G Sonkawade[2], P. K. Kulriya[2], Fouran Singh[2], D. K. Avasthi[2] and S. Annapoorni[3] and R. C. Ramola[1]

[1]Dept. of Physics, HNB Garhwal University, Badshahi Thaul Campus, Tehri Garhwal
[2]Inter University Accelerator Center, Aruna Asaf Ali Marg, New Delhi - 67
[3]Department of Physics and Astrophysics, University of Delhi, Delhi - 110 007

Conducting polymers are the important class of materials due to their properties such as high electrical conductivity, large nonlinear optical responses and the good thermal stability. These properties are very important in various fields like light emitting diodes, molecular electronics, actuators [1] & gas sensors [2,3]. Due to commercial uses, polymers become a subject of scientific and commercial interest. Therefore use of ion irradiation is of great importance to modify properties of these materials. In general most of these modifications can be traced back to changes taking place in chemical structure of polymer.

Pyrrole monomer (Aldrich 99% used as received) and para-tolune sulphonic acid (PTS) (Lancaster, U.K., 98+ %) both of the normality 0.1M were dissolved in distilled water and the electrochemical polymerization of the pyrrole was carried out on Indium Tin Oxide (ITO). The films Polypyrrole (Ppy) of thickness 80~100 μm were irradiated by 100 MeV O^{+7} ion with a beam current of 1 pnA available from 15 UD Pelletron at Inter University Accelerator Centre, New Delhi using various fluences ranging from $1x10^{10}$ to $3x10^{12}$ ions/cm^2. XRD of the polypyrrole thin films were carried out for structure determination by a Bruker AXS, X-ray diffractometer with Cu-K_α radiation for a wide range of Bragg's angle 2θ ($15<2\theta<40$). UV-Visible Spectra were obtained using a U-3300 Spectrophotometer.

The XRD pattern of pristine and irradiated Ppy irradiated by oxygen beam is shown in Fig.1. The peak value observed at 26.25 degree is the characteristic peak of Ppy and other peaks observed at 21.5, 31 and 35.5 degrees are values of diffracted X-ray for pure cubic phase of ITO. The pristine polypyrrole shows the semi crystalline nature. After irradiation with SHI at low fluence, intensity of the peaks increases, which shows that the polymer crystallinity increases. This may be due to cross linking of the polymer chains or by the formation of single or multiple helices

[4], which produces more crystalline regions in the polymer film after SHI irradiation. The degree of crystallinity for the polymers calculated by following formula

$$K = \frac{A}{A'} X100\%$$

where A is the total area of the peaks (area of crystalline and amorphous peaks) and A′ is the total area under the diffractogram. The % crystallinity calculated by above relation is shown in Table 1.

The electronic structure and the carrier type in the polymers can be visualized by UV-visible spectra. The UV-visible spectra recorded for the O^{+7} ion beam irradiated polypyrrole is shown in Fig 2. The absorption peak around 450 nm is polaron absorption peak of the conducting polypyrrole [5]. A shift in the absorption peak towards higher wavelength was found indicating a decrease in the energy bandgap of the polymer after SHI irradiation which gives rise to an increase in the dc conductivity of polymers. This shift in the absorption may be produced in creation of free radicals or ions and thus have a capability of increasing the conductivity of the polymers. From the absorption spectrum the direct band gap of the polymers was calculated by linear part of the Tauc's plot. The band gap was found to be 3.4 eV for the pristine Ppy, which decrease upto 3.0 eV after irradiation, by oxygen beam. The calculated values of band gap are shown in Table 1.

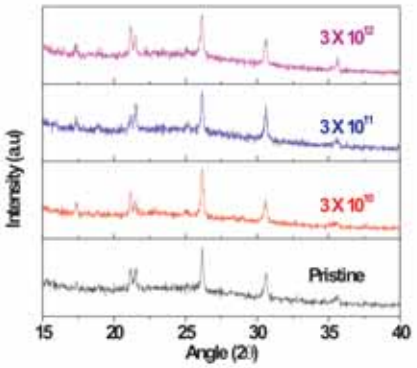

Fig. 1. XRD- Pattern of Polypyrrole

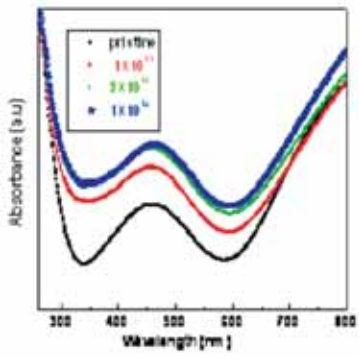

Fig.2. UV-visible of Polypyrrole

Table 1 : The % Crystallinity and the band gap variation in Polypyrrole thin films irradiated by 100 MeV oxygen beam

O^{+7} ion fluences (Ions/cm^2)	% K of Ppy	Band gap in Ppy
Pristine	23.02	3.4 eV
$3X10^{10}$	26.91	----
$1x10^{11}$	----	3.3 eV
$3X10^{11}$	30.39	3.2 eV
$1X10^{12}$	--	3.0 eV
$3X10^{12}$	32.21	--

REFERENCES

[1] E.Selma. J. Micromech. Microen. 9 (1999)1.

[2] J.M. Slater, E.J. Watt, N.J. Freeman, .J. May & Weir. Analyst (Cambrige,UK) 117 (1992) 1265.

[3] I. Lahesmaki, A. Lewenstam & A. Ivaska. Talanta 43 (1996) 125.

[4] Bruno Scrosati (Ed.), Appliations of Electroactive Polymers, Chapman & Hall, London, 1993.

[5] J. Chen. C.O. Too. G.G. Wallace. & G.F. Swierers. Electrochm. Acta 49 (2004) 691.

5.2.38 Modification of metal dispersed polymer composites by SHI

N.L.Singh[1], Anjum Qureshi[1], Sejal Shah[1], Dolly Singh[1] and F.Singh[2]

[1] Physics Department, M.S.University of Baroda, Vadodara-390 002
[2] Inter University Accelerator Centre, Aruna Asaf Ali Marg, New Delhi - 67

In recent years, technological devices at the nanometer scale are in demand. Therefore, there is a practical interest in the composites consisting of dielectrics with metal nanoparticles, which are encouraged by potential applications such as nonlinear optical switches, magnetic data storages, microelectronic devices, EMI shielding etc. The electromagnetic interference is serious problem in extremely sensitive electronic equipment. Polymer composites, with high dielectric constant and low loss can be used for the purpose of EMI shielding. This requirement can be fulfilled by incorporating fillers like metal powders i.e. Al, C, Au, Ag, Cu, etc. High energy ion irradiation induces significant modification in the material by electronic excitation or ionization. Irradiation also improves the dielectric properties of these composites.

We have prepared polymer composites by doping different concentrations (10, 20, 30 and 40%) of metals like Al, C and Cu in PMMA and PVC by chemical method. The films (thinckness ~ 0.3mm) were prepared by casting method. These films were irradiated with 140 MeV Ag^{11+} ion beam at the fluences of 10^{11} and 10^{12} ions/cm^2 using 15 UD Pelletron facility at Inter University Accelerator Centre, New Delhi.

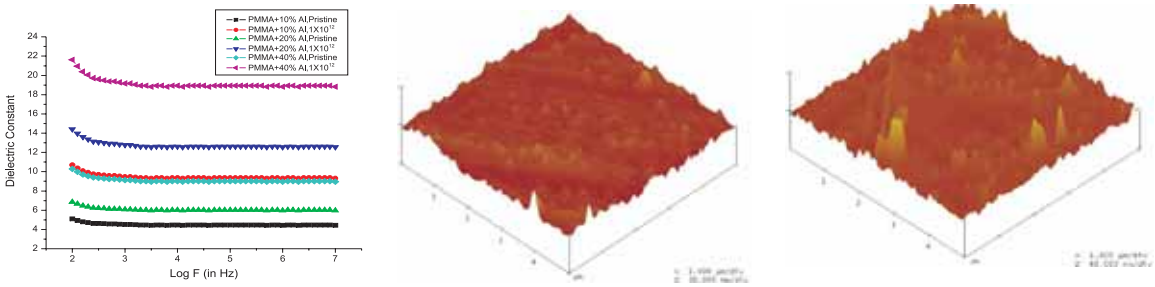

Fig. 1 (a) Dielectric constant vs Log F, AFM of (b) pristine (c) irradiated Al dispersed composite

Dielectric properties and surface morphology of pristine and irradiated samples were studied. It was observed that dielectric properties of the films vary with ion fluence, filler concentration and frequency of applied field. The dielectric constant/loss is observed to enhance significantly due to irradiation. This suggests that ion beam irradiation promotes (i) the metal to polymer bonding and (ii) convert the polymeric structure into hydrogen depleted carbon network. Surface morphology was studied by AFM in terms of average surface roughness. The result shows that average roughness of the films decreases after irradiation and surface becomes smoother. The decrease in surface roughness due to irradiation may be attributed to defect enhanced surface diffusion.

5.2.39 Production of pores by swift heavy ion induced dewetting of polymer thin film on GaAs

Jaskiran Kaur[1], S Singh[1], Rajesh Kumar[2], D Kanjilal[3], A Tripathi[3], Karunapathi Tripathi[4] and S K Chakarvarti[2]

[1] Department of Physics, Guru Nanak Dev University Amritsar
[2] Department of Physics, National Institute of Technology, Kurukshetra-136119
[3] Inter University Accelerator Centre, Aruna Asaf Ali Marg, New Delhi - 67
[4] Department of Physics, Jamia Millia Islamia New Delhi

We are reporting a technique for generating nano/micro pores in irradiated polymer film without etching. These pores were produced in thin polymer films (polycarbonate, 8um) on GaAs (P-doped) (111) substrate irradiated by heavy ions (50 MeV, Li^{+}) at room temperature ($29^{0}C$). Preparation of substrate was carried out at Inter University Accelerator Center (IUAC), New Delhi, India. Using the technique of resistive heating, a thin layer of gold of thickness (95nm) was deposited on the wafers then a thin layer of polycarbonate (Makrofol) by spin coating, thickness of polymer was around 10mm. The prepared samples were irradiated at room temperature with 50 MeV Li^{+3} ions at fluencies between $2x10^{7}$ and $5x10^{8}$ ions/cm^{2}. Before and after irradiation, the samples were characterized using AFM and SEM. AFM in tapping mode clearly distinguishes the pores with rim from the rest plane surface. Fig. 1. depicts the AFM pictures of the pores generated by ion assisted dewetting. Pattern formation is surprisingly similar to what is observed after heating thin polymer films on semi-conductor substrates above their melting point [1-3] and also in metal oxide coated semi-conducting film bombarded with swift heavy ions [4-6]. The Fig. 1 shows the 3D image of the pores with well-defined bright rims around big pores. The holes are surrounded by the rim like structures with heights up to 35 nm and are asymmetric in shape, as can be seen in the section analysis shown in the fig. 2.

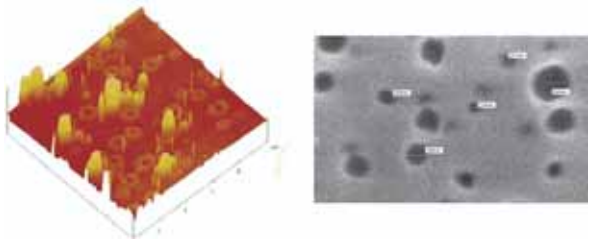

Fig. 1. 3D AFM and SEM image of 50MeV Li^{+3} ion irradiated Polymer coated GaAs

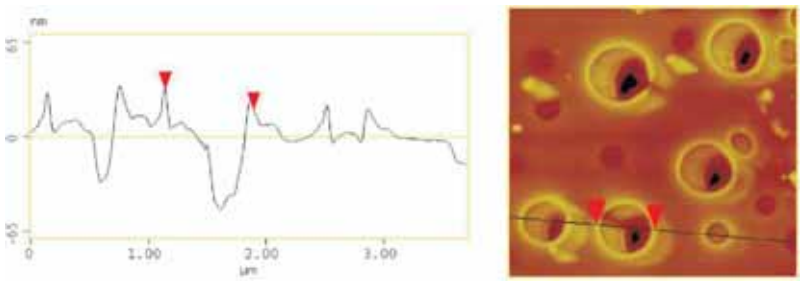

Fig. 2.Section analysis of the pores present on the Polymer coated GaAs

REFERENCES

[1] Gumter Reiter. Phy. Rev. Lett. Vol-87 (18) (2001) 186101.
[2] R. Seemann, S. Herminghaus, K. Jacobs Phy. Rev. Lett 87 (19) (2001) 196101.
[3] T. Bolse, A. Elsanousi, H. Paulus, and W. Bolse. Nucl. Instr. And Meth. B 244 (2006) 115-119.
[4] R. Seemann, S. Herminghaus, K. Jacobs, J. Phys.: Condens. Matter 13 (2001) 4925.
[5] W. Bolse Nucl. Instr. And Meth. B 244 (2006) 8-14
[6] T. Bolse , H. Paulus and W. Bolse. Nucl. Instr. And Meth. B 245 (2006) 264-268.

5.2.40 Effect of high energy ion beam irradiation on polypropylene

R. K. Dhillon[1], S. Singh[1], R. Kumar[2] and R. G. Sonkawade[3]

[1] Department of Physics, Guru Nanak Dev University, Amritsar-143005

[2] Department of Applied Physics, Z. H. College of Engineering and Technology, Aligarh Muslim University, Aligarh

[3] Inter-University Accelerator Center, Aruna Asaf Ali Marg, New Delhi - 67

Polypropylene is a well-known polymer because of its low cost, inert nature, good mechanical properties, weathering resistance and various commercial applications. The polypropylene samples for the present study were obtained from Goodfellow Ltd. (England) and were irradiated with C^{5+} (70MeV) and Ni^{11+} (150MeV) ions of fluences between 5×10^{10} to 5×10^{12} ions cm^{-2} in the Material Science Chamber of Inter University Accelerator Center, New Delhi. It is observed from UV-VIS spectroscopy that there is decrease in the energy gap of the polymer with the increase in ion fluence. The optical band gap of virgin polypropylene is 5.57eV. At the highest fleunce of 5×10^{12} ions cm^{-2} of Ni^{11+} (150MeV) ions, the optical band gap is reduced to nearly 57% *i.e.*, 5.57 to 2.39eV and for C^{5+} (70MeV), it is decreased by 4% *i.e.*, 5.57 to 5.37eV. Earlier studies have indicated that the C enriched domains created in polymers during irradiation are responsible for decrease in band gap [1-3].

XRD Analysis of virgin sample reveals four peaks at $2\theta = 15.302°$, 16.960°, 18.619° and 25.618°. On irradiation with C^{5+} (70MeV) and Ni^{11+} (150MeV) ions there is decrease in peak intensities and increase in FWHM for all four initial peaks. This indicates a significant loss of crystallinity of polypropylene with SHI irradiation. However, this change is more prominent for

Ni^{11+} ion than C^{5+} ion. Similar results have been observed by Zhu et al. [4] in PET irradiated with 35MeV/u Ar ions and by Liu et al. [5] in PET irradiated with high energy ions (Ar, Kr and Xe)

REFERENCES

[1] D. Fink, R. Klett, L.T. Chaddertan, J. Cardosa, R. Montiel, M.H. Vazquez, A. Karanovich, Nucl. Instr. and Meth. B 111 (1996) 303.

[2] A. Saha, V. Chakaraborty, S.N. Chintalpudi, Nucl. Instr. and Meth. B 168 (2000) 245.

[3] H.S. Virk, P.S. Chandi, A.K. Srivastava, Nucl. Instr. and Meth. B 183 (2001) 32.

[4] Z. Zhu, C. Liu, Y. Sun, J. Liu, Y. Tang, Y. Jui, J. Du, Nucl. Instr. and Meth. B 191 (2002) 723.

[5] C. Liu, Z. Zhu, Y. Jin, Y. Sun, M. Hou, Z. Wang, X. Chen, C. Zhang, J. Liu, B. Li, Y. Wang, Nucl. Instr. and Meth. B 166-167 (2000) 641.

5.2.41 UV-Visible Analysis of Pristine and Ion Irradiated Polymers

Ambika Negi[1], SubhashChandra [1], D.K.Kanjilal[2], R. G Sonkawade[2], J. M. S. Rana[1] and R. C. Ramola [1]

[1] Department of Physics, HNB Garhwal University Badshahi Thaul Campus, Tehri Garhwal

[2] Inter University Accelerator Center, Aruna Asaf Ali Marg, New Delhi - 67

High-energy ion bombardment induced modifications in polymeric materials have been attracting much attention nowadays. Polyethylene tetrathalate (PET) is polyester having a high melting point and very good mechanical strength due to the presence of aromatic ring in the polymeric structure.It is resistant to heat and moisture and virtually unatacked by many chemicals. Irradiation of polymers with swift heavy ions leads to a wide variety of property changes (1-4).

Ultraviolet-visible spectroscopy is an important tool for investigation as it gives an idea about the value of optical band gap energy (E_g). Ion beam interaction with polymer generates damage. We irradiated the PET (100 micron) with Li, Ni and Au. In the present study, effect of swift heavy ions in optical properties of (PET) had been investigated and observed that band gap continuously decreases with increasing fluences.

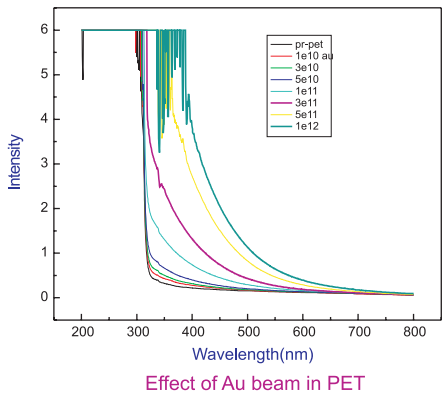

Fig. 1. Effect of Au beam in PET

REFERENCES

[1] A. Srivastava, T.V.Singh, S. Mule, C.R. Ranjan, S. Ponrathnam, Nucl. Instr. and Meth. B 192 (2002) 402.

[2] A. Srivastava, T. Singh, A.L. Sharma, P.K. Jain. C.R.Rajan, S. Ponrathnam, Radiat.Eff. Def. Solids 158 (2003) 561.

[3] J.P. Biersack, A. Schmoldt, D.Fink, G. Schiwietz, Radiat. Eff. Def. Solids 140 (1996) 63.

[4] P. Sonar, A.L. Shrma, A.Chandra, K. Mullen, A. Srivatava, Curr.Appl.Phys. (2003) 247

5.2.42 Optical band gap study of swift heavy ion irradiated polymers with UV-vis spectroscopy

Rajesh Kumar[1], S. Asad Ali[1], A.K. Mathur[1], H. S. Virk[2], F. Singh[3], S. A. Khan[3] and Rajendra Prasad[1]

[1]Department of Applied Physics, Z. H. College of Engineering & Technology, Aligarh Muslim University, Aligarh

[2]360 Sector-71, SAS Nagar (Mohali), Chandigarh-160071

[3]Inter University Accelerator Centre, Aruna Asaf Ali Marg, New Delhi - 67

The effect of ionizing radiation on polymers is generally classified in to main chain scission (degradation) and cross-linking. These may initiate modifications such as formation of chemical bonds between different molecules, intermolecular cross linking, irreversible cleavage of bonds (scission) in the main chain, resulting in to the fragmentation of molecules and the formation of saturated and unsaturated groups with stimulated evolution of gases [1]. At very high fluences of ions, carbonization may also take place [2]. In the present study modification in optical properties of four polymers induced by Si ion beam irradiation has been investigated by UV-Vis spectroscopy.

Significant changes of different amounts have been observed in optical response of the polymers after irradiation with Si ions. Ultraviolet-visible spectroscopy gives an idea about the value of optical band-gap energy (E_g) and thus provides an important tool for investigation. The absorption spectra with UV-Vis spectrophotometer are carried out on virgin and irradiated polymer samples. Optical absorption spectra of the virgin sample shows a sharp decrease with increasing wavelength up to a certain value, followed by a plateau region except in the case of PTFE spectra It is observed that optical absorption increases with increasing fluence and this absorption shifts from UV-Vis towards the visible region for all irradiated polymer samples as the fluence increases. The increase in absorption with irradiation may be attributed to the formation of a conjugated system of bonds due to bond cleavage and reconstruction [3].

Energy gap decreases with the increase in ion fluence in all the four polymers. But the percentage decrease is different in different polymers. At the highest fluence of ~10^{13} ions/cm^2 maximum decrease in energy gap of almost 40 % has been found for PES polymer samples and a minimum decrease of about 2.1% is found in PET. The cluster size showed a range of 79 to 454 carbon atoms per cluster for the polymers studied here.

REFERENCES

[1] D.M. Ruck, Nucl. Instr. and Meth., B 602(2000) 166.

[2] J.P. Durand, A.L. Moel. Nucl. Instr. and Meth. B 105(1995)71.

[3] L. S. Farenzena, R.M. Papaléo, A. Hallén, Araújo de., M. A., R.P. Livi, B.U.R. Sundqvist, Nucl. Instr. Meth. B105 (1995) 134.

5.2.43 Positron lifetime studies of the dose dependence of nanohole free volumes in ion-irradiated conducting poly-(ethylene-oxide) salt polymers

Rajesh Kumar[1], Udayan De[2], P.M.G. Nambissan[3], M. Maitra[4], S. Asad Ali[1], T. R. Middya[4], S. Tarafdar[4], F. Singh[5] and Rajendra Prasad[1]

[1] Department of Applied Physics, Z. H. College of Engineering & Technology, Aligarh Muslim University

[2] Variable Energy Cyclotron Centre, 1/AF, Bidhan Nagar, Kolkata

[3] Saha Institute of Nuclear Physics, 1/AF, Bidhan Nagar, Kolkata

[4] CMPR Centre, Department of Physics, Jadavpur University, Kolkata

[5] Inter-University Accelerator Centre, Aruna Asaf Ali Marg, New Delhi - 67

Free volume or holes, in solid polymer electrolytes (SPEs) or polymer solid electrolytes (PSEs) are required for ion movement and hence the electrical conduction. Since the work of Cohen and Turnbell [1], the transport processes in polymers are frequently described in terms of redistribution of the local free volume that appears due to the structural disorder in amorphous materials [2]. However a limited amount of experimental data has been reported on free volume and radiation induced modification due to lack of suitable probes for open volumes of molecular dimensions. Irradiation of polymers with swift heavy ion beams results into the change of free volume properties of polymeric material.

The present work has been carried out on PEO-salt complex with 17% salt. Free volume study by PALS for pristine sample and the samples irradiated with ions to different fluences has been undertaken to investigate the SHI induced modification in free volume properties. Solution-cast films each of total mass 3g of PEO (BDH, England) and of average molecular weight 600 Kg/mol complexed with NH_4ClO_4 (Fluka AG, 99.5% purity) were prepared in salt concentration of 17%. Pure PEO is non conducting while its complex $PEO_{(1-x)}(NH_4ClO_4)_x$ with weight fraction x = 17% is an ion conducting polymer. Polymer samples were exposed to 95 MeV oxygen ion beam at the 15 UD Pelletron accelerator at Inter University Accelerator Centre, New Delhi, India to different fluences.

Positron annihilation lifetime (PAL) and Doppler Broadening (DBA) measurements were carried out at the Saha Institute of Nuclear Physics (SINP), Kolkata, India, using a ^{22}Na source of approximately strength 400 kBq and a standard γ-γ coincidence setup.

Three lifetime components decomposed from the positron lifetime spectra arise from the annihilation of para positronium (p-Ps, τ_1~155-175 ps), free positron annihilation (τ_2~300-400 ps) and ortho positronium pick-off process (o-Ps, τ_3~1.5-3.5 ns) [3,4]. Based on a semi empirical model [5], the o-Ps pick off annihilation lifetime τ_{po} is related to the hole (assumed spherical) radius r_h .

The free volume radius r_h is calculated and the mean value of the free volume hole V_h is given as $V_h = \frac{4}{3}\pi r_h^3$.The fractional free volume F_v can be estimated as $F_v = C V_h I_3$ where C is a structural constant is ~ 0.0018 [5]. Table 1 shows the results obtained from o-Ps lifetime τ_3 for the values of the free volume hole radius r_h and volume of free holes V_h for the pristine samples and irradiated with 95 MeV O^{6+} ion beam.

Table 1 : The lifetime parameters of o-Ps, radius of free volume hole, mean free volume, fractional free volume and S parameter in poly-(ethylene oxide) salt polymer

Fluence (ions/cm^2)	τ_3 (ns)	I_3 (%)	r_h (Å)	V_h (Å^3)	Fv	S Parameter
Pristine	1.702	15.2	2.565	70.68	1.93	0.4059
10^{10}	1.685	15.0	2.544	68.95	1.86	0.4035
10^{11}	1.623	15.6	2.481	63.96	1.80	0.4040
10^{12}	1.820	14.0	2.684	80.98	2.04	0.4026
10^{13}	1.876	15.0	2.739	86.06	2.32	0.4018

o-Ps lifetime τ_3 obtained from PAL studies, free volume radius r_h and mean free volume decrease for the fluences 10^{10} and 10^{11} ions/cm^2 and then increase with 10^{12} and 10^{13} ions/cm^2. The results are contrary to our earlier study of SHI induced modifications in pure polymer [6-8] carried out through PAL measurements. The intensity of the o-Ps lifetime component I_3 shows only minor variation at highest fluence. The S parameter showed a continuous decrease with increasing fluence. The intermediate lifetime τ_2 also showed a similar decrease. These results indicate the occurrence of scission in the polymer chains and the fragmentation of larger free volumes into smaller ones.

REFERENCES

[1] M. H. Cohen, D. Turnbull, J. Chem. Phys. 31(1959)1164, D. Turnbull, M. H. Cohen, ibid. 52 (1970)3038

[2] J. Prez, Physics and Mechanics of Amorphous Polymers (A. A. Balkema, Rotterdamm, Brookfield, 1998).

[3] Y. C. Jean, Microchem. J 42(1990) 72; in Positron Annihilation, Proceedings of the 10th International Conference on Positron Annihilation, edited by Y.-J. He, B.-S. Cao, Y. C. Jean, Mater. Sci. Forum 175–178(1995)59.

[4] O. E. Mogensen, Positron Annihilation in Chemistry (Springer-Verlag, Berlin, Heidelberg, New York, 1995)

[5] Rajesh Kumar, S. A. Ali, A. K. Mahur, D. Das, A. H. Naqvi, H. S. Virk, Rajendra Prasad, Nucl. Instr. Meth.B244(2006)257.

[6] Rajesh Kumar, S. Rajguru, D. Das, Rajendra Prasad, Radiat. Meas. 36 (2003)151.

[7] Rajesh Kumar, A.K. Mahur, D. Das, K.K. Dwivedi, Rajendra Prasad, Indian. J. Phys. 78A (2) (2004) 225.

[8] Rajesh Kumar, Rajendra Prasad, Radiat. Meas. 40(2005)750.

5.2.44 Systematic measurements of energy loss and straggling for MeV heavy ions in polymers

Vishal Sharma[1], Pratibha[2], Tannu Sharma[2], P.K. Diwan[3], Shyam Kumar[2], V.K. Mittal[4], S.A. Khan[5] and D.K. Avasthi[5]

[1] Department of Physics, Chandigarh Engineering College, Landran, Mohali – 140 307

[2] Department of Physics, Kurukshetra University, Kurukshetra – 136 119

[3] Department of Physics, U.I.E.T., Kurukshetra University, Kurukshetra – 136 119

[4] Department of Physics, Punjabi University, Patiala – 147 002

[5] Inter University Accelerator Centre, Aruna Asaf Ali Marg, New Delhi – 67

Our group has been carrying out the energy loss and straggling measurements of heavy ions in different polymeric foils utilizing Pelletron accelerator facility at Inter University Accelerator Centre (IAUC), New Delhi. So far we have completed the measurements for Li, C, O, Si and Cl ions in Polypropylene, Mylar, Polycarbonate, Kapton and LR-115 polymers, covering the energy range ~ 1.0 – 6.0 MeV/u. Our measurements are highly precise and most of them are new and are being reported for the first time. Some new and interesting trends have been observed. None of the energy loss straggling formulations show agreement with the experimental data. We have made an attempt to develop fitted analytical expression for calculating the energy loss straggling compatible with the experimental values.

5.2.45 Effect of Lithium Ion Irradiation on Electrical Characteristics of High Speed NPN Power Transistor

C.M Dinesh[1], Ramani[1], M. C. Radhakrishna[1], S.A. Khan[2] and D. Kanjilal[2]

[1]Department of Physics, Jnanabharati, Bangalore University, Bangalore-560 056

[2]Inter-University Accelerator Center, Aruna Asaf Ali Marg, New Delhi - 67

The effect of high energy charged particles on the properties of microelectronic devices [1] e.g. NPN transistors are of academic interest due to its use in space and radiation rich environments. BJT's have important applications in analog and mixed – signal IC's and BICMOS (Bipolar Complementary Metal Oxide Semiconductor) circuits because of their current drive capacity, linearity, and excellent matching characteristics [2]. The present work aims to study the

effect of 50 MeV Li^{3+} ion irradiation on the electrical behavior of commercial BJT's. An attempt is made to explain the radiation degradation based on linear energy transfer (LET), total ionizing dose (TID), displacement damage (D_d) and its effect on depletion/diffusion capacitance, doping density, built in voltage and dielectric loss.

The silicon NPN power transistor (2N3866) manufactured by Bharat Electronics Limited (BEL), Bangalore, India, is selected for present investigation. The insulating silicon dioxide (SiO_2) thickness is of about 600 to 700 nm, the thickness of the emitter (n^+) is about 1μm and thickness of the base (p^+) is about 2 μm and intrinsic surface doping is about 5×10^{17} to 1×10^{18} cm^3. The n^- epitaxial layer thickness is 16 μm (silicon <111>, 2 Ω-cm) and the thickness of n^+ substrate is 200 μm (silicon <111>, 0.01 Ω-cm).

The transistor is irradiated by 50 MeV Li^{3+} ion beam using 15 UD Tandem accelerator facility at Inter University Accelerator Centre (IUAC). The fluence is varied from 1×10^{11} to 1.8×10^{12} ions cm^{-2}.

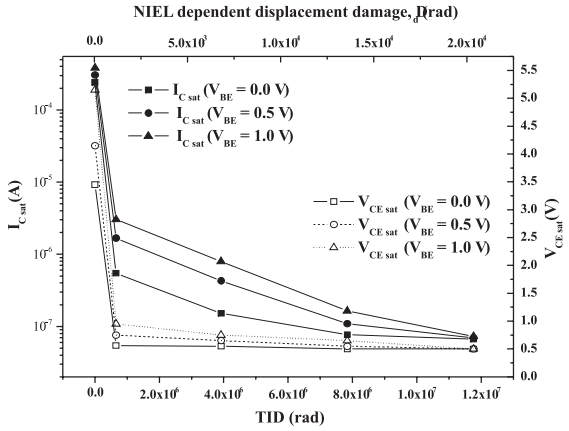

Fig. 1. Variation of output collector saturation current and collector – emitter saturation voltage of 50 MeV Li^{3+} ion irradiated transistor as a function of D_d and TID

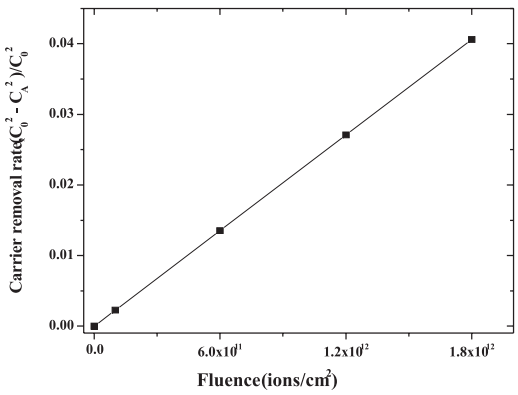

Fig. 2. Variation of carrier removal rate with fluence, $N_D = 5.75 \times 10^{16}$ cm^{-3}

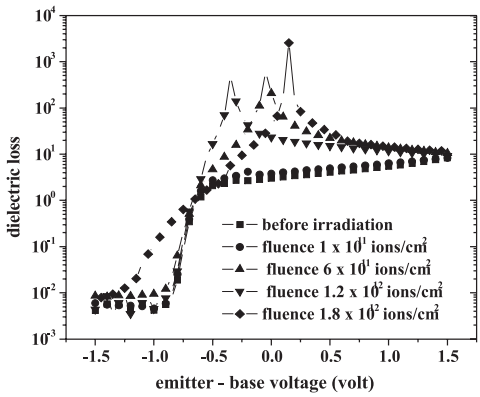

Fig. 3. Dielectric loss Vs emitter-base voltage of 50 MeV Li^{3+} ion irradiated transistor

With lithium ion irradiation, I_C is found to decrease with increase in ion fluence and I_B decreased initially for fluence of 1×10^{11} ions/cm^2, and then increases with further fluence increase. The MeV ion induced defects reduce the minority carrier lifetime and are responsible for the increase in series resistance and thereby reducing I_{Csat} and V_{CEsat}. The displacement damage increases the recombination in the neutral base region, which lead to the decrease of the collector saturation current. It is found that the number of recombination centers produced in silicon is proportional to the energy going into atomic displacement process. The non-ionizing energy deposition induced damage scaling of the gain variation of bipolar transistor is already observed for neutron and carbon ions [2,3]. The fluence dependent total ionizing dose (TID) and NIEL dependent displacement damage (D_d) versus saturation current and saturation voltage are plotted in figure 1. It shows correlation between the calculated defects and measured electrical parameters (I_{Csat} and V_{CEsat}). It is also observed that from figure 1, the saturation voltage and current abruptly decreased with ion fluence of 1×10^{11} ions/cm^2 and it remained constant with increase in fluence/dose. The BJT's are found to be very sensitive to the ionizing radiation and transistor gain degradation is the primary cause for the parametric shifts and functional failures. It is observed that the capacitance is reduced after the irradiation from nano-farad to pico-farad in the emitter-base region of the device (figure not shown). The change in capacitance is attributed to the reduction in the carrier density of the emitter-base region. This reduction in capacitance may be mainly due to the change in series resistance. Due to irradiation the shift in the built-in potential is observed, for unirradiated transistor it is found to be 0.437V and it increased to 0.445 V as the device is irradiated with 1×10^{11} ions/cm^2. The doping density of the emitter-base region decrease from 7.06×10^{16} cm^3 to 5.92×10^{16} cm^3 at the fluence 1×10^{11} ions/cm^2. These parameters play an important role in conduction of the device. Figure 2 shows the variation of carrier removal rate with fluence. From the figure the carrier removal rates seems to be small and it is found to be varying linearly with fluence of irradiation [4].

Figure 3 shows the plot of dielectric loss of the emitter-base region as a function of applied voltage. It can be seen that for unirradiated transistor the dielectric loss increases with the increase in the applied voltage. For irradiated device the curve shows similarity in the dielectric loss. As the fluence increases from 1×10^{11} ions/cm^2 to 1.8×10^{12} ions/cm^2 the dielectric loss increases, which indicates the decrease in its conducting property. However, the new peaks (at -0.05 V, - 0.15 V, and 0.15 V) show the production of new defects which are responsible for the decrease in its capacitance.

REFERENCES

[1] G.P. Summers, E.A. Burke, C.J. Dale, E.A. Wolicki, P.W. Marshall and M.A. Gehlhausen, IEEE Trans. Nucl. Sci. 34 (6), (1987) 1134.

[2] D. Codegoni, A. Colder, et. al., Nucl. Instr. and Meth. B 217, (2004) 65.

[3] A. Colder, N. Croitoru, et.al., Nucl. Instr. and Meth. B 179 (2001) 397.

[4] S.D. Kouimttzi, J. Phys. C: Sol. St. Phy. 19 (1986) 2427.

5.2.46 Influence of Irradiation Temperature on the characteristics of Deep Level Defects in Ag^{15+} Ion Irradiated Bipolar Junction Transistor

K.V. Madhu[1], Ravi Kumar[2], M. Ravindra[3] and R. Damle [1]

[1] Department of Physics, Jnanabharati, Bangalore University, Bangalore-560 056

[2] Inter-University Accelerator Center, Aruna Asaf Ali Marg, New Delhi - 67

[3] Components Division, ICG, ISRO Satellite Centre, Bangalore-560 017

In recent years, the study of deep level defects in semiconductor devices has become important to fabricate the devices for desired applications. In case of a bipolar junction transistor (BJT), the switching time depends on the recombination lifetime of the carriers which in turn depends on the concentration of the deep level defects or recombination centers [1-2]. Further, it is known that the introduction rate of the deep energy levels in silicon depends on the irradiation temperature [3-5]. This work describes the study of deep energy levels generated in the bulk of a commercial BJT by 200 MeV Ag^{15+}- ion irradiation. This BJT manufactured indigenously by Continental Device India Ltd. (CDIL) is planned for space applications. In the present study, the transistors are irradiated with Ag-ions at two different irradiation temperatures to study the effect of irradiation temperature on the characteristics of deep level defects.

The BJT used in the present study is a switching transistor with standard configuration (base thickness is 2.0 mm and oxide thickness is 1.2 mm). This BJT is suitable for low and high frequency operation. Decapped transistor is exposed to 200 MeV Ag^{15+}ions using 15 UD 16 MV Pelletron Tandem accelerator facility at Inter- University Accelerator Centre, New Delhi. The transistor is irradiated by Ag^{15+} ions with three different fluences 5.0×10^{10} ions cm^{-2}, 5.0×10^{11} ions cm^{-2} and 3.0×10^{12} ions cm^{-2} at two different temperatures 300 K and 77 K. I-V and Deep Level Transient Spectroscopy (DLTS) measurements are made before and after irradiation to study radiation induced transistor gain degradation and characteristics of deep level defects. After irradiation, it is observed that the base current increases with silver ion fluence. The extent of increase in base current is high in case of the transistor irradiated at low temperature. However, the collector current decreases as the ion fluence increases. The extent of decrease in collector current is also high in case of the transistor irradiated at low temperature. It is well known that the transistor gain degradation can occur due to the generation of recombination centers in the base region due to displacement damage caused upon irradiation. When recombination centers are generated in the base region of the transistor, it leads to an increase in the base current by decreasing the minority carrier lifetime. A decrease in the minority carrier lifetime will be reflected in the degradation of forward current gain of the transistor.

The deep level defects generated by irradiation of transistors by Ag^{15+} ions are characterized using DLTS technique. Figures 1 and 2 exhibit the DLTS spectra of the transistor irradiated with

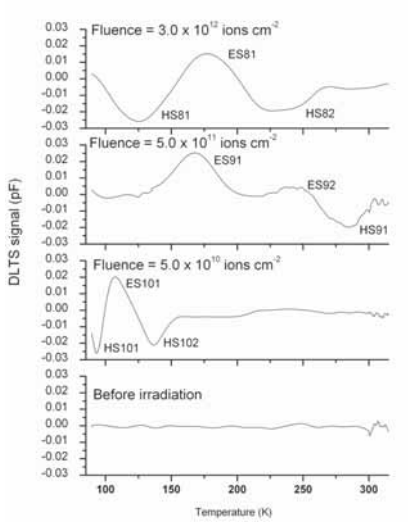

Fig. 1. DLTS spectra of silver ion irradiated (at low temperature) transistor for three different ion fluences. Rate window is fixed at 51.7 s^{-1}

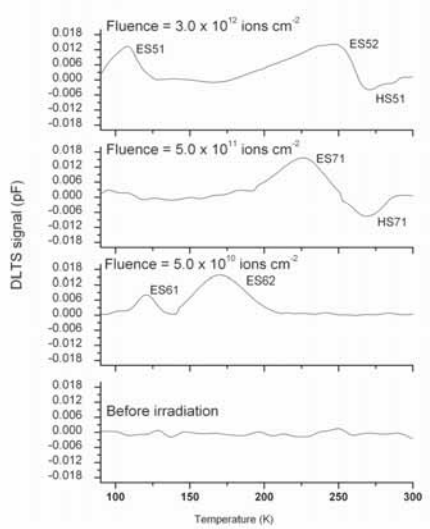

Fig. 2. DLTS spectra of silver ion irradiated (at room temperature) transistor for three different ion fluences. Rate window is fixed at 51.7 s^{-1}

Ag^{15+} ions at low temperature and room temperature respectively for three different ion fluences. The trap concentration (N_T) is determined by knowing peak height (dC_{max}) in the DLTS spectrum. In the DLTS spectra of the transistor irradiated at low temperature, four minority carrier and five majority carrier deep level defects are observed whereas five minority carrier and two majority carrier deep level defects are observed in the DLTS spectra of the transistor irradiated at room temperature. A comparison of I-V and DLTS results before and after annealing suggests that the transistors irradiated at low temperature are more vulnerable to high energy silver ion irradiation and this could be attributed to in-situ annealing of defects at high temperature. The defects which annihilate in the temperature range 350 °C to 450 °C have major contribution to the change in the base and collector currents and hence degradation of the forward current gain of the transistor.

REFERENCES

[1] S. M. Sze, Physics of Semiconductor Devices (2nd edition), John Wiley & Sons (1999) pp175.

[2] M. Nakabayashi, H. Ohyama, N. Hanano, E. Simeon, C. Claeys, K. Takakura, T. Iwata, T. Kudou, and M. Yoneoka, J. Mater. Sci. 16 (2005) 463.

[3] J. Boch, F. Saigne, V. Mannoni, F. Guistino, R. D. Schrimpf, L. Dusseau, K. F. Galloway, J. Fesquet, J. Gasiot, and R. Ecopett, IEEE Tran. Nucl. Sci. 49 (2002) 2990.

[4] H. Ohyama, K. Takakura, T. Watanabe, K. Nishiyama, K. Shigaki, T. Kudou, M. Nakabayashi, S. Kuboyama, S. Matsuda, C. Kamezawa, E. Simeon, and C. Claey, J. Mater. Sci. 16 (2005) 455.

[5] H. Ohyama, K. Takakura, H. Matsuoka, T. Jono, E. Simeon, C. Claeys, J. Uemura, and T. Kishikawa, J. Mater. Sci. 14 (2003) 437.

5.2.47 SEE Testing of PEMS and COTS Integrated Circuits

G R Joshi[1], S B Umesh[1], A R khan[1], M Ravindra[1] and Saif A Khan[2]

[1]ISRO Satellite Centre, Bangalore
[2]Inter University Accelerator Centre, Aruna Asaf Ali Marg, New Delhi - 67

All the electronic components used in the satellite system must meet the SEU, SEL & TID as per the ISRO specification. Some manufacturers give the SEE specifications for their components & some do not. For the components for which no radiation data is available either from the manufacturer or in the internet for the view of the users, SEE testing is done by our side to confirm if the component withstands the ISRO specified SEE limits.

The details of the devices are tabulated below

Sl. No.	Device Type	Function	Package Type	Manufacturer	Project	Radiation specification
1.	DS-5104ABTA	512Mb SDRAM	54 pin Plastic TSOP	Elpida/ 3DPlus	SSR- Oceansat onwards	Nil
2.	28C011T	1Mb EEPROM	32 pin DIP	Maxwell	SSR- Oceansat onwards	Rad-Pak SEU_{th}:18MeV-cm^2/mg
3.	RILV1616	16 Mb SRAM	48 pin Plastic TSOP	Renesas	Star Sensor IMS-1	Nil
4.	SJA1000	CAN controller	28 pin DIP	Philips	Star Sensor IMS-1	Nil
5.	HM62V8100	8 Mb SRAM	44 pin TSOP	Hitachi	Star Sensor IMS-1	Nil

512Mb SDRAM

The SDRAM mode register was configured to operate in Burst write and read mode. The data pattern of alternate 1's and 0's (checkerboard pattern) is written into and read from the memory array. As the data width is 4 bits, a pattern of 5_h(0101) and A_h(1010) is written alternatively in successive locations. Data is repeatedly read and compared with the expected values. In case of data mismatch error counter is incremented and the data is corrected in the error location and reading is further continued. The supply current I_{dd} is monitored during the test for recording of any SEL event.

128Mb EEPROM 28C011T

During the testing of write mode, EEPROM was in the erase-write mode programming of all the 1Mb locations. After the erase-write operation, a single read was made to verify the contents of the memory and again the device is subjected to programming mode. The I_{dd} is monitored during the test for recording of any SEL event.

RILV1616 & HM62V8100 SRAM

All the locations of SRAM are filled with alternate '0's and '1's (55_h & AA_h). The data is

continuously read back during irradiation. In the event of any mismatch in the read data, error counter is incremented and the error data is corrected and reading is continued. The test results are continuously monitored and recorded. The I_{dd} is continuously monitored for SEL event.

SJA 1000 CAN controller

The CAN device was tested for different modes.

1. Monitoring of the register set in the basic & Peli-CAN mode.
2. Monitoring the CAN protocol controller in self-test loop back mode.
3. The occurrence of upsets & I_{dd} are monitored and recorded.

The test result of 512 MB SDRAM indicates the susceptibility less than 17 MeV/mg/cm^2 LET and the device's sensitivity to upsets in the proton energy range. This device is sensitive for SEUs. EDAC (Error Detection and Correction) type of schemes or any other mitigation techniques can be employed for safer operation.

The EEPROM is found to be quite rugged and tolerant to heavy ion and proton-induced effects. The commercial 16MB SRAM is found to be sensitive to upsets and no Latch-up failures were observed. Upsets have to be mitigated.

The 16 MB SRAM device upset LET threshold is less than 17 MeV/mg/cm^2. The upsets were observed in command and control and status registers. This device is found to be very sensitive to upsets at lower LET values and also prone for Latch-up failure at higher LETs.

The CAN controller is very sensitive to upsets. As it has state machine, it is susceptible to controller failure. The device also exhibited a Latch – up failure. This device is found to be not suitable for the on – board application only with additional Latch up protection scheme to switch off the device in case of Latch-up.

Test Results

Sl No	Device type	ion	Energy MeV	LET MeV - cm^2/mg	Flux #P /cm^2/s	Fluence P/cm^2	SEU	SEL
1.	512MB SDRAM DS - 5104ABTA	$^{35}cl^{5+}$	60	17	1500	1.0 X 10^6	i. Errors @ 1 upset / 2k nibble/3.0 X 10^3 P/cm^2 ii. Observed stuck faults iii. No mode register failures	No Latch – up
		$^{107}Ni^{8+}$	100	31	1500	2.0 X 10^6	i. Errors @ 1 upset / 2k nibble/6.0 X 10^3 P/cm^2. ii. Observed stuck faults iii. No mode register failures	No Latch – up

2.	EEPROM 28C011T	$^{35}cl^{5+}$	60	17	1500	1.0×10^{6}	No upsets in write and read mode	No Latch – up
		$^{107}Ni^{8+}$	100	31	1500	2.0×10^{6}	16 upsets / 128k bytes in write mode	No Latch – up & SEGR
3.	16MBSRAM RILV1616	$^{35}cl^{5+}$	60	17	1500	1.0×10^{6}	Errors @ 500 upsets / 64k bytes/1.5×10^{4} P /cm^{2}	No Latch – up
		$^{107}Ni^{8+}$	100	31	1500	1.0×10^{6}	Errors @ 1500 upsets / 64k bytes/3.0×10^{4} P /cm^{2}	No Latch – up
4.	CAN controller SJA 1000	$^{35}cl^{5+}$	60	17	1500	1.0×10^{6}	Errors @ 1 upsets / 15 registers	No Latch – up
		$^{107}Ni^{8+}$	100	31	1500	1.0×10^{6}	Errors @ 5upsets / 15registers	Latch –up With Idd increased to 450mA

5.3 RADIATION BIOLOGY RESEARCH

The experimental parts of the projects involving heavy ion irradiation have been completed are from NEHU Shillong and BHU, Varanasi. For the project from NEHU, chromosome aberrations as a function of time are being studied in presence and absence of exogeneous glutathione in CHO cells. The project from BHU involved cells from rat spleen and bone marrow where Melatonin protection is being studied related to cell survival and apoptotic death under heavy ion irradiation.

Apart from these, the following research projects are going to start utlising the heavy ion beam.

1. Effect of swift heavy ions in MCF-7 carcinoma cell; MMH College Ghaziabad
2. Study of Low Dose Hyper-Radio-Sensitivity (HRS), in mammalian normal and tumour cells induced by heavy charged particles and the expression of apoptotic genes; Visva Bharati University, Shanti Niketan
3. Induction of apoptosis by heavy ion beam in Human Cervical Epithelial Carcinoma (HeLa) cells in presence and absence of PARP inhibitor; Kalyani University
4. Studies on heavy ion irradiated radiation damage in bacteria; WBUT, Kolkata
5. Studies on nanocrystal formation in microbes undergoing heavy ion irradiation; WBUT, Kolkata

5.3.1 Modulation of Endogenous Glutathione level and its role in High LET Radiation induced cellular damage

G. Pujari[1], A. Sarma[2], A. Chatterjee[3]

[1] Genetics Laboratory, Department of Zoology, NEHU, Shillong

[2] Inter University Accelerator Centre, Aruna Asaf Ali Marg, New Delhi - 67

[3]Molecular Genetics Laboratory, Dept. of Biotechnology and Bioinformatics, North Eastern Hill University, Shillong

Glutathione (GSH), a tripeptide (α-glutamyl-cysteinyl-glycin), was one of the first chemical compounds used as a radio-protector [1]. Intracellular GSH is the most important subsets of the endogenous sulfhydryls regarding the modification of cellular responses to both ionizing radiation and chemotherapeutic agents [2, 3]. Most studies of radioprotectors have employed γ or X-ray sources and, to a lesser extent, neutrons or other high-LET sources. Several studies have shown that chemical agents which modulate radiation sensitivity of mammalian cells exposed to low LET radiation are less effective with high LET radiation [4, 5]. In this investigation, an attempt has been made to study the influence of GSH on high LET radiation induced DNA damage and delay in cell proliferation.

Objective was to evaluate the influence of GSH pre-treatment on DNA damage and cell proliferation in cells irradiated by Carbon ion (^{12}C) beam and the Lithium ion (^{7}Li) beam.

The results and inference are briefed as following :

The frequency of aberrations induced by Carbon ion (^{12}C) beam is higher than the Lithium ion (^{7}Li) beam. The higher frequency of aberrations was scored in ion beam irradiated cells fixed at delayed hour. The cells whose division is delayed are carrying more aberrations than cells that enter mitosis early.

The most common aberration type is deletions, however, a good percentage of exchange aberrations are observed. Chromosomal aberration such as deletion and chromatid break showed an increase in the frequency with the increase in fluence and also in the presence of BSO. However, the frequency of exchange aberrations decreased in the presence of BSO. Since high LET irradiation is inducing more DNA double strand breaks which are spatially closer than low LET radiation and therefore the rate of rejoining of double strand breaks is higher and thus showing more exchanges. Reducing the frequency of exchanges indicates that the joining of DNA double strand breaks induced by high LET-radiation probably needs the presence of GSH.

No protection was observed when GSH was added before high LET radiation. The frequency of exchanges is observed to increase on exogenous addition of GSH. It indicates that the joining of DNA double strand breaks induced by high LET radiation probably needs the presence of GSH.

The induction of delay in cell cycle was more with ^{12}C beam than ^{7}Li beam irradiated cells. Both addition of exogenous GSH or BSO did not show any influence on the cell kinetics patter in the irradiated cells.

It has already been reported that the induction of CA and delay in cell kinetics by radiation may not always be interlinked (6).Usually both GSH and BSO reduced the delay induced by low LET radiation, but in the present study it failed to show any influence on such delay.

REFERENCES

[1] Latarjet R and Ephrati E,1948, C.R. Seanc. Soc. Biol., 142, 497.

[2] Clark EP,1986, Int. J. Radiat. Oncol. Biol. Phys., 12,1121-1126.

[3] Chattopadhyay A, Deb S, Chatterjee A,1999, Int. J. Radiat. Biol.,75, 1283-1291.

[4] Barendsen GW, Koot CJ, Van Kersen, Bewley DK, Parnell CJ, Field SB,1966, Int. J. Radiat. Biol.,10,317-327.

[5] Todd P, 1967, Radiat. Res.7, 196-207.

[6] Ray S and Chatterjee A, 2007, Int. J Radiat. Biol., 83: 347-354.

5.3.2 Studies on ionizing radiation irradiated metal induced radiation sensitization in Bacillus subtilis

S Das[1], P Nandy[1], S Chowdhury[1], A Sarma[3], A R Thakur[2] and S Ray Chaudhuri[1]

[1] Department of Biotechnology, West Bengal University of Technology, BF-142, Sector 1, Salt Lake, Kolkata-700064

[2] Department of Bioinformatics, West Bengal University of Technology, BF-142, Sector 1, Salt Lake, Kolkata-700064

[3] Inter University Accelerator Centre, Aruna Asaf Ali Marg, New Delhi-110067

The group has been able to isolate microbes from the environmental origin and characterize them at length. These microbes have the potential of metal accumulation and extracellular enzyme production. This property makes them potential candidate for bioremediation [1, 2, 3]. The ability to withstand radiation exposure would enable them to be used even under adverse conditions. The aim of the study is to look at the ability of these naturally occurring microbes to repair DNA DSB induced on its genome following ionizing radiation. The extent of metal accumulation inside the cell was tested and its effect on enzyme production as well as radiosensitization of the cell was studied. The over all investigation would give a better picture on the usability of these microbes for metal accumulation as well as enzyme induced bioremediation under adverse conditions.

The cells were grown and characterized as per the protocol of Nandy *et al* [4]. Metal salts of $Al(NO_3)_3.9H_2O$, $CuSO_4.5H_2O$, $AgNO_3$, $Pb(NO_3)$, $NiCl_2.6H_2O$, $HgCl_2$, $CoCl.6H_2O$, $FeSO_4$, $Cr_2O_3$and $CdCl_3$ were used for tolerance study. Stock solution of each metal was prepared on basis of molar concentration as per formulae M = Moles of solute/Volume of solution. In addition to $AgNO_3$, AgCl was also used in form of supersaturated stock solution. From an overnight grown culture of a single colony, 1% (v/v) was transferred to 3 ml of media supplemented with each metal separately. The initial metal concentration was taken as 1mM. The tolerance was measured on the basis of growth observed within 12 to 48 hours using spectrophotometer. If growth was observed, inoculum was added to the media with increasing concentration of the metal (1mm, 2mm, 10mm, 100mm and so on). This step was repeated for all the metals in each strain till Minimum Inhibitory Concentration (MIC) was obtained as visualized by cessation of growth.

The extent of accumulation was confirmed using EDXEF analysis as per the protocol reported elsewhere [5]. The localization of the metal inside the cells was confirmed through Transmission Electron Microscopy according to the protocols reported earlier [5]. The effect of metal on the cell was analyzed through Scanning Electron Microscopy [5]. For ionizing radiation study, the initial standardization was attempted using ^{60}Co γ rays. The DSB induction and its repair was studied using the protocol of Ray Chaudhuri *et al* [6,7]. 4×10^8 cells were used per plug for the Asymmetric Field Inversion Gel Electrophoresis experiments.

The cells show maximum accumulation of Pb. The cells can tolerate upto 6mM of $Pb(NO_3)$ in the culture with an associated accumulation of 421.38 ppb. The transmission electron micrograph shows accumulation on the periphery and also in the cytoplasm. The SEM image shows shortening of the cell in presence of metal indicating it to be a stress. The protease production in presence of metals decreases but this could also be attributed to less cell number. It has to be further studied to understand the correlation, if any. The DSB induction study indicates repairability of DSB by the

cells. It also emphasizes the increased damage in presence of metal as evident from the lanes showing repair in metal containing experiment. The result has to be further analysed through densitometric scanning for understanding the extent of damage and corresponding repair at different doses both in presence and in absence of metal.

By observing the dose profile, it seems 4 hours is not sufficient for the repair mechanism to take place, repair time has to be further standardized. The possible explanation of the apparent discrepancy in the time course study can be that the evident larger amount of DNA present in one of the lanes might have ligated back to form longer fragments which have receded back towards the groove in lane 1; still it has to be reconfirmed and interpreted after densitometric scanning.

REFERENCES

[1] Lloyd. J.R., Lovely. D.R. (2001) Microbial Detoxification of Metals and Radionuclides. Current Opinion in Biotechnolgy; 12: 248-253.

[2] Malekzadeh. F., Farazmand.A., Ghafourian. H., Shahamat. M., Levin. M., and Colwell. R.R. (2002). Uranium accumulation by a bacterium isolated from electroplating effluent. World Journal of Microbiology and Biotechnology; 18(4): 295-302.

[3] White. C., Wilkinson. S.C., and Gadd. G.M. (1995). The Role of Microorganisms in Biosorption of Toxic Metals and Radionuclides. International Biodeterioration and Biodegradation; 35: 17-40.

[4] Nandy. P., Thakur. A.R., and Ray Chaudhuri. S. (2007) Characterization of Bacterial Strains Isolated Through Microbial Profiling of Urine Samples.OnLine Journal of Biological Sciences; 7(1): 44-51.

[5] Adarsh. V.K., Mishra. M., Chowdhury. S., Sudarshan. M., Thakur. A.R., Ray Chaudhuri. S. (2007) Studies on Metal Microbe Interaction of Three Bacterial Isolates From East Calcutta Wetland. OnLine Journal of Biological Sciences; 7(2): 80-88.

[6] Raychaudhuri. S., Karmakar. P., Choudhary. D., Sarma. A., Thakur. A.R. (2003) Effect of heavy ion irradiation on DNA DSB repair in *Methanosarcina barkeri.* Anaerobe; 9(1): 15-21.

[7] Raychaudhuri. S., Karmakar. P., Thakur. A.R. (2000) α -Ray-Induced DNA Damage and Repair in *Methanosarcina barkeri.* Anaerobe;6(6): 325-331.

5.4 ATOMIC PHYSICS RESEARCH

We have continued to understand unusual features of beam-foil experiments using single as well as two-foil target. Such features indicate new phenomena having important relevance to astrophysics. One out these hints us a discovery of a new light source to be used for investigation of H-like highly charged ions.

Atomic and molecular physics experiments in the low energy ion beam laboratory have started yielding good results. Position sensitive multi-hit time-of-flight measurement system is used to study the fragmentation dynamics of complete and incomplete fragmentation process as presented below.

5.4.1 Atomic astrophysics experiments using highly charged MeV ions

T. Nandi

In the recent past we have succeeded in obtaining important results from atomic experiments having novel implications to astrophysics. Some are mentioned below.

(i) Formation of the circular Rydberg states in ion-solid collisions

We observed the circular Rydberg states populated in H-like Fe ions during fast ion-solid collisions. Time-resolved x-ray spectra obtained with 164 MeV $^{56}Fe_{26}$ ions colliding with a carbon foil do not show any lines due to H-like Fe ions at small delay times until 600 ps. However, Ly-a and Ly-b transitions appear after a while and attain maximum intensity at a delay of 920±5 ps. Such a delay is attributed to successive cascading from the circular Rydberg levels which find important implications in understanding the origin of radio recombination lines from interstellar spaces. Detailed can be seen in The Astrophysical Journal Letters 673**,** L103-L106 (2008).

(ii) Direct observation of large probability of collision-induced intrashell transition and its astrophysical relevance

We have observed intrashell transitions between 1s2s $^3S_1$ and 1s2p $^3P_2$ levels in He-like Ti ions by the beam-two-foil time-of-flight technique. The mean intrashell transition probability between these two sublevels obtained from this experiment is found to be quite large, (0.72 ± 0.05), which is attributable to the small energy splittings between them. A simple theoretical estimate using first Born approximation is found to be in close agreement with the experimental value. Such large intrashell transition probability is helpful in resolving a disagreement between theory and experiment on the relative intensity of Li-like C, N, and O ions in inter stellar medium.

(iii) Secondary beam-foil source: Confirmation of circular Rydberg states with projectile-like particle ions

We report the secondary beam-foil source for studying physics of projectile-like particle

ions. Projectile-like particle ions of $^{60}Ni_{28}$ and $^{63}Cu_{29}$ ions have been produced by Fe- and $^{62}Zn_{30}$ ions by Ni-ions, at beam energies above the Coulomb barrier, bombarding on thin carbon foil. Formation of circular Rydberg states has been confirmed in collision experiments with projectile-like particle ions on carbon foils. Merits and demerits of this novel technique are different from the beam-foil experiments. Its impacts on atomic collision physics, astrophysics, and nuclear transfer reactions are very interesting.

(iv) Experimental evidence of bare ions formed from nuclear reactions: its possible roles on astrophysics

We report that the projectile-like particle ions produced from nuclear pick up reactions are just bare ions. The x-ray emission spectra of the foil excited ions show a signature of transitions originated from higher charged states with slower projectile-like particle ions than the projectile ions. Such a novel ionization process can be responsible for producing the bare ions in the astrophysical plasma. This process will be useful in modeling chemical evolution of matter from which the solar system was formed.

5.4.2 Atomic and Molecular Physics Experiments at LEIBF

C P Safvan, Sankar De, Jyoti Rajput and A. Roy

Using the low energy ion beam facility, experiments were conducted to study the dissociation dynamics of multiply charged molecules. The experiments used the time of flight apparatus coupled with position sensitive detectors and post collision charge state analyser to determine the fragmentation patterns and dynamics.

Target molecules, in the form of an effusive gas jet were made to interact with multiply charged Ar projectiles. The fragmented molecular ions were detected with a position sensitive time of flight mass spectrometer and event by event analysis coupled with coincidence map techniques were used for data interpretation.

Molecules such as C_nH_m clusters are abundant in the astrophysical environment. Spectroscopic studies on comets such as Hale Bopp and Hyakutake, have confirmed the existence of C_2H_6 and C_2H_2 but not C_2H_4. Therefore a systematic study of formation and destruction of such species as a result of charged particle interaction is urgently needed to examine whether some intermediate "exotic" molecular ion is formed in the planetary atmosphere which prohibits or bypasses the formation of C_2H_4 giving preference to C_2H_6 and C_2H_2. Careful study of the dissociation products of C_2H_2 as a first member in this family of molecules might give us insight into some unknown realm of bond formation and rupturing processes to answer the above astrophysical phenomenon

A detailed study of the dissociation dynamics of acetylene was carried out. Fig.1 shows the fragmentation products from acetylene.

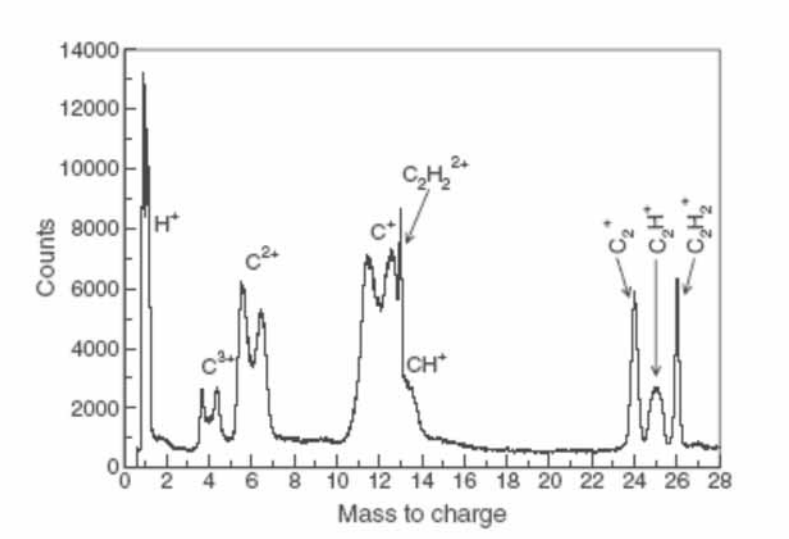

Fig.1. The fragmentation products from acetylene

Coincidence maps allow us to study the importance and relative ratios of the various dissociation channels. Fig.2 shows the coincidence map measured from acetylene.

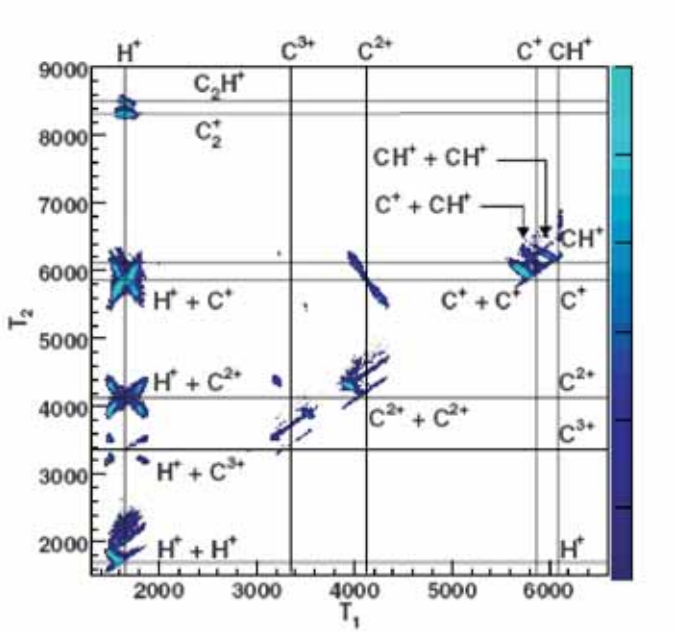

Fig.2. The coincidence map measured from acetylene

The projectile charge state dependence of fragmentation in small molecules like methane was also studied.